Radio Science Bulletin

ISSN 1024-4530

INTERNATIONAL
UNION OF
RADIO SCIENCE

UNION
RADIO-SCIENTIFIQUE
INTERNATIONALE

No 345
June 2013

URSI, c/o Ghent University (INTEC)
St.-Pietersnieuwstraat 41, B-9000 Gent (Belgium)

Contents

Editorial 3
URSI GASS 2014 5
Awards for Young Scientists - Conditions 6
Introduction to the Special Section on the Role of Radio Science in Disaster management 7
Topology Modeling and Network Partitioning : An Application to Forest-Fire Fighting 8
Causal Probabilistic Modeling with Bayesian Networks to Combat the Risk of Piracy Against Offshore Oil Platforms 21
Application of the Extended Ground Truth Concept for Risk Anticipation Concerning Ecosystems 35
Two-Tier Femto-Macro Wireless Networks : Technical Issues and Future Trends 51
An Analog of Surface Tamn States in Periodic Structures on the Base of Microstrip Waveguides 64
Book Reviews for Radioscientists 73
Conferences 76
News from the URSI Community 81
Call for Papers 89
Information for authors 92

Front cover: (top) The Faucon Noir unmanned aerial system in flight, with one its mapping payloads. (bottom) A mosaic created with the oblique images taken by the aerial system. See the paper by Antoine Gademer, Laurent Beaudoin, Loïca Avanthey, and J. P. Rudant in the "Special Section on the Role of Radio Science in Disaster Management."

For information, please contact :
The URSI Secretariat
c/o Ghent University (INTEC)
Sint-Pietersnieuwstraat 41, B-9000 Gent, Belgium
Tel.: (32) 9-264 33 20, Fax: (32) 9-264 42 88
E-mail: info@ursi.org
http://www.ursi.org

Editorial

In this issue, we have a special section on "The Role of Radio Science in Disaster Management." This special section has Tullio Joseph Tanzi, François Lefeuvre, and P. J. Wilkinson as Guest Editors. They have provided a separate introduction, highlighting the importance of radio science in disaster management. There are three invited papers in the special section in this issue. The balance of the papers in this special section will appear in the September issue.

Papers from the Special Section on "The Role of Radio Science in Disaster Management"

In their invited paper, Monia Hamdi, Laurent Franck, and Xavier Lagrange consider the topic of establishing and maintaining emergency networks. They do this in the context of networks for fighting fires. They begin with an overview of the importance of networks in responding to disasters, and the specific challenges for networks used in fighting fires. They assume that partitioning of the network is crucial, and that the nodes in the network have a satellite terminal. They introduce and describe the general topology of networks for emergency situations. They then describe topologies appropriate for forest-fire fighting. Three topological network models are considered: random walk, the reference region group model, and the fire mobility model. The characteristics of each of these three models are described. The three models were compared using simulations, with the radio range of the nodes varied over ranges appropriate to typical wireless-LAN ranges. The results of the simulations highlighted the strengths and weaknesses of each of the models with regard to their ability to capture the important characteristics of the dynamics of emergency networks. The authors then look at several clustering algorithms for mitigating the effects of partitioning in such networks. The aspects of cluster maintenance and node migration are examined. A new approach for cluster maintenance is introduced and compared to previous approaches, and is shown to ensure that the cluster structure remains consistent. This paper provides a nice introduction to the modeling of emergency networks, as well as some interesting new results.

The topic of the invited paper by Xavier Chaze, Amal Bouejla, Franck Guarnieri, and Aldo Napoli is the application of artificial-intelligence techniques to assess and respond to the risk of piracy attacks against offshore oil platforms. The paper begins with a brief introduction to the artificial-intelligence techniques and their use. It is noted that the ability to combine quantitative databases with qualitative human experience can provide an advantage. The use of a Bayesian network to do this is introduced. The problem of energy piracy at sea is explained. This includes a summary of facts and figures regarding attacks on energy installations, and a review of the categorization of the types of attacks that can occur. Examples of these are given. The International Maritime Organization's recommendations for protecting fixed installations and shipping are reviewed. The use of Bayesian networks to assess risk and recommend responses to risks is introduced and explained. The way some dedicated software was used to construct the Bayesian network is detailed. The use of the network to couple data from the Piracy and Armed Robbery database with expert knowledge to perform threat assessment and recommend countermeasures is described. A set of test attack scenarios was developed, and these are reviewed. The integration of the Bayesian network into an existing monitoring, assessment, and response system is described. The results of operating this system against the test scenarios are explained and analyzed. This paper presents a very interesting description of the application of artificial intelligence techniques to an important real-world problem.

Mapping and remote sensing are fundamental tools in the analysis and assessment of ecosystems, and in particular in the assessment of ecosystem disasters. The invited paper by Antoine Gademer, Laurent Beaudoin, Loïca Avanthey, and Jean-Paul Rudant presents a new concept, the Extended Ground Truth. This combines features of both mapping and remote sensing as a way of assessing and responding to attacks on ecosystems. The authors begin with a description of the use of dynamic cartography to map the changes resulting from an attack on an ecosystem. The example of invasion by a pest plant is used. The static and dynamic criteria for classifying plant species are reviewed. Manual and remote-sensing methods for mapping plant species are explained. The Extended Ground Truth concept is introduced. This is based on the use of images taken at a scale that allow unambiguous identification of individuals (e.g., individual plants or trees), combined with larger-scale mapping. The characteristics of the mapping and remote sensing necessary to implement Extended Ground Truth are identified. The methodologies for determining the size of the ground-sample distance; the type of sensor to be used; the flight speed, height, scan width, and overlap rate; and the choice of the type of vehicle to carry the sensor are explained. The application of the Extended Ground Truth method to a case study involving a French forest area is described.

This included the design and construction of a low-cost unmanned aerial system for low-level remote sensing and mapping. The details of the system are explained, and the results of applying the system and technique to the case study are analyzed. This paper introduces an interesting new approach to the use of a combination of mapping and remote sensing to assess ecosystem disasters.

Our Other Papers

Femto-cells are very small cellular networks that are typically user-installed, and connect the Internet to the cellular network. The use of femto-cells is seeing very rapid growth, leading to two-tier networks: networks in which existing large-scale cellular networks overlap with randomly distributed femto-cells. The invited Commission C paper by J. Zhang, Z. Xiao, X. Zhang, and E. Liu reviews the recent research and results relating to such networks. The paper begins with a review of the factors associated with femto-cell use, and the different types of access models used with femto-cells. Spectrum allocation in two-tier networks is explained, including the allocation of spectrum in two-tier networks using different access models, different approaches to spectrum allocation, and the efficiency of different spectrum-allocation approaches. Interference between the tiers of a two-tier network is discussed, including the various types of interference, and methods for mitigating these. Access approaches are reviewed, along with methods for selecting the tier of a two-tier network for a user device to use. Handover within a femto-cell network and between the tiers of a two-tier network is examined. The connection of such networks to the backhaul is reviewed, along with issues of protecting the mobility of user equipment and the energy efficiency of deploying such networks. The paper concludes with a look at future trends in research in the area. This paper provides a very insightful review of a type of network structure that is becoming much more common and important in real-world cellular communications.

The efforts of Sana Salous of Commission C in bringing us this paper are gratefully acknowledged.

Surface Tamm states appear at the boundary of two bounded periodic structures: for example, at optical frequencies at the boundaries of solid state lattices and photonic crystals. One important feature of such a state is that there is no transfer of energy along the boundary. There is also a very narrow transparency peak (the Tamm peak) that appears in the spectrum bandgap of a bounded periodic structure. The paper by D. P. Belozorov, A. A. Girich, and S. I. Tarapov introduces an analog to the surface Tamm state for a microwave microstrip waveguide structure. The paper begins with a review of Tamm states at the interface between bounded periodic media. The microstrip microwave structure is introduced. The Bloch equation is derived for an electromagnetic wave propagating along both an infinite and a finite periodic structure of such microstrip elements. The analog of the Tamm state is explored and demonstrated for such structures. A number of numerical examples are then presented in which the dimensions of the microwave structures are varied to demonstrate aspects of the behavior of the analog of the Tamm state. In particular, the dependence of the analog of the Tamm peak on the dimensions and parameters of the microwave structures is explored. Practical applications of this new analog of the Tamm state, particularly for measurements of the permittivity of fluids, are mentioned. This paper provides an introduction to an interesting new microwave propagation phenomenon.

Our Other Contributions

Kristian Schlegel has provided us with reviews of two books. One is a new book on space weather. The other is a review by a Young Scientist of a classic book on sequences for communication applications. We have reports on the Finnish Radio Science Days, an International Reference Ionosphere workshop, and the Swedish URSI national Member Committee's visit to a number of radio science groups in Latvia. There are also calls for papers for several important conferences in our field.

The call for papers and announcement of the application process for the Young Scientist Awards for the XXXIst URSI General Assembly and Scientific Symposium appears in this issue. This will be held August 17-23, 2014, in Beijing, China (CIE). This is going to be an outstanding conference, held in a fascinating and vibrant location. The venue will be the Beijing Conference Center, a modern conference center located in a park-like setting in the middle of Beijing. I urge you to start preparing your contribution, and to make plans to attend. You won't want to miss this!

XXXI General Assembly and Scientific Symposium of the International Union of Radio Science

Union Radio Scientifique Internationale

August 17-23, 2014 Beijing, China (CIE)

Announcement and Call for Papers

The XXXIst General Assembly and Scientific Symposium (GASS) of the International Union of Radio Science (Union Radio Scientifique Internationale: URSI) will be in Beijing. The XXXIst GASS will have a scientific program organized around the ten Commissions of URSI, including oral sessions, poster sessions, plenary and public lectures, and tutorials, with both invited and contributed papers. In addition, there will be workshops, short courses, special programs for young scientists, a student paper competition, programs for accompanying persons, and industrial exhibits. More than 1,500 scientists from more than 50 countries are expected to participate. The detailed program, the link to the electronic submission site for papers, the registration form, the application for the Young Scientists program, and hotel information are available on the GASS Web site: **http://www.chinaursigass.com**

Submission Information

All papers (a maximum of four pages) should be submitted electronically via the link provided on the GASS Web site: http://www.chinaursigass.com. Please consult the symposium Web site for the latest instructions, templates, and sample formats. Accepted papers that are presented at the GASS will be submitted for posting to IEEE Xplore.

Important Deadlines: Paper submission: February 15, 2014 Acceptance Notification: April 15, 2014

Topics of Interest

Commission A: Electromagnetic Metrology
Commission B: Fields and Waves
Commission C: Radiocommunication and Signal Processing Systems
Commission D: Electronics and Photonics
Commission E: Electromagnetic Environment and Interference
Commission F: Wave Propagation and Remote Sensing
Commission G: Ionospheric Radio and Propagation
Commission H: Waves in Plasmas
Commission J: Radio Astronomy
Commission K: Electromagnetics in Biology and Medicine

Young Scientists Program and Student Paper Competition

A limited number of awards are available to assist young scientists from both developed and developing countries to attend the GASS. Information on this program and on the Student Paper Competition is available on the Web site.

Contact

For all questions related to the GASS, please contact the GASS Secretary:
Cynthia Lian, e-mail: cynthia_nano@hotmail.com; Lucy Zhang, e-mail: yzha0943@gmail.com;
Yihua Yan, e-mail: yyh@nao.cas.cn; Tel: 008610-68278214

www.chinaursigass.com

AWARDS FOR YOUNG SCIENTISTS
CONDITIONS

A limited number of awards are available to assist young scientists from both developed and developing countries to attend the General Assembly and Scientific Symposium of URSI.

To qualify for an award the applicant:

1. must be less than 35 years old on September 1 of the year of the URSI General Assembly and Scientific Symposium;
2. should have a paper, of which he or she is the principal author, submitted and accepted for oral or poster presentation at a regular session of the General Assembly and Scientific Symposium.

Applicants should also be interested in promoting contacts between developed and developing countries. Applicants from all over the world are welcome, also from regions that do not (yet) belong to URSI. All successful applicants are expected to participate fully in the scientific activities of the General Assembly and Scientific Symposium. They will receive free registration, and financial support for board and lodging at the General Assembly and Scientific Symposium. Limited funds will also be available as a contribution to the travel costs of young scientists from developing countries.

The application needs to be done electronically by going to the same website used for the submission of abstracts/papers via http://www.chinaursigass.com/. The deadline for paper submission for the URSI GASS2014 in Beijing is 15 February 2014.

A web-based form will appear when applicants check "Young Scientist paper" at the time they submit their paper. All Young Scientists must submit their paper(s) and this application together with a CV and a list of publications in PDF format to the GA submission Web site.

Applications will be assessed by the URSI Young Scientist Committee taking account of the national ranking of the application and the technical evaluation of the abstract by the relevant URSI Commission. Awards will be announced on the URSI Web site in April 2014.

For more information about URSI, the General Assembly and Scientific Symposium and the activities of URSI Commissions, please look at the URSI Web site at: http://www.ursi.org or the GASS 2014 website at http://www.chinaursigass.com/

If you need more information concerning the Young Scientist Program, please contact:

The URSI Secretariat
c/o Ghent University / INTEC
Sint-Pietersnieuwstraat 41
B-9000 GENT
BELGIUM
fax: +32 9 264 42 88
E-mail: ingeursi@intec.ugent.be

Introduction to the Special Section on the Role of Radio Science in Disaster management

Guest Editors:
Tullio Joseph Tanzi, François Lefeuvre, P. J. Wilkinson

Natural or man-made disasters inflict dreadful losses on the regions that experience them, in both material wealth and human lives. In extreme cases, survivors may feel death was preferable, especially months after the disaster, when recovery appears to have stalled. While the media draws everybody into these events, the scale of the publicized devastation can be mind-numbing to the point of being an anesthetic, and time can erode the remaining compassion of the moment.

Disasters demand action, from anticipating their potential to responding and mitigating their effects. Risks associated with all phases of a disaster are a measure of our ability to cope in a dynamic and highly stressful environment. These risks may refer to anything from the safety of an individual to the economic well-being of a region. Irrespective of the exact nature of the risk, we believe that knowledge, correctly applied, will reduce the risks associated with a disaster.

Science has achieved much in alleviating some of the worst aspects of disasters, from providing warnings of impending weather events (cyclones, tornadoes, floods, fires, droughts, tsunamis, and pestilence) to mitigating the worst effects of the initial impact. This is an ongoing undertaking that engages the interest, if not the participation, of all scientists.

Radio science pervades society, and plays an integral role in disaster management and mitigation. This role is often taken for granted, even though it forms a significant part of the response to disasters. For instance, the role of communications during and after a disastrous event is pivotal for assessing damage and providing relief. Each URSI Commission is a reservoir of specialist knowledge and contributions, and specialists' assistance from all URSI Commissions can contribute to new operational and efficient approaches to manage the diverse events that arise in our everyday lives. With these objectives in mind, an Inter-Commission Working Group on Natural and Human Induced Hazards and Disasters was created at the 2008 URSI GASS.

The effectiveness is even greater when applied in conjunction with other disciplines, represented by the other scientific unions of the International Council for Science (ICSU). In fact, this can open an even wider space of new applications for radio science. To this end, the International Society for Photogrammetry and Remote Sensing (ISPRS) and URSI have been working together. This activity was initiated by Prof. Francois Lefeuvre, when he was President of URSI, and Prof. Orhan Altan, the President of ISPRS. Joint meetings took place in Antalya, Istanbul, and most recently in Melbourne, Australia. The joint approach will enable more complex problems to be recognized and addressed.

The first of two parts of special sections containing papers drawn from the recent joint ISPRS – URSI Symposium, held during the ISPRS General Assembly in Melbourne, July 2012, starts in this issue of the *Radio Science Bulletin*. These papers provide an example of cross-Union interdisciplinary research. There will be a further joint meeting at the URSI GASS in Beijing in August 2014.

Tullio Joseph Tanzi, Télécom ParisTech – LTCI/CNRS, Paris, France; e-mail: tullio.tanzi@telecom-paristech.fr

François Lefeuvre, LPC2E/CNRS, URSI, Orléans, France; e-mail: lefeuvre@cnrs-orleans.fr

P. J. Wilkinson, IPS, Bureau of Meteorology, Australia; e-mail: phil_wilkinson@internode.on.net

Topology Modeling and Network Partitioning : An Application to Forest-Fire Fighting

Monia Hamdi
Laurent Franck
Xavier Lagrange

Abstract

This contribution is about emergency networks, and how to counter partitioning occurring in a mobile ad hoc network. Our approach is based on clustering, where a distributed election process is run in order to identify a node called the *clusterhead*, which will provide interconnection services with the rest of the network. While the election process is based on a published protocol called KCMBC, this contribution focuses on an aspect not covered by KCMBC, which is cluster maintenance. Cluster maintenance makes sure that the election process stays valid even though the partition topology changes: nodes join and leave the cluster. In this context, we propose and evaluate a maintenance protocol called passive maintenance, which generates few control messages while maintaining cluster integrity. Because our solution is assessed by means of simulation, it is important to set a representative framework for evaluation. For this reason, the contribution starts with a discussion of modeling network topology. Different models that are used for representing forest-fire fighting are compared, considering simplicity and the ability of the model to represent what is being modeled.

1. Introduction

When a disaster strikes, the existing telecommunication infrastructure – if present – is either destroyed or saturated. Dedicated solutions, called emergency telecommunication systems, are deployed to (a) enable communication among teams on the field, and (b) make it possible for the outposts to report back to the headquarters and to receive orders. Currently, these solutions take the form of professional mobile radio (PMR) systems, such as analog HF/UHF/VHF radios and digital APCO25/TETRA/TETRAPOL systems. Satellite phones and transportable communication hubs are also used to provide wired/wireless Internet access and telephony backhauling over geostationary satellite links.

As far as civil-protection forces are concerned in France, there is currently no proposed network solution supporting broadband integrated services, and that includes field responders. The reasons are many; one facet is the necessity to find a technology providing the right mixture of flexibility and reliability at an affordable cost. Enabling service provision in the field is one of the most-challenging issues. In that respect, mobile ad hoc networks are among the candidate technologies, and they are the motive for this contribution. However, such networks are exposed to the impairments typical of mobile wireless communications, yielding unreliable radio links. One outcome of radio unreliability is the chance of experiencing partition in the field network, where graph connectivity is lost, and the topology is split into two or more isolated islands of nodes.

We make the assumption that network partitioning is a reality that should be tackled. For that purpose, we also assume that nodes in the network have a satellite terminal. In the event of network partitioning, one of these terminals is activated, and the corresponding node serves as a gateway for connecting the other nodes in the partition with the rest of the network. While detecting a partitioning event is out of the scope of this paper, electing the node to serve as a gateway is based on a clustering protocols published in the literature. Clustering algorithms and protocols were initially designed to cope with scalability issues in mobile ad hoc networks. Such algorithms and protocols consist of electing a *clusterhead*, and affiliating the other nodes to this clusterhead, thereby forming a cluster. For this purpose, we rely on the KCMBC (K-hop Compound Metric Based Clustering) protocol [1], as justified later. However, cluster formation is only one side of the problem, and cluster maintenance also has to be dealt with. Cluster maintenance is needed because of network dynamics, where nodes join or leave the partition, potentially making the current cluster structure obsolete. The first contribution of this paper is to propose a maintenance mechanism that is compatible with KCMBC and keeps cluster consistency, while dedicating a low amount of signaling traffic.

Monia Hamdi and Laurent Franck are with the Microwaves Department, Télécom Bretagne-Institut Mines Télécom; e-mail: Laurent.Franck@telecom-bretagne.eu. Xavier Lagrange is with the Network, Security, and Multimedia Department, Télécom Bretagne-Institut Mines Télécom.

This invited paper is part of the special section on the "Role of Radio Science in Disaster Management."

However, before proceeding with the evaluation of clustering and cluster maintenance, the context of the study has to be clearly defined. This step is mandatory, because it is likely that the performance of the protocols will be tightly dependent on the network topology. We assume here a network composed of firemen and trucks deployed in the framework of forest-fire fighting. This network provides services such as location and sensor-data collection (e.g., for detecting the presence of volatile organic compounds), geographical information distribution, and, more generally, Internet access. The second contribution of this paper is therefore to compare three approaches to modeling such a network topology, and to work out whether tradeoffs can be achieved between the expressiveness of such models and their simplicity.

Section 2 addresses topology modeling, describing the different categories of generic and dedicated models. The section ends with a discussion of topology models for emergency situations. Section 3 presents generic and dedicated topology models for forest-fire fighting. These models are then compared, based on metrics capturing properties such as network-node density and the dynamics of network partitioning. In Section 4, the use of the KCMBC algorithm is evaluated in the context of a partitioned network. Finally, Section 5 presents the challenges of cluster maintenance. A new maintenance protocol is discussed that shows good maintenance properties at a low signaling cost.

2. Topology Models

Topology modeling consists of representing a network's layout and dynamics by means of mathematical laws. These laws depict properties such as the location and motion of the nodes, and whether nodes switch on/off during the lifetime of the network. Topology models range on a continuum from generic models, where node motion is mostly driven by random laws, to dedicated models, which are derived from the observation and representation of field activity. A generic model is supposed to apply to a wide span of activities, while a dedicated model is expected to be more focused and accurate, yet more complex.

2.1 Generic Models

Generic models are further subdivided into random, space-correlated, and time-correlated models.

In random models, each node randomly and individually chooses its destination and motion speed. Popular random models are the *random walk* [2] and the *random waypoint* [3]. Random walk is a step-by-step motion, while random waypoint is a sequence of trajectories split by random stops and turns. In 2006, Kurkowski [4] screened all contributions presented during the MobiHoc conferences from 2000 to 2005. It appeared that 64% of the contributions requiring a topology model for evaluation purposes were based on the random-waypoint model.

Space-correlated models are random models where the motion of some nodes is spatially correlated. These models target group mobility, where clusters of nodes tend to move in the same direction, seeking a common objective. *Reference point group mobility* (RPGM) [5] and *Reference region group mobility* (RRGM) [6] are two examples of such models.

Finally, with time-correlated models, the laws governing the motion of a node display a correlation over time. Assuming a node has a limited fuel capacity, the range a node can move at time t depends on earlier stages. *Gauss-Markov mobility* [7] is an example where the speed of a node is correlated over time according to a Gauss-Markov stochastic process.

2.2 Dedicated Models

Dedicated models mitigate the impact of randomness by introducing constraints on the node mobility, so as to mimic conditions present in the environment, or the activity to which a model relates.

Models with a geographic restriction fall in this category. Some models use maps to define the paths that nodes may follow [8]. This approach is suited for urban modeling, where a network of roads constraints the directions nodes may go. Other models are based on a playground where obstacles are laid out, calling for avoidance maneuvers from these nodes [9].

Trace-based models are derived from actual field situations where the motion patterns of the nodes were recorded and then played back for simulation purposes [10]. The following paragraph focuses on models targeting emergency situations.

2.2.1 Topology Models for Emergency Situations

In [11], the authors described a disaster scenario where the area is split into three rescue zones. Nodes representing responders moved within their zone according to a random pattern at low speed (1 m/s). Two vehicles commuted on a line between zones at higher speed (5 m/s), and provided inter-zone communication capabilities. A similar model was used in [12], where the number of zones and vehicles was increased. [13] relied on a random-waypoint mobility to model the motion of emergency vehicles in an urban environment. The random waypoint was constrained according to the mesh pattern displayed by the street network.

[14] proposed a topology model targeting emergency medical care. Victims were transported from the field to a field hospital, and then evacuated to fixed hospitals. The model was highly specific, and relied on a tactical map describing the positions of various zones (field, transit point,

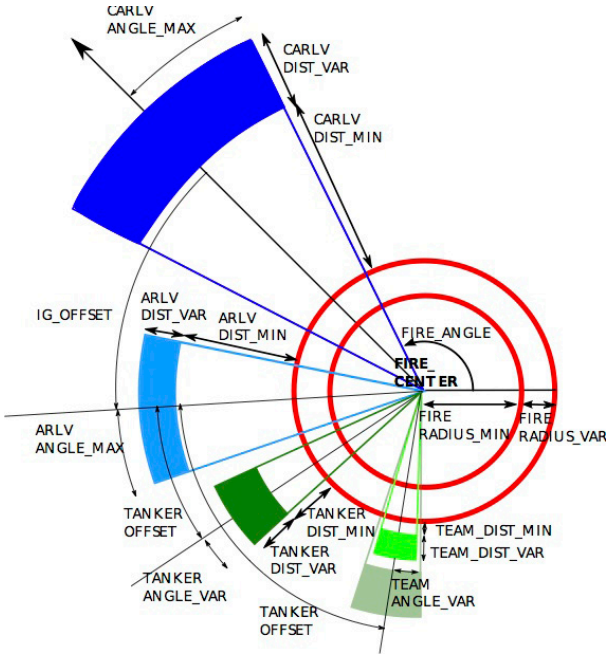

Figure 1. The layout of a single intervention group and a column command car around a fire. IG = intervention group; ARLV = IG command car; CARLV = Column command car [17].

field hospital). The map dictated the rules of node motion (rescuers commuted among the different zones). The same team developed a model [15] based on real-world traces for describing the mobility of ambulances as they were dispatched to the scene of an incident.

In [16], a complex event-based mechanism modeled the mobility of first responders (police and emergency medical care) at the scene of a disaster. The model defined events such as "a victim calls for assistance" or "a car is on fire." These events could either "attract" first responders passing by, or generate an avoidance/protective trajectory. The rationale of such an agent-based approach was that given a set of basic and individual rules (e.g., "go for care," "avoid fire,"...), it was expected that the patterns of motion observed at the global level would be consistent and realistic.

3. Topology Modeling and Network Properties

Different topology models yield different patterns of motion. In this section, the impact of the topology model on the network properties is investigated. The scenario for this study is a forest fire, where firefighters are equipped with communication devices and form a mobile ad hoc network (MANET). Three topology models are considered: *random walk*, *reference region group model* (RRGM), and *fire mobility*, in increasing order of faithfulness with respect to the field activity.

The next paragraphs provide a description of these models, and then proceed with the comparison. The description starts with the fire-mobility model, since the parameters of the model will later be used to parameterize the random walk and RRGM so as to ensure a fair comparison among the three models.

3.1 Fire Mobility

The fire-mobility model was designed in our lab from interviews with French Civil Protection personnel and national operation guides. It models the layout and motion of one or more *firefighter columns*. The model was fully described in [17]. The fire is modeled as a disk with a random trajectory. A column is made of one command car plus four groups, each composed of one command car, four tankers, and four firefighter pairs, yielding a total of 37 nodes. The groups are dispatched so that one is in front of the fire and the two others are flanking it. As the fire moves, each entity checks its position against safety distances and operational rules, and redeploys if necessary. Relocating a single tanker can trigger the redeployment of

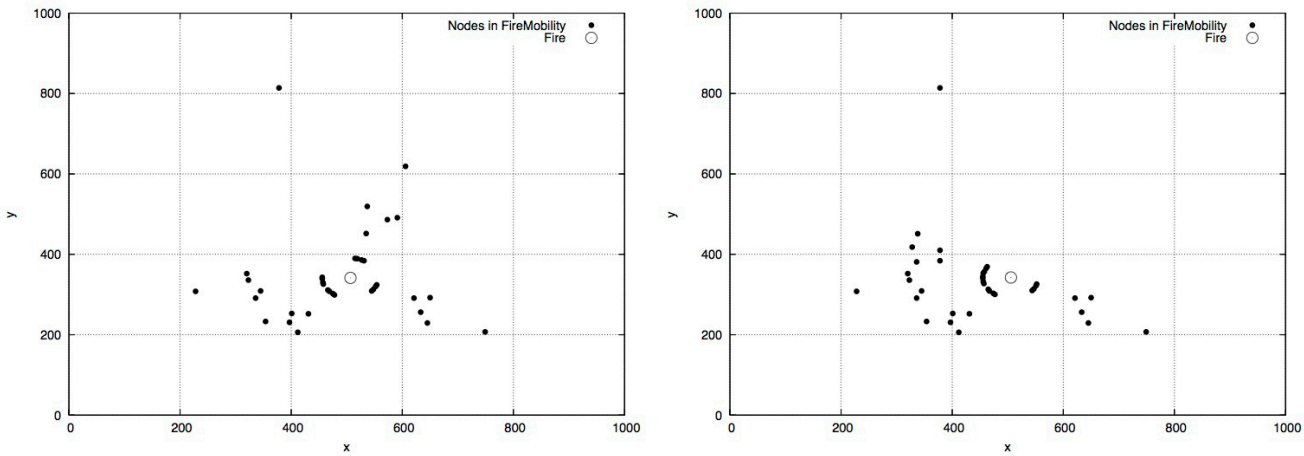

Figure 2. Snapshots of the fire-mobility topology. The fire is represented by a circle. In (a), the three groups are separated, while in (b), the two groups on the left overlap.

Parameter	Value
Playground size	1000 × 1000 m
Fire radius	50 m
Number of nodes	37
Number of intervention groups	4
Step duration of fire motion	1 s
Fire speed	0.3 m/s
Average node speed	4.4m/s
Column command car distance from the fire	$U[400,600]$ m
Group command car distance from the fire	$U[150,300]$ m
Tanker distance from the fire	$U[100,200]$ m

Table 1. The parameters of the fire-mobility model.

the whole group so as to guarantee consistence within the group. Figure 1 shows the parameters driving how group entities and the column car are dispatched around a fire. Table 1 lists all parameters used to configure the model, and Figure 2 shows two snapshots of the network layout.

3.2 Reference Region Group Mobility

The reference region group mobility model [6] implemented in this contribution aims to model the group behavior of firefighters. However, the model is not as accurate as the fire-mobility model, since it does not take into account the actual organization in terms of command cars, tankers, etc. It also does not include any consideration about the distances among team members. The fire is defined by a disk, the motion of which follows a random trajectory. The intervention area is a disk of larger diameter, centered on the fire. At the initialization of the model, nodes cluster with each other, forming at most five groups. Each cluster leader picks up a random destination within the intervention area, and the cluster proceeds to that destination at random

Parameter	Value
Playground size	1000 × 1000 m
Fire radius	50 m
Intervention area radius	300 m
Number of nodes	37
Step duration of node and fire motion	1 s
Fire speed	0.3 m/s
Average node speed	4.4 m/s

Table 2. The parameters of the reference-region group mobility model.

speed. The journey to the destination is made up of a sequence of intermediate reference regions. A cluster may proceed to the next reference region when all nodes belonging to the cluster have reached the current reference region. If the destination of the group is outside the intervention area because of the fire's motion, a new destination is picked up. The parameters are listed in Table 2, and Figure 3 shows two snapshots of the reference-region group's topology.

3.3 Random Walk

The random-walk model is a step-by-step-motion model where all nodes are randomly dispatched on a rectangular playground. At the start of each step, all nodes individually choose a direction and speed of motion. Compared to the other models, random walk does not implement the group behavior of the firefighters. The parameters of the model are provided in Table 3. Figure 4 shows two snapshots of the topology.

3.4 Comparing the Three Models

The three models were first compared on the basis of the network properties that resulted from the topology layout. The models were compared pairwise: random walk with fire mobility, and fire mobility with RRGM. For each

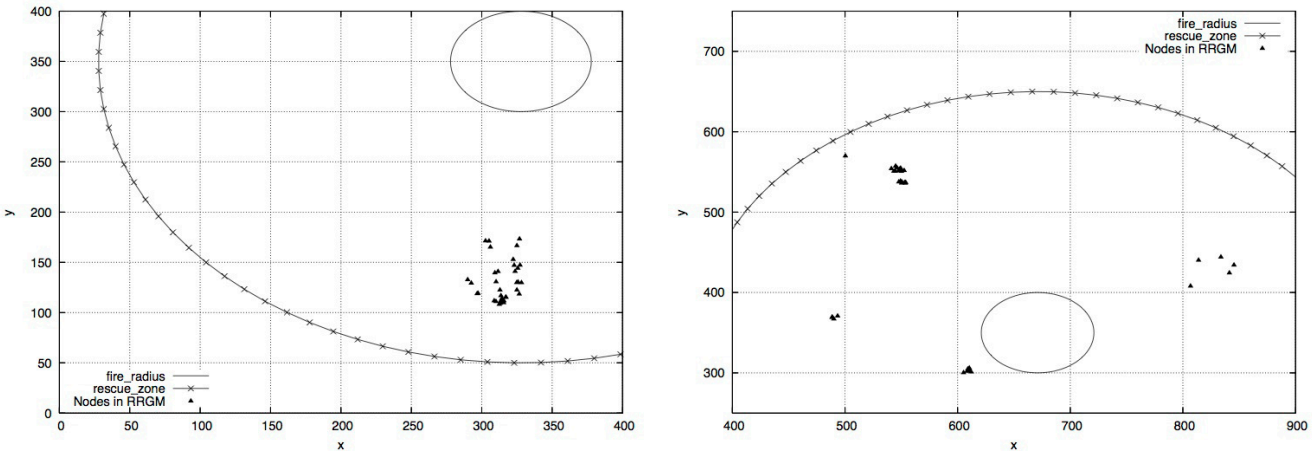

Figure 3. Snapshots (close-up) of the RRGM topology for (a) $t = 0$ s and (b) $t = 9000$ s. On these close-ups, the inner circles represent the fire, and the outer circles are the intervention area.

Parameter	Value
Playground size	370 × 370 m
Number of nodes	37
Step duration	1 s
Average node speed	4.4 m/s

Table 3. The parameters of the random-walk model.

case, the radio range of the nodes was varied from 70 m to 100 m (this corresponded to a typical wireless-LAN range). Each simulation set lasted for 10000 s, and was repeated 10 times with a different random seed. The results were averaged.

The focus was initially put on network partitioning. Network partitioning occurs as a consequence of the nodes' motions and the radio-frequency link budget: the network is split in two or more clusters that are unconnected. In a forest-fire-fighting scenario, this may translate into a group leader being unable to report to the column leader, or to call for support.

Figure 5 shows the duration (as a percentage of the total simulation time) the network suffered from partitioning. The random-walk and fire-mobility models displayed similar trends, with a decreasing duration of partitioning as the radio-frequency range increased. On the other hand, the RRGM model showed a higher and steady partitioning duration. This was due to the dynamics of RRGM, and the uncorrelated motion of the different groups. When the various groups were isolated from each other, they rarely managed to get back within radio range, whatever the radio range. This situation is illustrated in Figure 3b. As far as the RRGM model was concerned, it lacked correlation among groups, in addition to the existing correlation among group members.

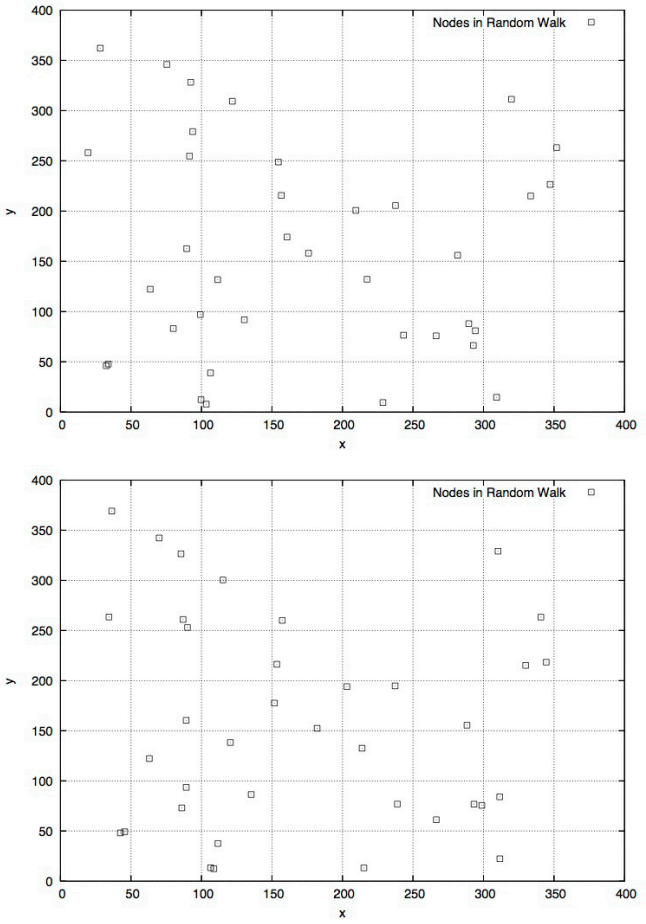

Figure 4. Snapshots of the random walk topologies.

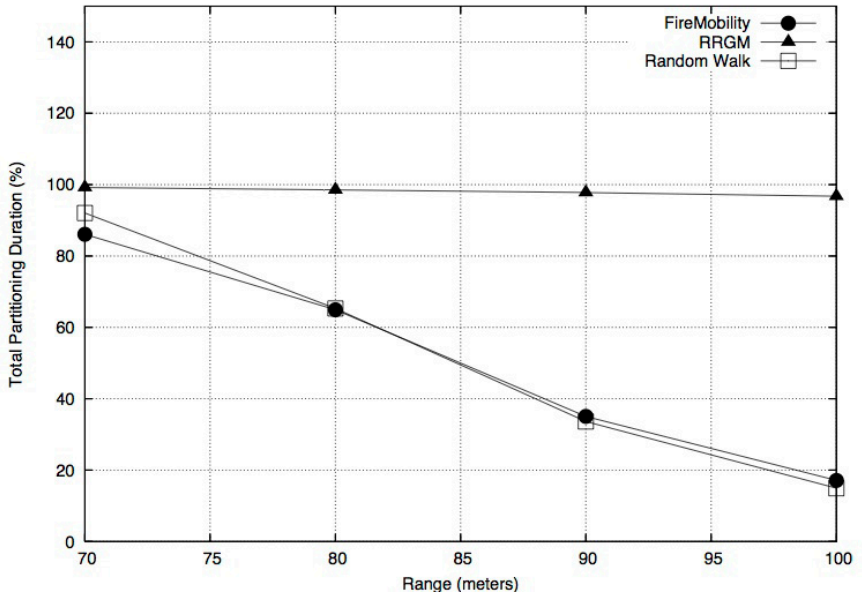

Figure 5. The duration (as a percentage of the simulation duration) the network was partitioned as a function of the radio-frequency (RF) range for the random-walk, RRGM, and fire-mobility models.

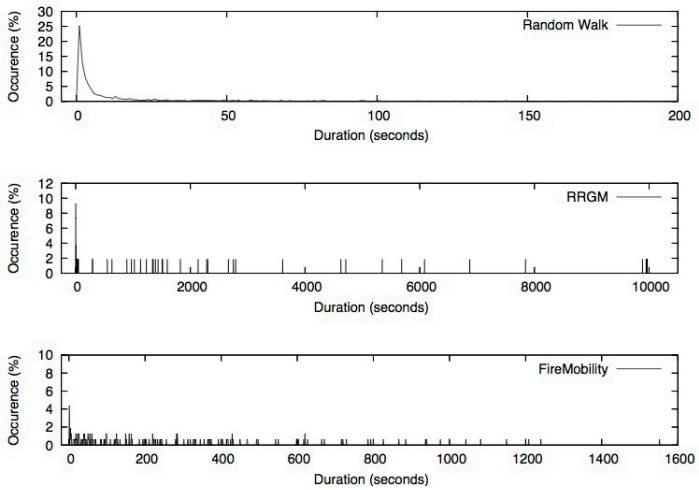

Figure 6. The distribution of the duration of partitioning events for the random-walk (top), RRGM (middle), and fire-mobility (bottom) models. The radio-frequency range was fixed at 70 m.

For a radio-frequency range of 70 m, one might consider that the three models behaved similarly, and this also held true for the random-walk and fire-mobility models at longer RF ranges. However, when looking closely at the duration distribution of partitioning events (Figure 6), the three models displayed different trends. For the random-walk model, partitioning – although frequent – did not last more than 10 s. Indeed, with random walk, a node may change its direction of motion at every move. Partitioning events in these circumstances are likely to be short lived. The fire-mobility and RRGM models displayed less short-lived partitioning events, and longer events happened: up to 1600 s (fire mobility) or the whole simulation duration, 10000 s (RRGM). These observations were a direct consequence of the basic properties of the network, such as the number of neighbors a node may have (node degree, Figure 7) and the link lifetime (Figure 8). Both characteristics were evaluated for a radio range of 70 m.

Nodes in random walk often had neighbors, which was an advantage in mitigating partitioning. On the other hand, the links among neighbors were often going up and down. For the RRGM and fire-mobility models, the links tended to be more stable (e.g., in RRGM, 6% of the links that were established lasted for the whole simulation). However, the node degree displayed a larger standard deviation, which was an indicator of the clustered layout of the nodes. This clustering caused long-term partitions, especially at low radio-frequency ranges. Comparing the RRGM and fire-mobility models, the former suffered from a more significant clustering effect, which was the cause of such a large span in the duration of partitioning events.

To summarize this first part, the random-walk or RRGM models are easy to implement, but they do not accurately represent the network topologies deployed during forest-fire fighting. This was striking for the RRGM model, where the parameters were selected to approach those of fire mobility. The reason for this failure was found when looking at core properties, such as node degree and link lifetime. While we do not claim that the fire-mobility model faithfully reflects the operations on the field (the impact of terrain topology on the fire and the deployment of the units are not taken into account), the fire-mobility model is the best approach so far. It shows how the other models fell short of capturing important characteristics of the network

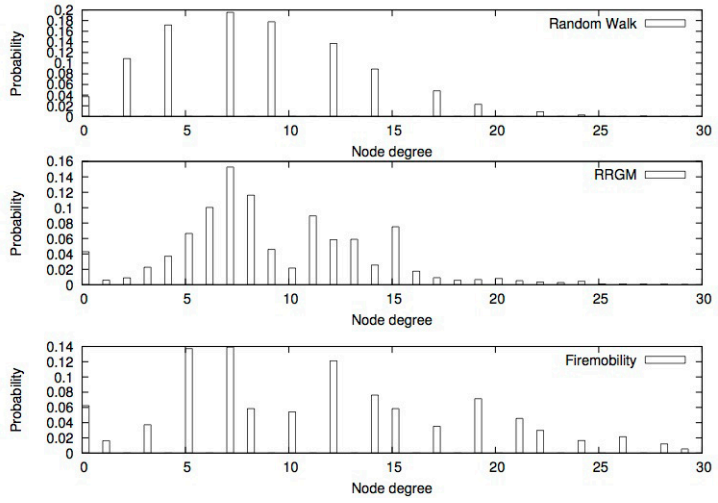

Figure 7. The distribution of the node degree (number of neighbors) for the random walk (top, $\bar{X} = 3.61$, $\sigma = 1.99$), RRGM (middle, $\bar{X} = 9.16$, $\sigma = 4.87$), and fire-mobility (bottom, $\bar{X} = 6.61$ $\sigma = 4.01$) models. The radio-frequency range was fixed at 70 m.

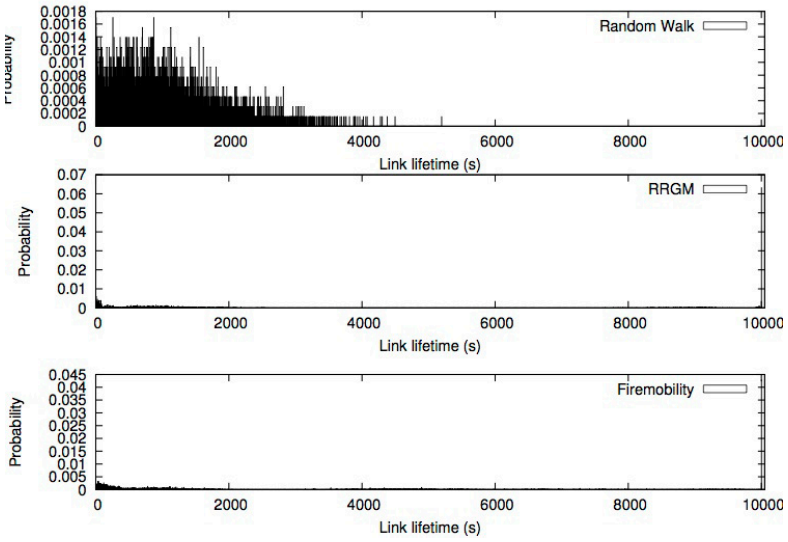

Figure 8. The distribution of the link lifetime for the random-walk (top), RRGM (middle), and fire-mobility (bottom) models. The radio-frequency range was fixed at 70 m.

dynamics. Finally, it might be possible to modify a model, such as the RRGM model, so as to approach the ability to represent the situation of the fire-mobility model. However, the effort required in this direction would be similar to the design of a dedicated model.

The next section addresses the use of clustering algorithms in a partitioned network.

4. Clustering Algorithms for Mitigating Partitioning

The use of clustering techniques was originally proposed to solve scalability issues in large MANETs [18]. The network is divided into virtual groups of mobile nodes, called clusters. A clusterhead is elected among mobile hosts to be the local coordinator. In *k*-hop clustering, each node is at most *k*-hops distant from its clusterhead.

We propose to extend the application of clustering to partitioned networks, where a clustering algorithm is used within a partition to elect the node providing interconnection with the rest of the network. In the context of forest-fire fighting, trucks and command cars are equipped with mobile satellite terminals, similar to maritime or aeronautical equipment, providing several hundreds of kbps. In this work, it was assumed that all vehicles were equipped. While this is unrealistic, constraining the choice to a subset of vehicles can be considered later since, as shown below, the selection of candidate gateways in the solution we have adopted depends on a metric that can be tailored.

We start by describing clustering algorithms, and then explain the choice of the most-suitable clustering algorithm for our scenario. MaxMin [19] was the pioneering algorithm in this field. Cluster formation is composed of two phases (FloodMax and FloodMin), and each phase comprises *k* rounds of message exchanges. MaxMin inspired several later works. The KCMBC algorithm [1], based on MaxMin, introduced an expiration-time metric, to take into account the impact of node mobility and to possibly rule out nodes that are not eligible. It is also interesting to note that the election mechanism of KCMBC could be extended to other metrics, such as satellite-link quality or energy considerations.

Unlike MaxMin, k-lowestID and k-CONID [20] rely on flooding clustering requests and decisions. Huang [21] improved these algorithms by introducing clusterhead backup mechanisms, and a weight factor based on link quality. However, like its ancestors, this leads to broadcast storms. In DSCAM [22], the cluster-based network structure forms an (r,k)-dominating set, where r is the minimum number of clusterheads per node, and k is the maximum number of hops between a node and its clusterhead. The construction of an initial dominating set is solely based on node identifiers.

As already stated, the node properties impact the suitability of a node to serve as a satellite access point. Therefore, the approaches where clusterhead selection is not based on these node properties are excluded. In addition to that, [1] proved that MinMax-based approaches outperform k-LowestID-based approaches with respect to cluster-formation overhead. As a result of the previous analysis, the KCMBC algorithm was selected for this study.

The performance of the KCMBC algorithm has been already simulated and validated in a mobile environment [1]. However, prior works assumed dense networks, where each node can communicate over multi-hop paths with any other node of the network. This is the first time a clustering algorithm has been evaluated in a scarce-density network where partitioning may occur. These partitions are dynamic: nodes can leave a partition to join another one. Our aim is to analyze the KCMBC behavior in this context, and to re-use the mechanism of clustering to identify suitable satellite gateways.

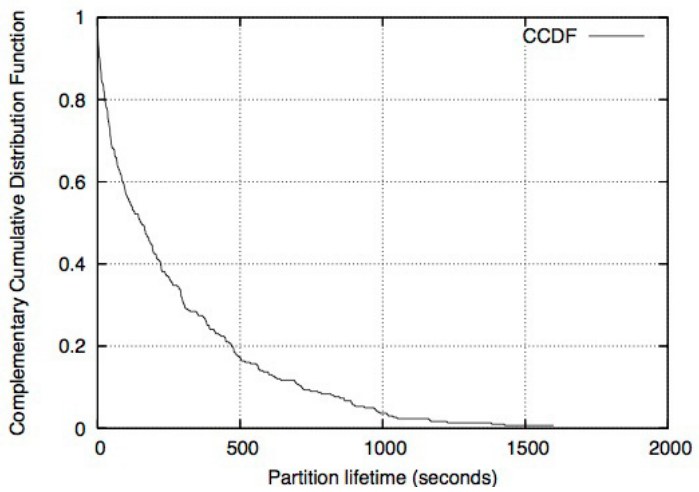

Figure 9. The complementary cumulative distribution function (CCDF) of the partition lifetime for a radio range of 70 m.

4.1 KCMBC Overview

The KCMBC algorithm comprises three main steps. The first step is node-metric computation, using the degree and the so-called expiration time. The purpose of this metric is to assess whether a node will be able to maintain durable connections with its neighbors, and therefore be an eligible clusterhead. The second step is the clusterhead election, based on the FloodMax and FloodMin protocols. The third step is the cluster maintenance, where the cluster structure is updated according to nodes joining and leaving the cluster.

During the second step (clusterhead election), each node broadcasts its metric value to the *k*-hop neighbors and, upon reception of other nodes' metrics, proceeds with the election of a candidate clusterhead. This decision is then broadcast back to the *k*-hop neighbors. Consolidation mechanisms are then used to make sure that there is a consensus among nodes as to which node serves as clusterhead.

4.2 KCMBC Evaluation

The simulation scenario relies on the fire-mobility model described before, with the parameters listed in Table 1. All nodes were equipped with WLAN devices, displaying a communication range from 70 m to 100 m. Each simulation was conducted for 10 000 s, and then repeated 10 times with a different pseudorandom seed. The results were averaged.

We ran the KCMBC clustering algorithm against the network topology every time a network partition was detected. However, before proceeding with the actual evaluation of KCMBC, it was necessary to measure the characteristics of partitioning so as to tune the functioning of KCMBC. Furthermore, running the clusterhead election should not have been an issue (the network was considered to be stable during this phase, which lasted for about a second). However, there were questions about the further maintenance of the cluster's integrity. Indeed, it could happen that a clusterhead became isolated, or that other nodes joined or left the cluster, significantly impacting its topology. The study of the topology dynamics of a formed cluster and its impact on the maintenance are covered later in this contribution.

A first task was to assess the necessity of using satellites for the recovery of network connectivity by examining the partitioning-lifetime distribution with a communication radio range equal to 70 m, which represented the worst case. Figure 9 revealed that over 60% of partitioning events

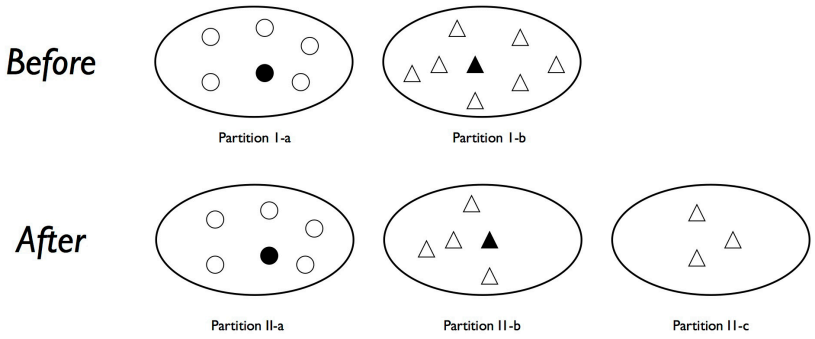

Figure 10. Splitting: partition 1-b was split into two subsequent partitions.

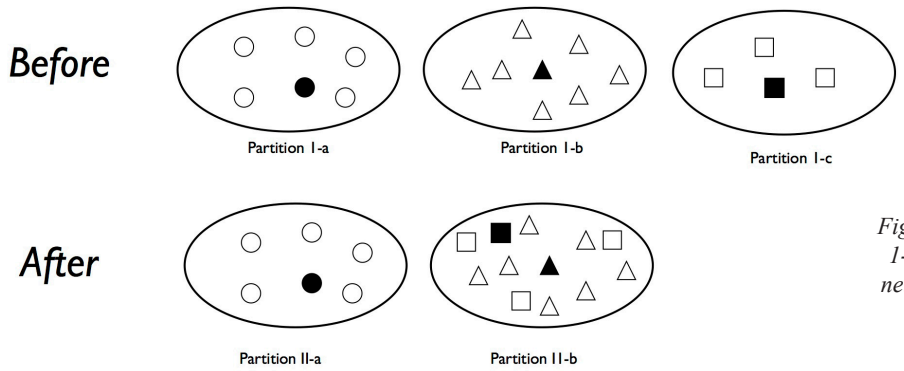

Figure 11.Merging: partitions 1-b and 1-c merged, but the network was still partitioned.

had a lifetime greater than 100 s, and 19% of the network partitioning events lasted longer than 500 s. Recovering partitioning was therefore a necessity. As pointed out in [23], tactical networks usually deploy a single gateway in each part of the network. It was therefore assumed that one cluster should be defined per partition. In order to meet this requirement, the parameter k in KCMBC, corresponding to the maximum number of hops between a cluster member and its clusterhead, should be properly tuned. This parameter is bounded by the diameter of the network partitions. According to our simulation results, k had to be set to a value of 12.

The next section covers the protocols that can be used to maintain cluster consistency, especially considering that the nodes are mobile, and may leave or join clusters.

5. Cluster Maintenance

This part describes the topology changes in a partitioned network, evaluates how KCMBC responds to these events, and proposes guidelines for implementing cluster maintenance. Three cases represent the possible evolution of a network partition: splitting, merging, and node migration. For each case, the topology evolution is illustrated, the KCMBC behavior is analyzed, and simulation results based on the fire-mobility model are presented.

5.1 Splitting and Merging

Splitting occurs when two groups of nodes, initially located in the same partition, move away from each other and form two different partitions (Figure 10). The nodes, located in a partition where there is no clusterhead, trigger reclustering. In this context, reclustering consists of a new clusterhead election from this subset of so-called orphaned nodes. According to the KCMBC design, if an orphan node detects more than d orphan neighbors, all those orphans attempt to trigger a new cluster formation. This rule guarantees that there is at least one clusterhead per partition. However, the authors who proposed KCMBC did not provide the details of how to detect the loss of a clusterhead.

Partitions may also move towards each others to form a single partition (merging). After merging, full network connectivity may be recovered. In this case (the use of satellite communications), clustering is not required. The network may also remain partitioned (Figure 11). In KCMBC, two clusterheads upon partition merge keep their status, unless they become close neighbors. This is contradictory to a functional requirement in this work, which is to have only one clusterhead per partition. In order to manage partition merging, a clusterhead should therefore be able to detect the presence of other clusterheads in the same partition, and possibly resign.

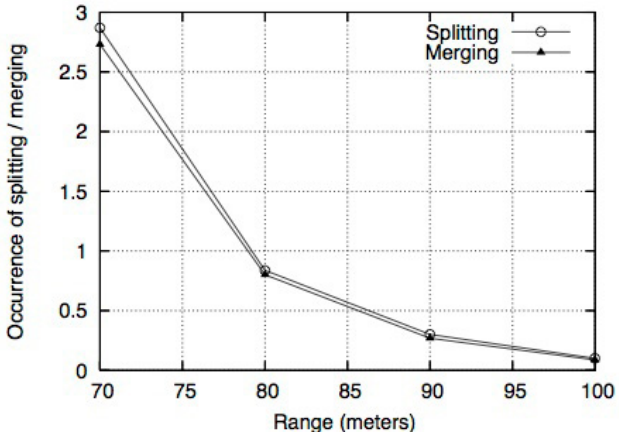

Figure 12. The average number of splitting and merging events during the lifetime of a partition event as a function of the radio range.

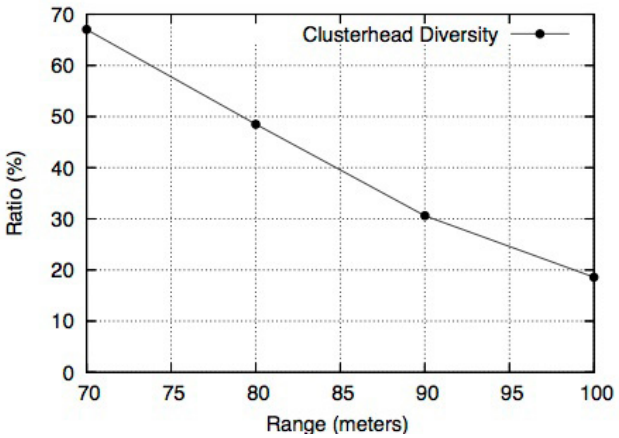

Figure 13. The occurrence of clusterhead diversity (i.e., more than one clusterhead per cluster) as a function of the radio range during a partitioning event.

Figure 12 shows that splitting and merging occurrences are approximately similar. During a partitioning event, there is a continuous oscillation between splitting and merging. It can also be noted that the lower the radio range, the more dynamic the topology. For a radio range lower than 80 m, partition merging and splitting occurred at least once every partitioning event. As a result, each clusterhead should detect the presence of other clusterheads in its partition, each cluster member should detect the loss of its clusterhead, and orphan nodes should trigger reclustering.

Because of partition merging, several clusterheads may be located in the same partition. As already stated, KCMBC does not support in its standard design the detection of multiple clusterheads in a single partition. This may be an important drawback, depending on how often it happens in our scenario. Figure 13 shows that during a partitioning event, several clusterheads were observed in the same partition for at least 20% of the time. As a result, the standard maintenance procedure in KCMBC does not totally meet the needs of our scenario.

5.2 Node Migration

Because of the mobility, a node may move to a different partition. This node may be a cluster member that joins an already-formed cluster (Figure 14a). In KCMBC, if a node loses the path to its clusterhead and detects a new neighbor (i.e., because of new link), it joins the cluster to which the neighbor belongs. This rule implies that nodes communicate the clusterhead identifier to their neighbors. The migrating node may also be a clusterhead (Figure 14b). If a clusterhead has no more affiliated neighbors, it joins another cluster. Otherwise, it keeps its clusterhead status. The latter case is similar to merging, resulting in a partitioned network. A clusterhead should therefore be able to detect the presence of other clusterheads in its partition.

From a maintenance standpoint, clusterhead migration is similar to partition merging. Contrarily, cluster-member migration is different, and its relevance in the scenario has to be assessed. It is defined as the number of cluster members leaving their partitions during a partitioning event. Figure 15 shows that cluster migration happened on average twice during a partitioning event for a radio range of 80 m. Consequently, the maintenance procedure should make it possible for nodes leaving their partition to detect clusterheads in their new partitions.

In KCMBC, each node includes the identifier of its clusterhead in neighborhood-sensing messages, called "Hello" messages, that are sent (one per second, in this work). However, to be able to make relevant decisions, the information sent by a node to its neighbors should also be updated. For instance, if a node leaves its cluster and joins another cluster, the information sent in earlier "Hello" messages is no longer relevant. Moreover, if a node loses its clusterhead status, its affiliated members have to be informed. The KCMBC authors supposed that each node had the required information to make relevant decisions, without specifying the underlying signaling mechanism.

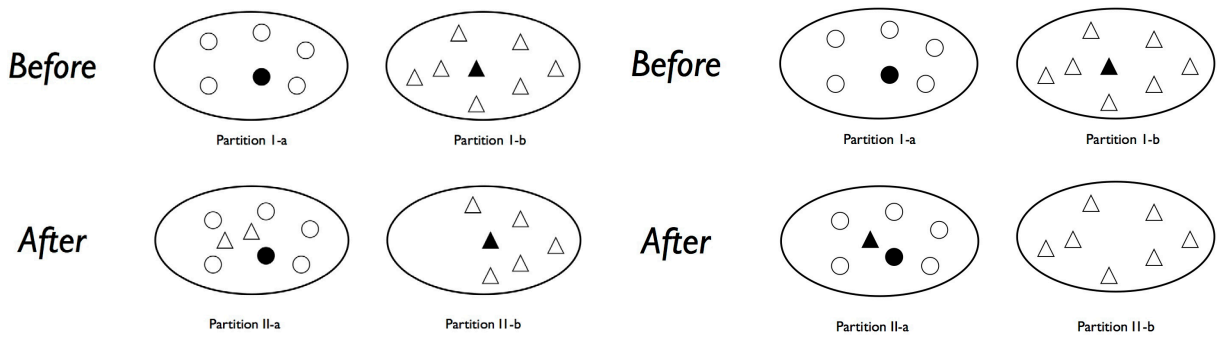

Figure 14. Node migration: (a) cluster member migration, (b) clusterhead migration.

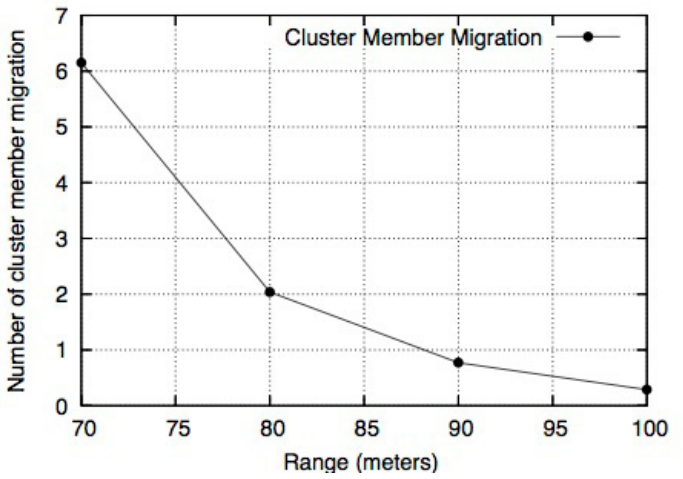

Figure 15. The average number of cluster member migrations during a partitioning event as a function of the radio range.

In conclusion, the maintenance procedure in KCMBC does not meet all the needs of the scenario using the fire-mobility model. For partition splitting or clusterhead migration, KCMBC does not detail how a node detects the loss of its clusterhead. Furthermore, in the case of partition merging, clusterheads keep their status, which transgresses the functional requirement of one clusterhead per partition. This study allows highlighting additional cluster maintenance requirements: (a) each clusterhead should detect the presence of other clusterheads in the partition, (b) each cluster member should detect the loss of its clusterhead, and (c) the presence of neighboring clusterheads and (d) orphan nodes should trigger reclustering.

5.3 An Updated Maintenance Procedure

In [24], we provided a review of existing maintenance protocols for clustering algorithms. Among them, the work from Bellavista and Magistretti [25] was interesting, as it coped with *k*-hop clustering, and sought to minimize the signaling traffic required for maintenance. This method will be designated as *Periodical Broadcast*, as it is based on a periodical broadcast (every *Refresh_Period*) of state information within the cluster.

In [24], we also proposed a new maintenance procedure, called *passive maintenance*, which was based on a combination of two mechanisms: (a) the piggybacking of time-stamped clusterhead identities in existing *Hello* messages that are sent by every node in KCMBC every *Hello_Period*, and (b) the transmission of dedicated messages (called *CH_REQ* and *CH_REPLY*, for resolving ambiguities resulting from a clusterhead leaving a cluster and duplicate clusterheads being in the same cluster. Upon clusterhead disconnection and cluster connection, several nodes may quasi-simultaneously send CH_REQs. To avoid traffic peaks, a node is allowed to send or relay only one CH_REQ during a period of *Hello_Period* seconds. In the same manner, a clusterhead is allowed to send only one CH_REPLY during a period of *Hello_Period* seconds. Similarly, simultaneous CH_REQs may yield packet collision. To tackle this problem, a node, *u*, waits for a

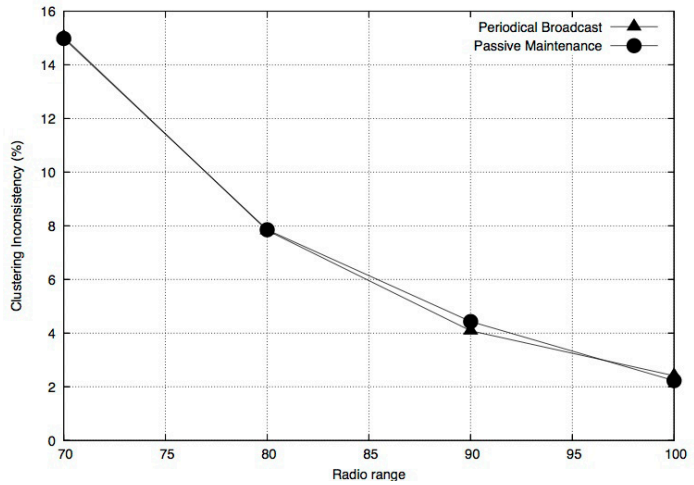

Figure 16. The clustering inconsistency as a function of the radio range.

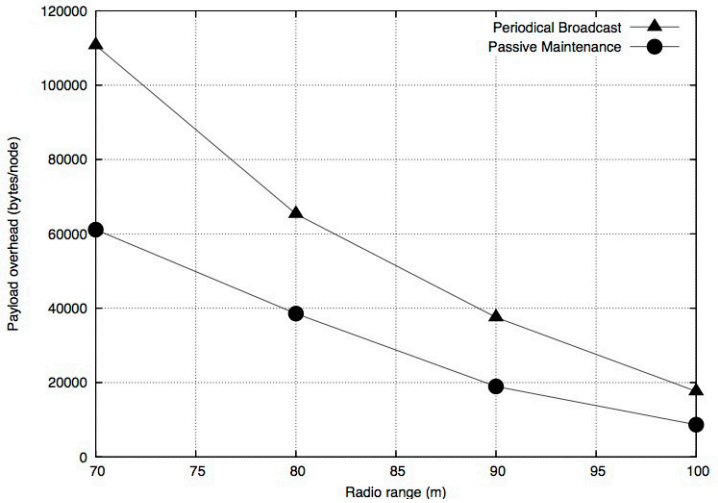

Figure 17. The cost for passive and periodic maintenance as a function of the radio range. The cost was expressed in the number of bytes sent per node for the complete simulation duration (10000 s).

back-off interval ($T_{backoff}$) before sending a CH_REQ. In this work, $T_{backoff} = ID_u / N$, where ID_u is the identifier of the node u, and N is the network's size.

5.3.1 Comparing Periodic and Passive Maintenance

The comparison was based on two aspects: the quality of maintenance, and the cost of maintenance. The quality was expressed in terms of cluster inconsistency, which measured how often the rules driving cluster structure were breached for the duration of partitioning. The higher the inconsistency, the poorer the quality of maintenance. The cost of maintenance accounted for the number of bytes that were sent in the network for maintenance purposes. For the sake of fair evaluation, both maintenance solutions were parametrized, so as to offer similar cluster inconsistencies (as shown in Figure 16), and the evaluation covered maintenance cost.

Figure 17 compares the cost of maintenance in bytes sent per node for the duration of the simulation. The byte accounting included all messages sent for the purpose of maintenance, and also the extra information added to *Hello* messages in the case of passive maintenance. It showed that for an equal quality of maintenance, passive maintenance generated about 50% less signaling traffic than broadcast maintenance.

A similar trend as shown in [24] was observed when the number of signaling messages was considered, rather than the actual payload size. The better performance of passive maintenance – whatever the dynamics of partitioning – was due to its reactive nature, which made it possible to avoid useless transmission of maintenance messages when the cluster structure was stable.

6. Conclusion

This paper covered two contributions. The first was about topology modeling, and showed how dedicated topology models are by no means a luxury. Indeed, generic models, such as the random-walk model or the reference-region group-mobility model, failed to capture the specifics of the application (here, forest-fire fighting), resulting in strongly biased modeling. The second contribution was about the use of clustering algorithms and protocols in order to identify nodes that can provide interconnection facilities when the network is partitioned. More precisely, we proposed and evaluated a maintenance protocol that tracked changes in the network topology and ensured that the cluster structure – as determined by the published KCMBC protocol – remained consistent. This maintenance protocol was also shown to be efficient in terms of signaling traffic, when compared to other solutions.

As far as the prospects of this work are concerned, two directions exist. The first one calls for revisiting the network architecture and to consider (rather than an ad hoc network) a wireless-mesh network, where a subset of nodes (the backbone nodes of the wireless-mesh network) would be eligible for hosting satellite gateways. This direction is motivated by the complexity that stems from the use of KCMBC and the maintenance process. In this perspective, we are currently investigating gateway-placement strategies based on genetic algorithms. The second direction is the extension of KCMBC in order to (a) restrict the nodes that are eligible for the clusterhead role, and to (b) integrate metrics reflecting the constraints of satellite communications (such as link budget) during the computation and maintenance of the cluster. The complexity does not reside in the modification of KCMBC, which offers convenient support for different metrics, but rather in a choice of relevant metrics with regard to the performance obtained.

7. References

1. S. Leng, Y. Zhang, H-H. Chen, L. Zhang and K. Liu, "A Novel k-Hop Compound Metric Based Clustering Scheme for Ad Hoc Wireless Networks," *IEEE Transactions on Wireless Communications*, **8**, 1, January 2009, pp. 367-375.

2. R. A. Guerin, "Channel Occupancy Time Distribution in a Cellular Radio System," *IEEE Transactions on Vehicular Technology*, **36**, 3, August 1987, pp. 89-99.
3. J. Broch, D. A. Maltz, D. B. Johnson, Y-C. Hu and J. Jetcheva, "A Performance Comparison of Multi-hop Wireless Ad hoc Network Routing Protocols," 4th ACM/IEEE International Conference on Mobile Computing and Networking (MobiCom), 1998, pp. 85-97.

4. S. Kurkowski, T. Camp and W. Navidi, "Two Standards for Rigorous MANET Routing Protocol Evaluation," IEEE International Conference on Mobile Adhoc and Sensor Systems (MASS), 2006, pp. 256-266.

5. X. Hong, M. Gerla, G. Pei and C-C. Chiang, "A Group Mobility Model for Ad hoc Wireless Networks," 2nd ACM international Workshop on Modeling, Analysis and Simulation of Wireless and Mobile Systems (MSWiM), 1999, pp. 53-60.

6. J. M. Ng and Y. Zhang, "A Mobility Model with Group Partitioning for Wireless Ad hoc Networks," 3rd International Conference on Information Technology and Applications (ICITA), **2**, 2005, pp. 289-294.

7. B. Liang and Z. J. Haas, "Predictive Distance-based Mobility Management for PCS Networks," 18th Annual Joint Conference of the IEEE Computer and Communications Societies, **3**, 1999, pp. 1377-1384.

8. J. Tian, J. Hahner, C. Becker, I. Stepanov and K. Rothermel, "Graph-Based Mobility Model for Mobile Ad Hoc Network Simulation," 35th Annual Simulation Symposium, 2002, pp. 337-344.

9. A. Jardosh, E. M. Belding-Royer, K. C. Almeroth and S. Suri, "Towards Realistic Mobility Models for Mobile Ad hoc Networks," 9th Annual International Conference on Mobile Computing and Networking (MobiCom), 2003, pp. 217-229.

10. V. Vetriselvi and R. Parthasarathi, "Trace Based Mobility Model for Ad hoc Networks," 13th IEEE International Conference on Wireless and Mobile Computing, Networking and Communications (WiMOB), 2007, pp. 81.

11. P. Johansson, T. Larsson, N. Hedman, B. Mielczarek and M. Degermark, "Scenario-Based Performance Analysis of Routing Protocols for Mobile Ad hoc Networks," 5th Annual International Conference on Mobile Computing and Networking (MobiCom), 2009, pp. 195-206.

12. S. Kumar, R. K. Rathy and D. Pandey, "Design of an Ad Hoc Network Model for Disaster Recovery Scenario Using Various Routing Protocols," International Conference on Advances in Computing, Communication and Control (ICAC3), 2009, pp. 100-105.

13. K. Gyoda, N. Hoang Nguyen, K. Okada and O. Takizawa, "Analysis of Ad hoc Network Performance in Emergency Communication Models," 22nd International Conference on Advanced Information Networking and Applications Workshops (AINAW), 2008, pp. 1083-1088.

14. N. Aschenbruck, E. Gerhards-Padilla, M. Gerharz, M. Frank and P. Martini, "Modeling Mobility in Disaster Area Scenarios," 10th ACM Symposium on Modeling, Analysis, and Simulation of Wireless and Mobile Systems (MSWiM), 2007, pp. 4-12.

15. M. Schwamborn, N. Aschenbruck and P. Martini, "A Realistic Trace-based Mobility Model for First Responder Scenarios," 13th ACM International Conference on Modeling, Analysis, and Simulation of Wireless and Mobile Systems (MSWIM), 2010, pp. 266-274.

16. Y. Huang, W. He, K. Nahrstedt and W. C. Lee, "Corps: Event-Driven Mobility Model for First Responders in Incident Scene," IEEE Military Communications Conference (MILCOM), 2008, pp. 1-7.

17. C. Giraldo Rodriguez, *MANET Routing Assisted by Satellites*, PhD dissertation Télécom Bretagne-Institut Mines Télécom, 2011.

18. P. Krishna, N. H. Vaidya, M. Chatterjee and D. K. Pradhan, "A Cluster-Based Approach for Routing in Dynamic Networks," *ACM SIGCOMM Computer Communication Review*, **27**, 2, April 1997, pp. 49-64.

19. A. D. Amis, R. Prakash, T. H. P. Vuong and D. T. Huynh, "Max-Min d-Cluster Formation in Wireless Ad Hoc Networks," 19th Annual Joint Conference of the IEEE Computer and Communications Societies (INFOCOM), 2000, pp. 32-41.

20. G. Chen, F. G. Nocetti, J. S. Gonzalez and I. Stojmenovic, "Connectivity Based k-Hop Clustering in Wireless Networks," 35th Annual Hawaii International Conference on System Science (HICSS), 2002, pp. 2450-2459.

21. T-C. Huang, H-C. Ke and L.-C. Shiu, "A Double- Manager k-Hop Clustering Algorithm in Mobile Ad Hoc Networks," 4th International Conference on Computer and Information Technology (CIT), 2004, pp. 640-645.

22. V. S. Anitha and M. P. Sebastian, "Scenario-Based Diameter-Bounded Algorithm for Cluster Creation and Management in Mobile Ad Hoc Networks," 30th IEEE/ACM International Symposium on Distributed Simulation and Real Time Applications (DS-RT), 2009, pp. 97-104.

23. B. Xing, M. Deshpande, S. Mehrotra and N. Venkatasubramanian, "Gateway Designation for Timely Communications in Instant Mesh Networks," 8th IEEE International Conference on Pervasive Computing and Communications Workshops (PERCOM Workshops), 2010, pp. 564-569.

24. M. Hamdi, L. Franck and X. Lagrange, "Novel Cluster Maintenance Protocol for Efficient Satellite Integration in MANETS," AIAA International Communications Satellite Systems Conference (ICSSC), 2011.

25. P. Bellavista and E. Magistretti, "How Node Mobility Affects k-Hop Cluster Quality in Mobile Ad Hoc Networks: A Quantitative Evaluation," IEEE Symposium on Computers and Communications (ISCC), 2008, pp. 750-756.

Causal Probabilistic Modeling with Bayesian Networks to Combat the Risk of Piracy Against Offshore Oil Platforms

Xavier Chaze
Amal Bouejla
Franck Guarnieri
Aldo Napoli

Abstract

Pirate attacks against offshore oil platforms are multiplying. To reduce the vulnerability of this critical, highly strategic infrastructure, operators are actively investigating potential new information and communication technologies. Among the available options, techniques from artificial intelligence and, in particular, Bayesian networks offer promising avenues for research. This article describes the development and assessment of a prototype Bayesian network designed to assess the risk of attack against offshore oil platforms.

1. Introduction

More than seven thousand oil rigs are scattered across the world's oceans. These high-tech facilities offer a range of facilities to extract, process, and temporarily store oil. Vessels that transport oil between the place of production and consumption form another essential part of the operation.

Modern maritime piracy is undoubtedly a major threat to the security of both energy production sites and maritime oil transport. It is clear that current monitoring methods have major weaknesses in terms of threat detection and, in particular, in the defensive procedures to be implemented in response to a threat. This was demonstrated by the fact that in 2011, 552 attacks were registered with the International Maritime Bureau (http://www.icc-ccs.org/home/imb), compared to 487 attacks in 2010. It is clear that an effective and efficient system that can guarantee the safety of all facilities and stakeholders (operators, subcontractors, etc.) involved in the exploitation of oil fields is needed.

There are two aspects to data and domain knowledge: quantitative (databases containing information about the operating conditions of oil fields, and particularly about acts of piracy), and qualitative (the expertise and experiences of operators and stakeholders who organize prevention and the response to attacks). An approach that couples both quantitative and qualitative aspects of data seems particularly useful. Methods and models from artificial intelligence have repeatedly demonstrated the benefits of such an undertaking. Similarly, Bayesian networks have been mobilized, as much for their ability to formalize knowledge resulting from various worlds as for predictive reasoning capabilities that can provide decision support.

This article is organized into three sections. It first outlines the current situation related to acts of piracy against energy infrastructure. We then introduce the concept of Bayesian networks. In this section, we focus on the development of a methodology that led to the construction of a Bayesian network based on two data sources (the Piracy and Armed Robbery database of the International Maritime Organization, and the collection and formalization of expert knowledge). The last section presents and discusses our results obtained through simulations of comprehensive and realistic pirate-attack scenarios.

2. "Energy" Piracy at Sea

This part is organized into three sections. The first section outlines some baseline data concerning piracy in general, and the energy sector, in particular. The second establishes a typology of threats, and the third provides a short summary of the tools currently available for alerting and securing oil installations.

Xavier Chaze, Amal Bouejla, Franck Guarnieri, and Aldo Napoli are with MINES ParisTech, Centre for research on Risks and Crises (CRC), 1 Rue Claude Daunesse , CS 10207, 06904 Sophia Antipolis Cedex, France; Tel: +33(0)4 93 95 75 43; Fax: +33(0)4 93 95 75 81; E-mail: {firstname.surname}@mines-paristech.fr.

This invited paper is part of the special section on the "Role of Radio Science in Disaster Management."

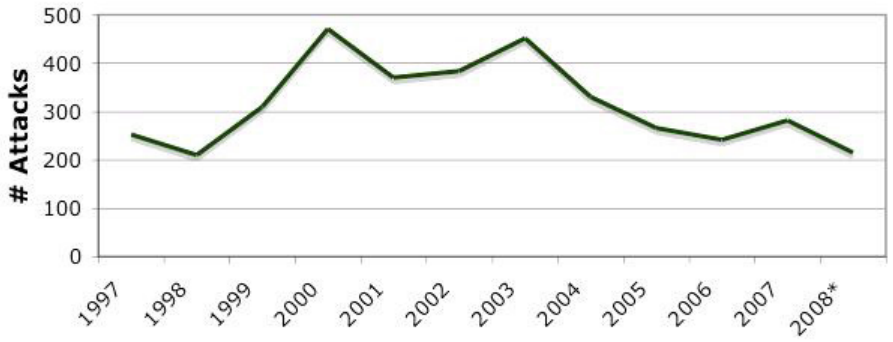

Figure 1. Global maritime pirate attacks, January 1997-September 2008. The total number of attacks was 3,566. (source: IMO database).

2.1 Piracy Facts and Figures, and Attacks on Energy Installations

On average, 5.9 vessels are attacked per 1,000 trips made [1]. In 2007, a pirate attack was reported on average every 31 hours. In the early 1980s, the international community responded by setting up a regulatory framework (the United Nations Convention on the Law of the Sea [2]). This defined "piracy" and the ways in which states and vessels can protect themselves and, if necessary, respond to attacks. In the 1990s, the number of attacks considerably increased. The International Maritime Organization (IMO) (http://www.imo.org), under the aegis of the United Nations, was made responsible for creating a database of incidents, and providing monthly, quarterly, and annual reports [3]. The IMO produced its first report in 1998. So far, nearly 4,000 attacks have been documented. Figure 1 is a summary of attacks in the ten-year period up to September 2008.

The IMO has estimated that the costs (losses) are 13 to 15 billion dollars per year in the Pacific region [4]. Other sources suggest a sum of 16 billion dollars [5, 6]. Losses include direct costs, such as the theft of ships and goods, but also indirect costs due to the act of piracy (delays, higher insurance premiums, etc.). The human cost is also very high. In 2006, 15 sailors were killed, 188 were taken hostage, and 77 were kidnapped and released in exchange for a ransom. Since 1995, more than 350 sailors have lost their lives.

Attacks on vessels carrying energy products represented a significant percentage of incidents. In 2006, they averaged about 12% of attacks, and reached more than 24% in 2007 (Figure 2). Most of these attacks aim to steal an asset. They take place either while the vessel is still in port, or with the help of small, very fast boats. The number of instances of hijackings, hostage-taking, and ransom demands have also sharply increased. In August 2003, the Malaysian tanker *Penrider* was seized while off the coast of Indonesia, and a 100,000 dollar ransom was demanded.

Clear targets for pirates are vessels that are attacked for the goods they are transporting. In 1998, the *Petro Ranger* was attacked outside the territorial waters of Singapore. It was carrying nearly 12,000 tons of petroleum products. Pirates went to the lengths of renaming the ship *Wilby*, and assigning it a Honduran flag. For a time, the *Petro Ranger* became a ghost ship [7].

As Figure 3 shows, the vast majority of attacks against vessels carrying energy products concern tankers transporting oil and liquid gas. About 3% (4,000 vessels) of the total tanker fleet (120,000 vessels) are energy tankers. In 2007, pirates started to take an interest in mobile oil platforms and liquid gas carriers, with some success. Two platforms were attacked in 2007, one in Indonesia and the other off Singapore. Three fixed drilling platforms were also attacked, two in Nigeria (including a kidnapping and a ransom demand), and one in India. These events show that pirates are able to tackle any type of target.

Figure 4 shows that most pirate attacks are concentrated in Indonesia and the Malacca Straits. In 2007, Nigeria suddenly emerged as a dangerous area, particularly for vessels transporting energy products, which accounted for 29% of attacks, although Indonesia still led the field with over 35% of attacks. However, in 2008, Somali pirates

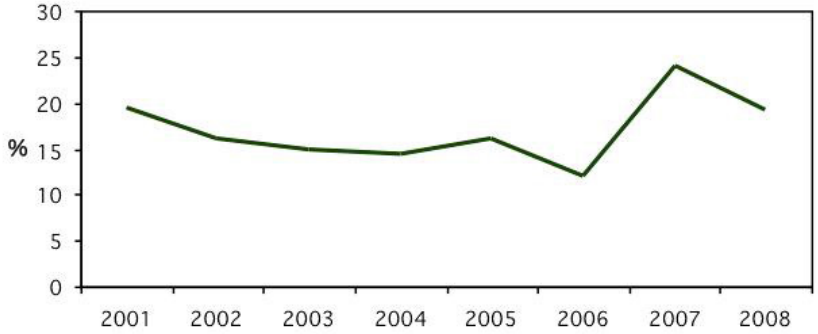

Figure 2. The percentage of attacks on energy vessels, January 2001-September 2008 (source: IMO database).

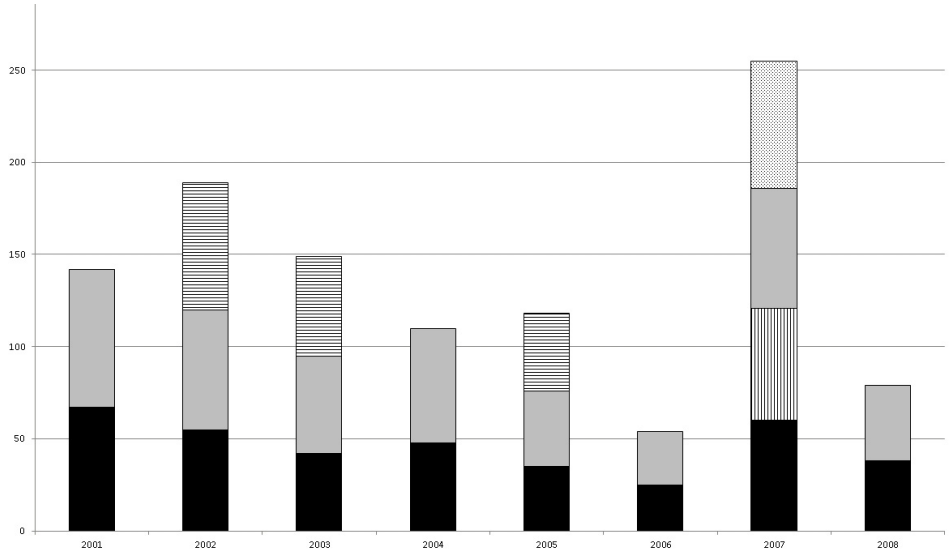

Figure 3. The number of attacks by vessel type, 2001-2008 (source: IMO database).

increased their response capacity beyond 200 nautical miles. Consequently, in 2008, more attacks occurred in Nigeria and Somalia than in Indonesia and the Malacca Straits. By the end of 2008, the IMO had recorded more than 60 attacks.

2.2 Typology of Threats Against Oil Platforms

Jenkins [8] established the first typology of threats to oil platforms based on feedback from reports. He identified:

- The bomb scare: this aims to disrupt operations by forcing an evacuation and generating an expensive and extensive search in order to end the alarm, which is usually false. However, Jenkins includes cases where a real bomb has been placed, either by platform personnel or by underwater divers.
- Floating mines: remnants of the Second World War, they pose a very low level of risk.
- Sabotage: mainly by installation personnel or terrorist organizations.
- Boarding (or collision) by a non-governmental organization: usually to bring to the public's attention an environmental cause.
- The destructive attack: a terrorist attack by a guerrilla or regular army.
- Hostage-taking: this hypothesis was formulated by Jenkins based on the example of planes and trains. At the time the typology was established (1988), he had no feedback about it, and estimated the risk to be low because of the resources that would have to be deployed and the difficulty of accessing an offshore platform.
- "Kamikaze" ships or an aircraft (piloted or not).

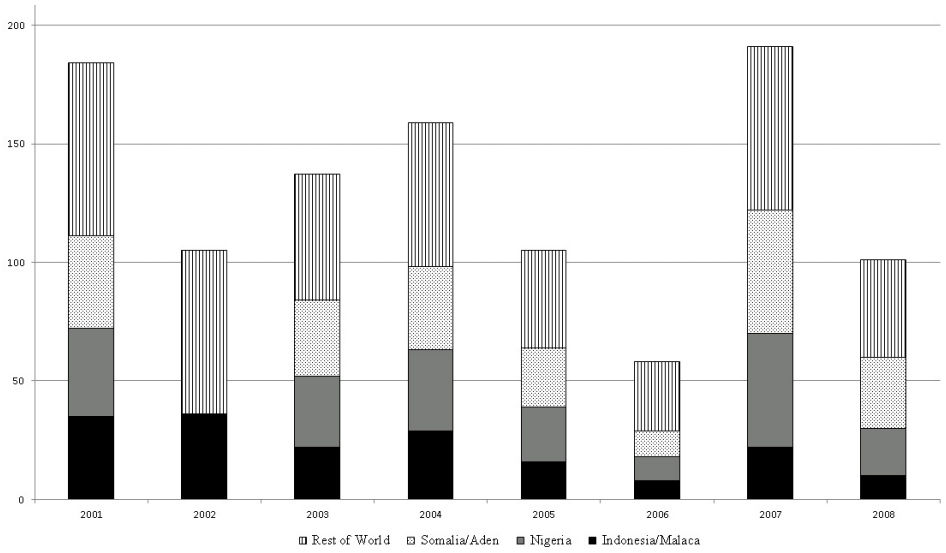

Figure 4. The number of pirate attacks by country, 2001-2008 (source: IMO database).

- Attacks against platform personnel: although this is similar to hostage-taking, here it relates to intercepting personnel before they assume their duties.

Acts of piracy against offshore oil installations have increased considerably since 1988. In 2008, Kashubsky [9] conducted a very detailed study of Nigeria. Here we have selected a few significant events as illustrations:

- On June 12, 2005, an armed group boarded the Jameston FPSO (floating production, storage and offloading unit) and took 45 hostages. They were released following the payment of a ransom three days later.
- On January 11, 2006, a Shell platform was attacked and four people were taken hostage from the maintenance vessel anchored to the platform.
- On January 15, 2006, a very violent attack against a Shell facility resulted in a fire, extensive damage, and 17 deaths.
- On February 18, 2006, a speedboat attacked an installation, and nine personnel were wounded.
- On October 2, 2006, Shell barges were attacked. Three soldiers were killed protecting the facility.
- On April 1, 2007, an installation suffered a dual attack. The maintenance ship was diverted by pirates who were then able to come alongside.
- On April 19, 2007, a security vessel was attacked. The pirates managed to strip it of its own weapons.
- On May 3, 2007, the FPSO Mystras was attacked: the attackers used the anchor chain to board. Eight employees were kidnapped.
- On October 21, 2007, a large armed group simultaneously attacked two maintenance ships.
- On June 19, 2008, the FPSO Bonga was attacked and damaged, production stopped, and losses were estimated at more than 200,000 barrels of oil per day.
- On September 14, 2008, platforms belonging to Shell and Chevron were simultaneously attacked.
- On September 16, 2008, eight speedboats loaded with dynamite and hand grenades attacked the Shell (Orubiri) pumping station, causing extensive damage.
- Etc.

These events highlight the extent of the human, material, and economic damage. They also highlight the forms of criminal action and strategies used by pirates: surprise, extreme mobility, rapid action, a small number of assailants, and the weapons they use.

2.3 Protection of Installations and Shipping

Military authorities consider it impossible to protect all of the world's merchant fleet. It is the same for ships carrying energy products. The IMO has therefore issued a set of recommendations for ship-owners and crews aimed at ensuring the safety of persons, property, and equipment. The IMO does not recommend arming ships and oil platforms in order to avoid violent confrontations. This is especially relevant given that pirates are particularly well-armed (with automatic rifles, grenades, etc.), and seem to favor hostage-taking and ransoms. This leads to hope that hostages will be well-treated and the rejection of a policy of armed and violent responses to attacks.

Merchant ships have two ways to respond to an attack: they can either seek to avoid it by changing routes, and/or increasing ship security. The first option is not possible for oil platforms that are anchored to the sea bed. For them, detection and warning systems are essential.

The IMO has issued a series of recommendations that include:

- Increased and permanent vigilance.
- Increased use of detection technologies (radar, infrared, searchlights, etc.).
- Installation of audible alarms, illuminating suspicious vessels.

Despite these recommendations, some owners and operators have resorted to security companies. Most use non-lethal means to repel attacks. In November 2008, in the Gulf of Aden, a security team defeated heavily armed pirates using water cannon combined with a noise repulsion device.

Action Taken by Vessel	Number of Vessels Taking Action	Applicable to Off-shore Platforms?
Raised alarm	21	Yes
Took evasive maneuvers	28	No
Increase speed	16	No
Crew mustered	8	Yes
SASS activated	2	Yes
Coalition warship advised/responded	12	Yes
Fire hoses activated	6	Yes
Sent distress signal	1	Yes
Fired flares	1	No
Sounded ship's whistle	1	Yes

Table 1. Actions taken by ships to protect themselves against attack in Somalia, January-September 2008. The number of attacks was 67 (source: IMO Database).

Table 1 provides an overview of the defensive actions implemented in Somalia in 2008 to prevent pirate attacks. The final column indicates whether the measure can be applied to offshore oil platforms.

The United States Department of Homeland Security has produced a set of recommendations for the protection of vessels. The document, entitled "Port Security Advisory (2-09) (REV 1)," advocates the following responses to an attack:

- Activate the alert system (in conjunction with the United States Coast Guard).
- Make a mayday call on the VHF channel.
- Inform local authorities.
- Inform the management of the operating company.
- Deploy the anti-aggression plan.
- Ensure that the AIS (Automatic Identification System) is operational.
- Send a distress message via systems such as Inmarsat-C.
- Prepare to move to the refuge area.
- Begin escape maneuvers aimed at outrunning the attackers or enabling external intervention (for ships).
- Use non-lethal means aimed at stopping the intrusion and repelling the attackers.
- Owners and operators are asked to provide notification of the attack (and suspected attacks) to the United States' authorities.

It is clear that the proposed methods and solutions are simple, limited, and to say the least, rustic. New technologies should be able to improve on these current prevention systems.

3. The Contribution of Bayesian Networks to Reducing the Vulnerability of Offshore Oil Installations

This second part is organized into three sections. The first briefly outlines the operational requirements and constraints inherent in the design and development of a high-performance detection, alert, and threat-processing system. The second introduces the concept of the Bayesian network, and the software tool used in development of the system. Finally, the third section describes how to construct a Bayesian network based on both quantitative data and expert knowledge.

3.1 Operational Requirements and Technical Issues

To date, there is no technological solution on the market that manages the entire processing chain of a threat. The main systems currently available independently manage the detection and the response to a threat. Among detection tools, radar-based systems (pulses[1]) are able to locate large or medium-sized mobile vessels, but they perform poorly in the detection of small craft (such as fishing boats, motor boats, etc.) and in rough seas. Moreover, they are relatively slow to analyze a wide geographical area [10]. There are also optronic surveillance systems[2], which, despite their strengths in the long-range detection of small targets, remain handicapped by problems of solar reflection on the sea surface, and have proven to be very sensitive to weather conditions [11]. As for counter-attack systems (water hoses, noise guns, etc.), they are often inappropriate or misused.

In terms of threat response, oil platforms that are the victim of an attack are able to broadcast warnings to security vessels deployed in the area, but their diffusion is geographically very restricted. Moreover, even if the security vessel is notified, its ability to intervene remains uncertain, particularly if it is remote from the location of the attack.

The goals of our research are therefore limited. Taking into account work undertaken so far, we aim to improve the ability of an installation to detect a threat, raise the alert, and secure the installation if the threat is verified. There are many constraints inherent in this problem. The first challenge is a direct consequence of the large number of attack parameters. These include input and output system parameters related to the target (platform or mobile vessel), the danger (type, criticality, vulnerability, on-board security facilities, etc.), the threat (vessel used by the attackers, its speed, weapons, etc.), and the environment (time of day, visibility, sea state, etc.). The second challenge is that these parameters may interact. For example, whether it is relevant to request the intervention of the security vessel depends in particular on the time needed for it to reach the installation under attack, and the weaponry and speed of the threat. A second constraint therefore lies in the management of the many interdependent relationships among system variables.

A further constraint is the need to take into account the uncertainty of threat data. The alert report not only contains aggregated data from detection instruments such as FMCW (frequency-modulated continuous-wave) radar (the type of vessel detected, number of occupants, potential weapons, etc.), but also mathematical calculations based on dynamic variables (distance between the target and the attacker, time before they are able to board the platform, etc.). This necessarily leads to the question of how to manage errors and false alarms. For example, despite the improved performance of radar, the information it provides becomes increasingly unreliable as the distance to the threat increases, and as the sea state deteriorates.

These constraints suggest the design and development of a decision-support system based on graph theory [12] that is able to translate and exploit (by means of a graph) a large number of variables, their dependency relationships, impacts, etc. When the uncertainty inherent in the data is taken into account, the need to find a solution that is based on probability theory and probabilistic calculations is clear. We therefore propose a model based on Bayesian networks. This tool should be able to automatically prepare response plans tailored to the nature of the detected intrusion.

3.2 Bayesian Networks and *BayesiaLab* Software

Depending on the application, the practical implementation of a Bayesian network is similar to that of other models: neural networks, expert systems, decision trees, data analysis (linear regression) models, fault trees, and logical models. Naturally, the choice of method depends on criteria such as ease of use, and the cost and time needed to implement a solution. In addition to theoretical considerations, the following aspects of Bayesian networks in many cases make them a better choice than other models [13]:

- Knowledge acquisition. This is the ability to collect and merge different kinds of knowledge in the same model: feedback (historical or empirical data), expertise (expressed as logical rules, equations, statistics or subjective probabilities), and observations.
- Knowledge representation. The graphical representation provided by a Bayesian network is explicit, intuitive, and understandable by a non-specialist. This facilitates both the validation of the model, its possible extension, and, in particular, its use. A decision-maker is more likely to rely on a model that they understand and know how works than to trust a black box.
- Knowledge use. A Bayesian network is versatile: the same model can be used to assess, predict, diagnose, and optimize decisions, all of which helps to recover its initial development costs.
- Quality of software. Nowadays, there are various software tools available to understand and process Bayesian networks. These tools offer functionality that is more or less advanced: probabilistic learning, learning the structure of the Bayesian network, the option to integrate continuous, utility, and decision variables, etc.

A Bayesian network can both represent knowledge and make it possible to calculate conditional probabilities. Widely used for diagnosis (medical or industrial) [14], such networks can capitalize and exploit knowledge, and are particularly suitable for the assessment of uncertainty [15, 16].

A Bayesian network, *BN*, is a directed acyclic graph defined by a set of nodes corresponding to attributes, *H*, and by $E \subset H \times H$, the set of arcs of the graph. A conditional probability distribution, $P_{A_i|\Pi_{A_i}}$, is associated with each node, where $\Pi_{A_i} = \left\{ A_j \middle| \left(V_{A_j}, V_{A_i}\right) \in E \right\}$ are the parents of node A_i. One of the properties of a Bayesian network is that it uniquely defines the joint probability distribution over *H*:

$$P_H^{RB} = \prod_{i=1}^{n} P_{A_i} \left| \Pi_{A_i} \right. . \quad (1)$$

An association rule, *R*, is a pattern $X \Rightarrow Y$, where *X* and *Y* are itemssets, such as $Y \neq \varphi$ and $X \cap Y = \varphi$. *X* denotes the left side of the rule and *Y* denotes the right side. Let *I* be an itemset. The support for *I* in database *BD*, denoted $supp_{BD}(I)$, is the set of records (or transactions) of *BD* that contains *I*.

Given a database, *BD*, defined on a set of attributes, *H*, and a Bayesian network, *BN*, we thus obtain the confidence of the association rule $R = X \Rightarrow Y$ [17]:

$$Conf_{BD}(X \Rightarrow Y) = P_{Y|X} \quad (2)$$

$$= \prod_{i=1}^{m} P_{Y_i} \left| \Pi_{Y_i} \right. .$$

From data estimates,

$$Conf_{BD}(X \Rightarrow Y) = \frac{\text{supp}_{BD}(X \cup Y)}{\text{supp}_{BD}(X)} . \quad (3)$$

In our study, the Bayesian network is used to develop a tailored, graduated, and progressive response to a threat. Database records and the knowledge of experts in the maritime and oil domains are used to overcome the initial lack of knowledge and feedback from the application domain.

BayesiaLab software was used to construct the Bayesian network. This is a decision-support tool for modeling uncertain knowledge. It provides analysis, diagnosis, simulation, optimization, and risk-management functions, and offers two methods to develop a Bayesian network:

- Automatic "data mining" modeling. This module makes it possible to collect and merge various kinds of knowledge in the same model (e.g., historical or empirical data). The software provides several functions for constructing a Bayesian network from an imported data source: definition of missing and filtered values, definition of an initial network, supervised learning,

clustering, probabilistic structural equations, integration of continuous, utility, and decision variables, etc.

- "Brainstorming" modeling. This enables the construction of a Bayesian network based on expert knowledge. The benefit of this model is the constructive discussion between experts that makes it possible to model situations that are rare or have not yet occurred. The drawback is that expert knowledge is often incomplete, partially incorrect, and subjective. The development of a Bayesian network through brainstorming involves three key steps. The initial step is to clearly define objectives, prepare a list of dimensions, and define the variables related to each dimension (their type and states), taking into account the need to minimize the number of states. Next, structural modeling consists of determining the cause and effect relationships, and adding new variables that simplify the network. Finally, parametric-modeling techniques are used to elicit knowledge.

These two types of modeling are complementary, and are used to construct a Bayesian network based on data mining and expert knowledge. The usefulness of the graphical representation of a Bayesian network is very dependent on the number of nodes that compose the network. The software offers two algorithms for automatic positioning:

- A dynamic algorithm, suitable for arborescent or weakly connected structures, which takes account of parental relations between nodes, the force of arcs, and the weight of nodes, defined according to the number of children and parents of each node.

- A genetic algorithm for processing more-complex networks. This algorithm can take into account the relationships between nodes, the force of arcs, overlapping nodes, and the intersection of arcs with other arcs and nodes.

For the analysis of results, the software provides four tools:

- Arc analysis is provided by a comprehensive tool that highlights the force of arcs. Arc thickness reflects the strength of the probabilistic relationship it represents in the associated probability law.

- Target-node analysis is a more localized tool. The analysis focuses on a target variable, which enables the user to see the amount of data contributed by each node to the knowledge of the target node.

- The target-node state-analysis tool makes it possible to visualize two pieces of information for each node related to its probabilistic relationship with the target variable: the influence of the variable on a particular state of the target variable, and the information gain provided by the node to the knowledge of the target state.

- Causal analysis is a tool to remove the orientation of arcs the orientation of which can be inverted without changing the joint probability law.

In addition to these analysis tools, the software makes it possible to edit the report. This HTML report provides a description of all observed variables, probability distributions, etc. The software can also prepare a second report, focused on a global analysis of all observations. The purpose of this report is to determine whether there are contradictory findings, or if they all point in the same direction.

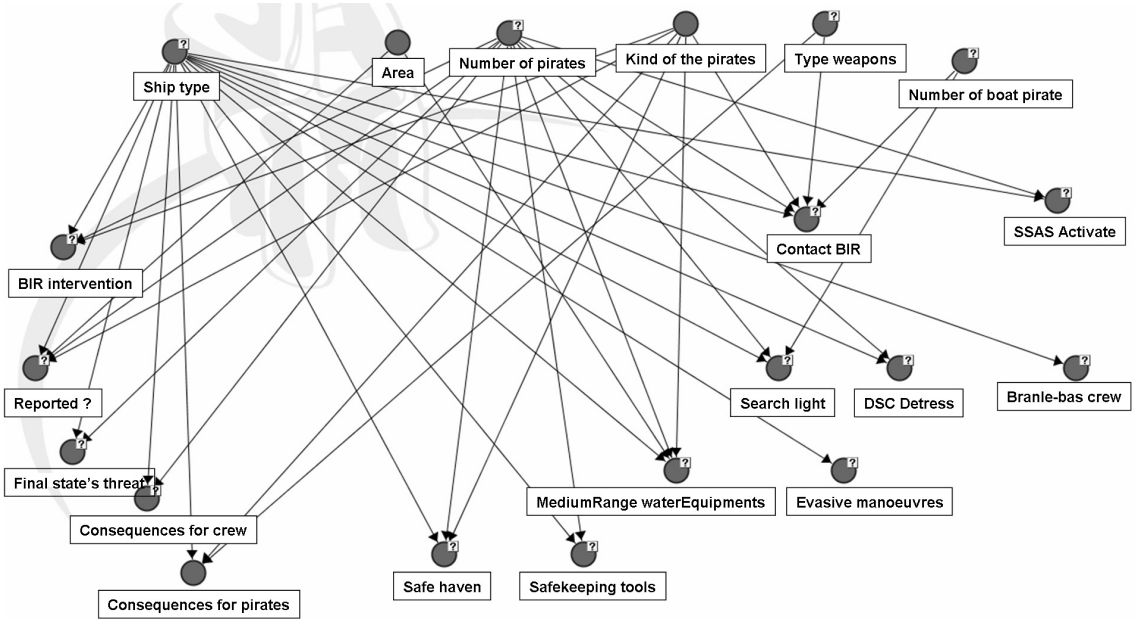

Figure 5. The Bayesian network generated from IMO data.

3.3 Coupling of Quantitative and Qualitative Knowledge

A key feature of our Bayesian network is that it combines quantitative knowledge from the IMO database and qualitative knowledge acquired from experts in the maritime domain.

The first step was to construct a Bayesian network from records related to attacks against vessels and offshore platforms. The second step used expert knowledge to refine the results and add countermeasures.

Quantitative data was provided by the IMO's Piracy and Armed Robbery database. This is the only database in existence containing records (dating back to 1994) of piracy attacks in the maritime environment. In July 2011, it contained 5,502 records, and data included the name of the asset attacked, the number of people involved in the attack, the type of weapons used, the measures taken by the crew in order to protect themselves, the impact on the crew and the pirates, etc. The software automatically generated a Bayesian network from this data, and suggested dependency relationships between the main database elements. The software also offers various unsupervised learning methods (e.g., data-segmentation algorithms or target-node characterization). We decided to use an association discovery algorithm, as it generated the most relevant model.

Figure 5 shows the Bayesian network built from the IMO database. Information such as longitude, latitude, name of the asset attacked, etc., was not retained, as these fields were not listed for all attacks. The network contained around twenty nodes related to the type of vessel attacked, the location of the attack, the type of weapons used by the pirates, their numbers, etc. The relationships among these variables were identified through an automatic learning process.

A classical statistical analysis of this data provided a first set of information. The most interesting results included the following: most ships that are attacked are bulk carriers or tankers, 48% of attacks take place in international waters (due to the absence of security controls), and pirates benefit from attacking in numbers (68% of attacks are carried out by teams of five or more). As a result of this network, a clear picture emerged of pirate tactics, their weapons, and in particular, the number of people involved.

In the example that follows, specific threat-node characteristics were set in order to identify countermeasures used by the crew of the attacked target. Figure 6 illustrates the selected hypothesis:

- The asset under attack: a tanker.
- The location of the incident: international waters.
- The type of attackers: thieves.
- The type of weapon: gun.

In this example, the Bayesian network indicated that (as in most cases) the assailants fired shots at the target, and that the crew, to protect themselves from this danger, applied evasive maneuvers and used water hoses on the attackers.

This analysis of the IMO database made it possible to identify the main actions taken by most entities when attacked, namely: initiate evasive maneuvers, activate the SSAS alert system, contact the security vessel, secure the crew, activate searchlights, etc. The network created from

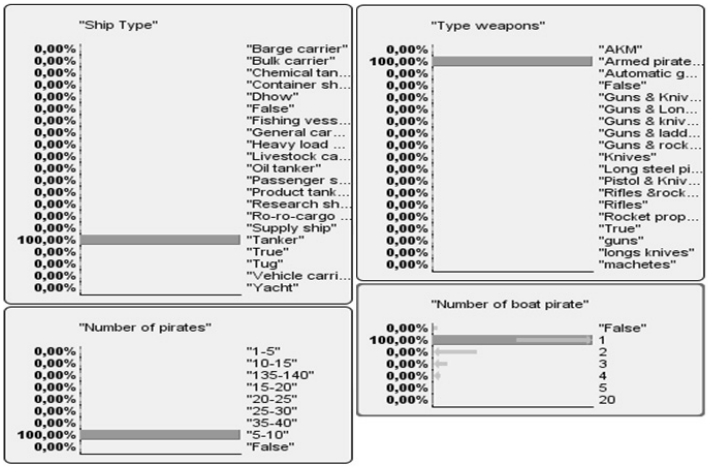

Figure 6. The attack scenario against a tanker.

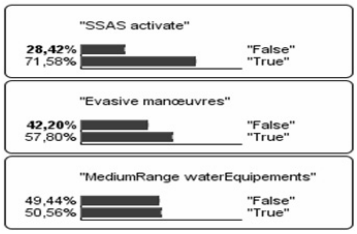

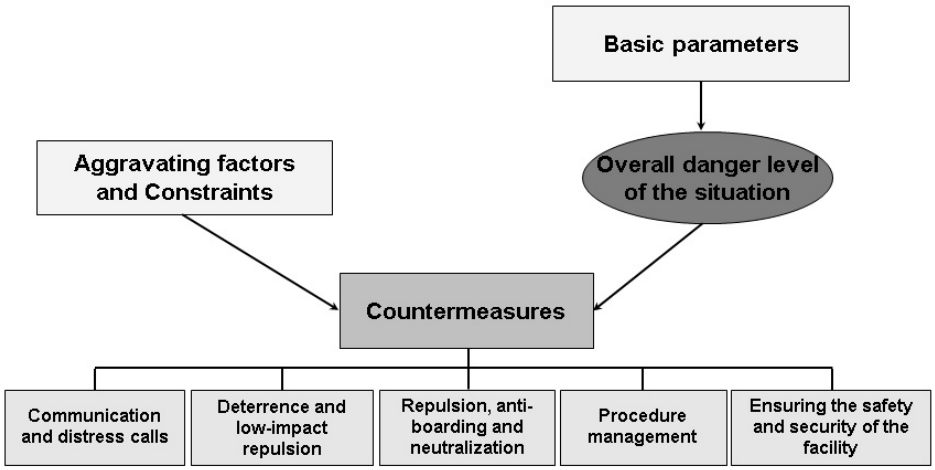

Figure 7. The structure of the Bayesian network.

the IMO database also made it possible to determine the principal tools and methods used by the crew of attacked entities to protect themselves, to evaluate the effectiveness of these tools, and to define the probability of certain types of attacks.

This Bayesian network, through its states and conditional probabilities, provided a formal framework into which maritime domain experts were able to add their knowledge in order to build a second Bayesian network.

The second step of the methodology consisted of the analysis of information extracted from the IMO Bayesian network by maritime and oil experts. The IMO database primarily contains information related to attacks on shipping. Experts were able to contribute knowledge that made it possible to transpose the results to oil fields; nodes and arcs were added to make the model as versatile as possible. Although each Bayesian network is unique for the two broad categories of target (shipping or oil platforms), the input variables are the same regardless of the nature of the target (type of ship, threat, kinematics, etc.). However, the countermeasures recommended by the network are tailored to the type of target (for example, evasive maneuvers are not proposed for an offshore platform).

This new Bayesian network, tailored to the constraints and conditions found on oil platforms, was developed as a result of numerous brainstorming sessions, during which maritime and security experts shared their experiences and discussed network states and probabilities [18].

The complementarity of the IMO data and the knowledge of maritime and offshore security experts made it possible to generate a response-planning network. The architecture consisted of four modules and five sub-modules (Figure 7). The scope of each of these modules was directly related to the meaning of its constituent nodes. The classification included basic parameters, the overall danger level of the situation, aggravating factors and constraints, communication nodes, those related to requests for help and countermeasures, given in Table 2.

In this Bayesian network, each module or sub-module consisted of one or more nodes that received and/or transmitted causal relationships to other nodes. Each node was composed of a matrix of conditional probabilities that was calculated taking into account the various interactions with other nodes, and the actual reality that the node itself represented. For example, the probability distribution of activating searchlights ("Activate Search Light") was directly subject to interactions with visibility, time of day, and technical constraints, such as availability and remote control.

The probabilities of base nodes were standardized, and elements characterizing a specific attack were not included. The initial probability distribution for activation of the sonic cannon ("Activate LRAD") was therefore distributed as follows: stand-by, 99.51%; Activate LRAD Loudspeaker, 0.27%; Activate LRAD Sonic Weapon, 0.22%.

In the next section, we assess the relevance of our Bayesian network, using a set of attack scenarios.

4. Attack Scenarios and Discussion

This last part is organized into two sections. The first describes the test scenarios. The second describes the integration of the Bayesian network into a global system for the management of alerts and responses, namely SARGOS.

4.1 Attack Scenarios: Case Studies

Several scenarios were developed to test the ability of the Bayesian network to prepare real-time response

<table>
<tr><th colspan="4">Basic Parameters</th></tr>
<tr><td colspan="4">Static or dynamic physical data that characterize the threat and the target. They can be the direct result of the alert report, or are derived from intermediate calculations. They constitute the minimum level of modeling that is sufficiently detailed to give a full understanding of the threat/ target in the response scenario.</td></tr>
<tr><th colspan="4">The Overall Danger Level of the Situation</th></tr>
<tr><td colspan="4">Calculated from basic parameters, this level ranges from 1 to 4 (maximum overall danger level), and changes in real time in response to the situation in order to plan appropriate countermeasures.</td></tr>
<tr><th colspan="4">Aggravating Factors and Constraints</th></tr>
<tr><td colspan="2">Aggravating factors make it possible to take into account the potential deterioration of the situation and to therefore anticipate alternative plans (such as environmental factors: visibility and time of day).</td><td colspan="2">Constraints are represented by parameters that can influence the effectiveness of the response. They are directly related to the ease of use of countermeasures (such as the immediate availability of an operator or whether the device can be remotely operated).</td></tr>
<tr><th colspan="4">Countermeasures</th></tr>
<tr><td colspan="4">These are defensive measures that are implemented by the target under attack in order to protect itself against an identified threat and to normalize the situation as soon as possible. Countermeasures are the physical manifestation of the response plan and are increasingly forceful, depending on the nature of the threat detected.</td></tr>
<tr><th>Communication and the Request for Help</th><th>Low-Level Repulsion Measures</th><th>Repulsion, Anti-Boarding and Neutralization Measures</th><th>Procedure Management</th></tr>
<tr><td>Objectives:
• Alert relevant personnel.

• Warn, at various levels of intervention, maritime security actors (security vessels, coastal countries).

This enables installations and vessels in the oil field to anticipate their response plan and to find out if outside intervention is possible.</td><td>Objectives:
• Advise the attackers that the target knows their intentions and is able to respond.

Small-scale repulsion is the ability of the target to repel the attackers using low-level methods (searchlights, fire hoses, sound guns).</td><td>Objectives:
• Slow down the progress of the attack to give the crew enough time to prepare other security measures.

• Slow down or neutralize the attackers.

These active countermeasures have a high impact and rely on equipment that can repulse an attack from a distance while remaining within the framework of non-lethal self defense.</td><td>Objectives:
• If there is a security alert, sound action stations and gather crew at pre-defined assembly points.

• Secure the installation (activate the citadel, stop production, secure access to sensitive areas, etc.).</td></tr>
</table>

Table 2. The Bayesian network modules.

plans tailored to a detected intrusion. These scenarios were developed in collaboration with experts (Table 3).

Figure 8 shows in detail the results of the insertion of parameters modeling an attack on an FPSO unit by an unknown assailant (scenario 1). This example showed that the danger level of the situation was 2 with a 64.68% probability of occurrence. In this case, countermeasures to be applied were to inform the crew master; request the intervention of the security vessel; broadcast a loud, clear message using the long-range loudspeaker; activate searchlights; engage the safety post; and activate repulsion equipment.

Planning can be tailored to the danger level of the situation and is adapted as threat and target parameters change. The generation of attack scenarios makes it possible to refine probabilities, and to test the reaction of the Bayesian network by varying threat, target, and environment parameters. These scenarios made it possible to assess the relevance and consistency of the countermeasures proposed by the network, which could be iteratively improved.

4.2 Integration of the Bayesian Network into the SARGOS System

The SARGOS system ("Système d'Alerte et de Réponse Graduée OffShore," ProjetANR-09-SECU-009, Programme CSOSG 2009) [19] was designed to meet the emerging need for security on offshore civilian infrastructure that is vulnerable to malicious acts of piracy or terrorism conducted at sea. The aim is to develop a system that ensures a coordinated, global protection chain (Figure 9). It includes:

- Monitoring and automated monitoring. The combination of a specialized radar (FMCW technology) and conventional sensors helps to detect intrusions from small boats and commonly used vessels.
- Assessment of the danger level. An intelligent analysis of the characteristics of the detected object makes it

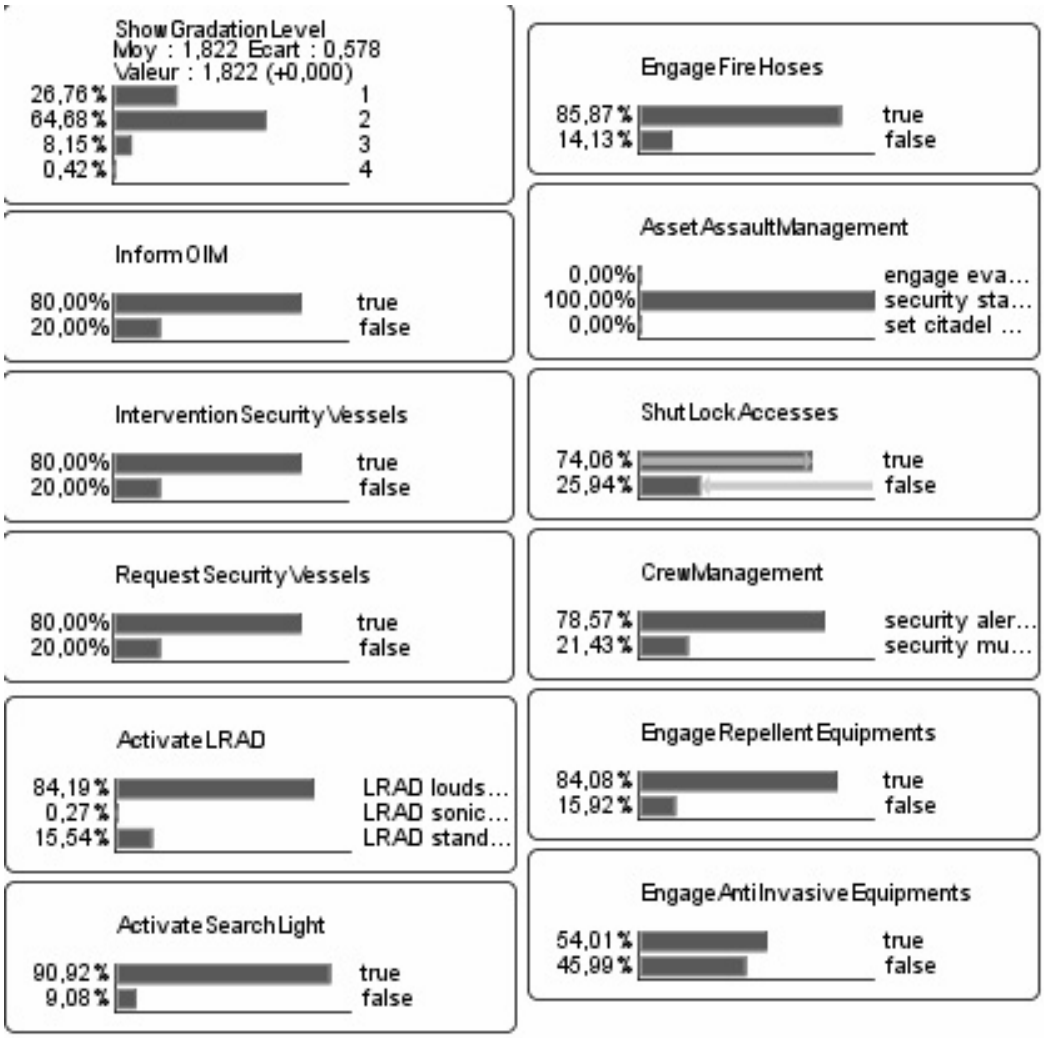

Figure 8. Response planning following the insertion of an attack on an FPSO unit from an unknown source.

Threat Type	Target Type	Context	Distance Target/Threat	Time Target/ Threat	Time for Security Ship to React	Danger Level
Unknown	FPSO (critical importance)	Good visibility Daytime	200 < d < 500 m	900 s < t	t < 300 s	**2 (64.68%)**
Highly maneuverable vessel (firearms detected)	FPSO (critical importance)	Poor visibility Night	d < 50 m	t < 300 s	900 s < t	**4 (79.79%)**
Unknown	FPSO (normal importance)	Poor visibility	200 < d < 500 m	t < 300 s	300 < t < 900 s	**2 (50.73%)**
Unknown (handguns detected)	FPSO (critical importance)	Good visibility	50 < d < 200 m	300 < t < 900 s	900 s < t	**3 (45.21%)**
Inconnu (handguns detected)	FPSO (critical importance)	Good visibility Dawn-dusk	d < 50 m	t < 300 s	t < 300 s	**3 (56.40%)**

Table 3. Test scenarios developed in collaboration with experts.

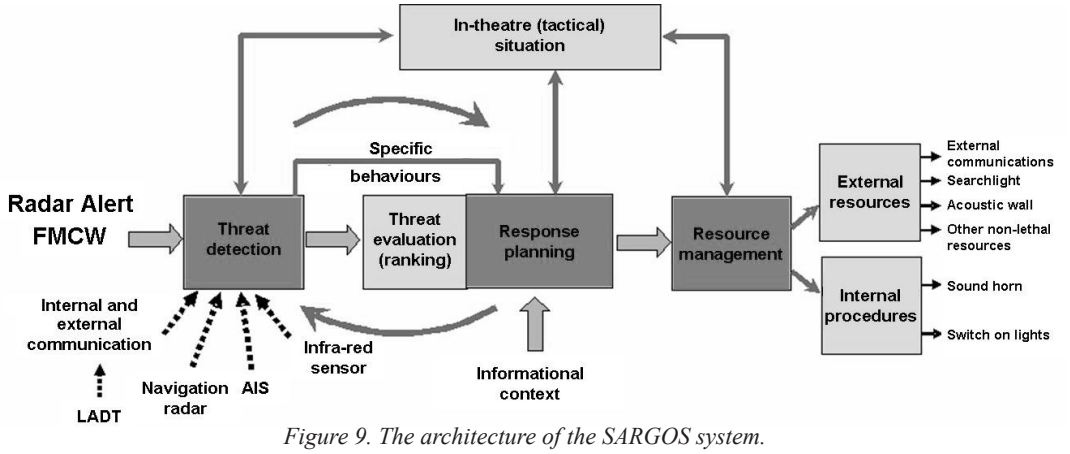

Figure 9. The architecture of the SARGOS system.

possible to classify and assess the danger level. When the level exceeds the pre-set alarm threshold, an alarm is generated, and the operator is alerted via a message sent to a mobile terminal.

- Development of a graduated response plan that can be controlled in real time. From the Bayesian networks, a situation analysis automatically creates response plans tailored to the nature of the detected intrusion. The plan takes into account the infrastructure's operating modes, and the regulatory and legal context of the oil field.

One of the key capabilities of the SARGOS system is a comprehensive threat-response strategy that can ensure personnel safety, raise the alarm, coordinate external means of assistance, and recommend non-lethal deterrents. It was implemented using a transverse system approach, and is based on innovative technologies that were developed using the complementary skills of project partners[3]. It can ensure the automatic protection of offshore infrastructure faced with new forms of piracy by triggering the relevant actions at the appropriate time.

We have developed a prototype that integrates the Bayesian network into the SARGOS system. The prototype takes an alert report as input, and generates a planning report as output. The output report contains all the countermeasures to be applied, either manually by the crew or automatically by the system.

The results of intermediate calculations are fed into the Bayesian expert knowledge network. *BayesiaEngine* software provides an application programming (API) interface and a *Java* library. Through this module, attack parameters can be inserted into the network.

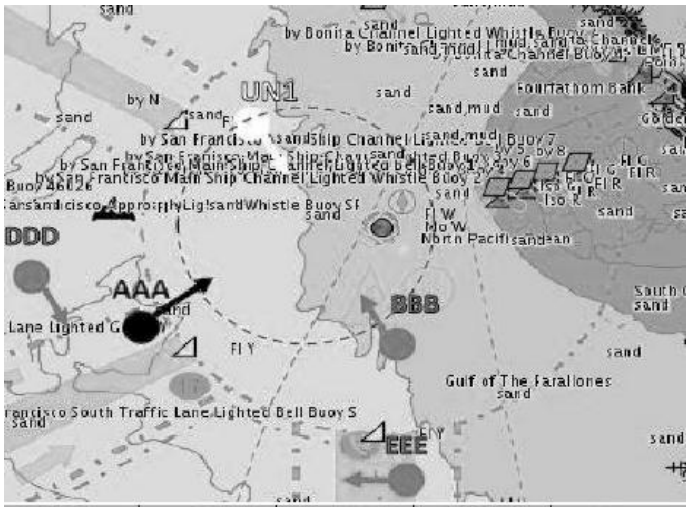

Class	ID	CPA	TCPA	Type
Enemy	AAA	2. 3 m	3. 30 mn	Small Boat
Unknown	UN1	1.5 m	2.20 mn	
Friend	BBB	2.8 m	4.15mn	Tanker
Friend	CCC	0		Tanker
Friend	DDD	0		Small boat

Figure 10. The SARGOS man-machine interface, showing threat classifications.

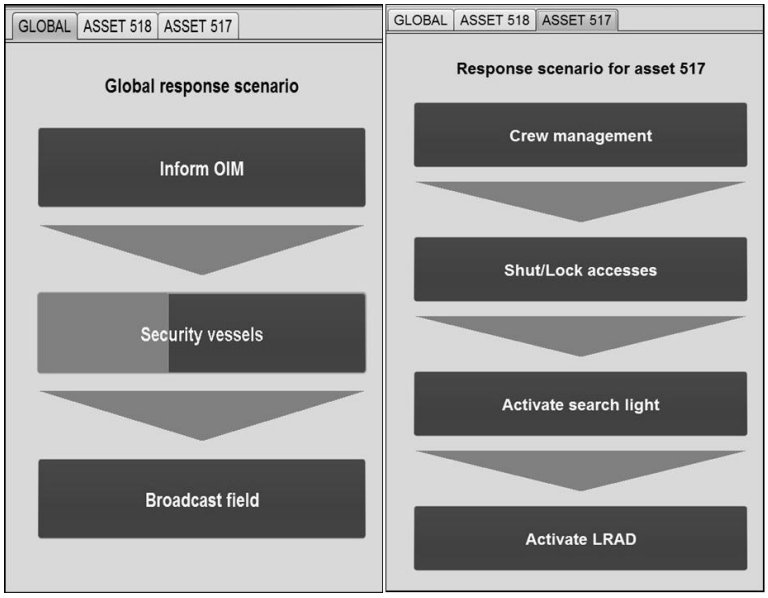

Figure 11. The SARGOS man-machine interface, showing global (left-hand side) and local (right-hand side) countermeasures to be applied.

The selection of countermeasures varies according to the situation. It is therefore possible to set an activation threshold in order to only include those countermeasures that are most appropriate at a particular time, in a given situation. We decided to set this threshold at 70%. This means only those countermeasures where the probability of one of its states is greater than 70% are integrated into the planning report. This threshold was selected by domain experts, as it is actually the case in more than two-thirds of incidents encountered in real life. After numerous trials and adjustments, the output of the network corresponded to realistic and reliable responses.

Once appropriate countermeasures have been selected, they are included in the planning report, where they are displayed in a specific order. The main factors affecting the priority are the action mode of the countermeasure, its ease of implementation, whether it can be activated automatically or manually, the time required before it becomes effective, and any additional functions.

The SARGOS system can handle multiple threats in one alert report. The first threat to be processed is always that which has the shortest response time for the most exposed potential target. Figure 10 demonstrates the interface of the SARGOS system, and shows the simultaneous processing of multiple threats.

In this example, the system detected a set of entities that were heading towards an oil field. It classified them as "Enemy," "Unknown," or "Friend." An alert was only generated for entities classified as "Enemy" and "Unknown." Following this initial processing, the planning report was divided into two parts. The first applied to the whole oil field, and concerns communication and a request for support (the left-hand side of Figure 11). The second related to the specific target in danger, and displayed a prioritized list of the countermeasures to be activated (the right-hand side of Figure 11). On the left-hand side of Figure 11, the vertical division visible in the request for the intervention of the security vessel represents the resulting probability.

5. Conclusions and Future Work

The problem of acts of piracy against oil infrastructure is complex. In an open space that is subject to many environmental constraints, the difficulty of assessing a potential threat, the constant evolution of a dangerous situation, as well as the need to manage a large number of parameters weaken the effectiveness of protection measures.

The use of a Bayesian network for planning the response to a threat therefore represents real progress. The network can manage potential interactions among threat characteristics, the target under attack, the environment, and crew and facility management. Most importantly, it can adapt in real time to changes in the danger level of the situation. The proposed response is translated into a planning report, which is the output of the intelligent processing of successive warning reports that reflect the evolution of the situation. The network can be scaled through the integration of feedback from previous attacks managed by the system. Through this mechanism, the planning module is progressively better adapted and iteratively improved.

Dynamic Bayesian networks [20] provide another avenue for exploration. Interest in these networks has seen significant growth as a way to generalize hidden Markov models or Kalman filters in applications such as speech recognition, state estimation in dynamic models, etc. A dynamic Bayesian network is a factored representation of a Bayesian network, where the nodes are time-indexed on a discrete scale. The nodes are indexed over adjacent time steps. There are two types of links: classic Bayesian network links and so-called temporal relationships. The latter make

it possible to define conditional probability tables for a node depending on the state of its parents at an earlier point in time. The application of a dynamic Bayesian network to the SARGOS system makes it possible to integrate notions of time into the decisions to be taken in response to an attack, and its influence on the evolution of the threat.

Finally, another interesting approach would be to draw upon a tailored ontology [21]. This would potentially improve the model of knowledge integrated into the Bayesian network. It would make it possible to formalize knowledge upstream, and to consolidate threat-detection and identification steps.

6. References

1. N. Brown, "Taking the Fight to the Pirates," Jane's Information Group, 2006.

2. United Nations, "United Nations Convention on the Law of the Sea," 1982, available at www.un.org/Depts/los/convention_agreements/convention_overview_convention.htm.

3. International Maritime Organization, "Reports on Acts of Piracy and Armed Robbery Against Ships,"2001-2008, www.imo.org.

4. M. Ryan, "Captain Counts the Cost of Piracy," *BBC News*, 2006, news.bbc.co.uk.

5. J. S. Burnett, *Dangerous Waters, Modern Piracy and Terror on the High Seas*, New York, Dutton, 2002.

6. D. R. Dillon, "Piracy in Asia: A Growing Barrier to Maritime Trade," *Heritage Foundation Backgrounder*, #1379, 2000, available at www.heritage.org.

7. D. J. Nincic, "Maritime Security as Energy Security: Current Threats and Challenges," in G. Luft and A. Konin (eds.), *Energy Security: Challenges for the 21st Century*, Washington DC, Greenwood Publishing in collaboration with the Institute for the Analysis of Global Security (IAGS), 2009.

8. B. M. Jenkins, "Potential Threats of Offshore Platforms," Rand Corporation, 1988.

9. M. Kashubsky, "Offshore Energy Force Majeure: Nigeria's Local Problem with Global Consequences," *Maritime Studies*, 2008.

10. M. Morel and J. Broussolle, "I2C, Interoperable Sensors and Information Sources for Common Detection of Abnormal Vessel Behaviours and Collaborative Suspect Events Analysis," Maritime Systems and Technology (MAST) 2011, Marseille, 2011.

11. M. A. Giraud, B. Alhadef, F. Guarnieri, A. Napoli, M. Bottala-Gambetta, D. Chaumartin, M. Philips, M. Morel, C. Imbert, E. Itcia, D. Bonacci and P. Michel, "SARGOS: Système d'Alerte et Réponse Graduée OffShore," Workshop Interdisciplinaire sur la Sécurité Globale (WISG) 2011, Troyes, 2011.

12. B. Harris, "Graph Theory and its Applications: Proceedings," Academic Press, University of Michigan, 2011.

13. A. Becker and P. Naïm, *Les Réseaux Bayésiens, Modèles Graphiques de Connaissances*, Editions Eyrolles, 1999.

14. C. Lee and K. J. Lee, "Application of Bayesian Network to the Probabilistic Risk Assessment of Nuclear Waste Disposal," *Reliability Engineering and System Safety*, **91**, 5, 2006, pp. 515-532.

15. L. D. Hudson, S. W. Bryan, S. Mahoney and K. Blackmond, "An Application of Bayesian Networks to Antiterrorism Risk Management for Military Planners," 2002.

16. J. E. Martín, T. Rivas, J. M. Matías, J. Taboada and A. Argüelles, "A Bayesian Network Analysis of Workplace Accidents Caused by Falls from a Height," *Safety Science*, **47**, 2, 2009, pp. 206-214.

17. K. Kalev and R. Dechter, "Stochastic Local Search for Bayesian Networks," 7th International Workshop on Artificial Intelligence and Statistics, 1999.

18. X. Chaze, A. Bouejla, F. Guarnieri and A. Napoli, "The Contribution of Bayesian Networks to Risk Management in Oil Field Piracy," Workshop on Information Technologies for the Maritime Sector (ITEMS) 2012, Busan, 2012.

19. A. Bouejla, X. Chaze, F. Guarnieri and A. Napoli, "Bayesian Networks in the Management of Oil Field Piracy Risk," 8th International Conference on Risk Analysis and Hazard Mitigation, Island of Brac, 2012

20. T. Dean and K. Knazawa, "A Model for Reasoning About Persistence and Causation," *Computational Intelligence*, 1989, pp. 142-150.

21. A. Vandecasteele and A. Napoli, "Spatial Ontologies for Detecting Abnormal Maritime Behavior," OCEANS 2012, Yeosu, 2012.

Footnotes:

[1] *A radar emits microwave pulses towards the target. These signals are then reflected and intercepted by the radar receiver, which also collects an electric signal, called the "echo."*

[2] *These systems bring together optics and electronics. They usually consist of an optical sensor, an image-processing system, and a display or data-recording system.*

[3] *The SARGOS project partners are:*
SOFRESUD, 777 av. de Bruxelles, 83500 La Seyne sur Mer
ARMINES/CRC, Rue Claude Daunesse, 06904 Sophia Antipolis
CDMT, 3 avenue Robert Schuman, 13628 Aix en Provence Cedex 1
CS Communication & Système, 230 Rue Marcellin Berthelot, 83130 La Garde
DCNS Division Systèmes d'Information et de Sécurité, BP 403, 83055 Toulon Cedex
ROCKWELL COLLINS France (RCF), 6 avenue, Didier Daurat, BP 20008, 31701 Blagnac Cedex
TESA, Télécommunications Spatiales et Aéronautiques, 14-16 Port Saint Etienne, 31000 Toulouse

Application of the *Extended Ground Truth* Concept for Risk Anticipation Concerning Ecosystems

Antoine Gademer
Laurent Beaudoin
Loïca Avanthey
Jean-Paul Rudant

Abstract

Mapping is a fundamental tool in the study of ecosystems. It is usually done by field records, but this method consumes a lot of time and resources. Remote sensing is a complementary tool, but still needs ground-truth certification, due to the scale factor. In this article we present a concept, the *Extended Ground Truth*, which tries to keep the advantages of both mapping and remote-sensing techniques. The concept offers the use of imaging tools while providing a ground truth. We then develop this concept using one example concerning ecosystem analysis.

1. Introduction: Dynamic Cartography of Ecosystems

Mapping vegetation and its dynamics are major challenges for the study of ecosystems. Beyond the interest in fields such as forestry or agriculture, we place this article in the context of risk prevention: erosion, invasive spreading of weeds (plant species initially foreign to the environment where the species added itself [1]), health risks, etc.

1.1 Pest Plants

Indeed, among the plants brought by men from abroad, some have become invasive to a point where they gradually force the disappearance of the native vegetation, and form large homogeneous patches. These species are referred to as pest plants [2, 3]. These invasive species have several formidable qualities. They generally produce much fruit that is widely disseminated, by birds, small mammals, or, more rarely, by the wind, and they generally do not suffer from parasites or pathogens. They form massive homogeneous patches that slow or block the forest dynamics, and they can also affect the herbaceous undergrowth. Colonization occurs mainly by taking advantage of an opening in the environment, whether natural or artificial. Once installed, by their ability of vegetative or sexual multiplication plant pests quickly become dominant over the natural vegetation, blocking any alternative process of native settlement. By the deep modification of the ecosystems (soils, flora, fauna, etc.) plant pests can thus provoke serious problems in many human activities (agriculture, fire, diseases, etc.), and cannot be put aside.

The risk management of biological invasions is difficult to conduct. Controlling illegal imports of plants is quite illusory. In addition, the behavior of newly imported plants is unpredictable, and the risk of having a new plague is greater than ever. To illustrate the importance of plant pests, we can take, for example, the case of Réunion Island. Réunion Island is particularly sensitive to biological invasions of plants and animals. The biological reasons are fundamental: isolated for millennia (about three million years), this island was not immediately settled by many species, as only a few of them have had the opportunity to move there, brought by air currents or by marine birds. Before the arrival of humans, the flora of Réunion was unique but fragile, and relatively poor. Exceptionally protected, Réunion was discovered and colonized by humans until the seventeenth century. Since that date, there have been many introductions, and no equilibrium has been established among the indigenous communities and invasive plants, with invasions taking place before our eyes. However, today it is generally accepted that 30% of the surface of the island (60,000 ha) is still covered with primary formations. The wild flora of Réunion is composed of about 650 flowering plants, native or endemic, and more than 450 exotic species, brought by humans since the seventeenth century.

Antoine Gademer, Laurent Beaudoin, and Loïca Avanthey are with the Laboratoire ATIS, ESIEA Paris, France; E-mail: antoine.gademer@gmail.com; laurent.beaudoin@esiea.fr. Jean-Paul Rudant is with the Laboratoire ESYCOM, Cellule TIG – Universite Paris-Est-Marne-La-Vallee.

This invited paper is part of the special section on the "Role of Radio Science in Disaster Management."

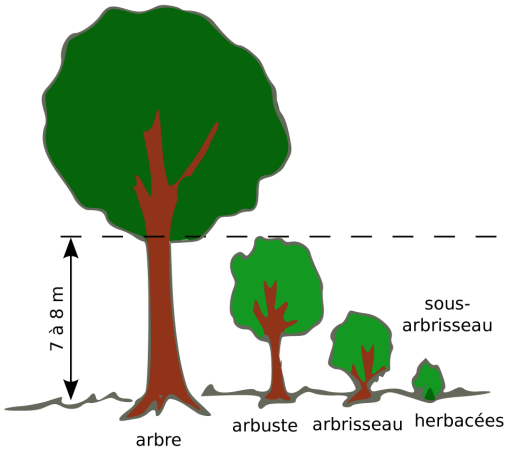

Figure 1. The scale distinctions between plants (source: Gademer).

The case of *Prosopis juliflora* is quite illustrative. It was deliberately imported in the 1920s [3] on the island of Réunion to reforest the lower slopes of the West Island, and for livestock feed. The plant has not fulfilled any of these functions. However, it quickly colonized much of the coastal plains, where it behaves as a dangerous invader.

Mapping is thus necessary to understand the complex interactions of plant species with each other, their environment, and the animal species. Mapping allows monitoring and anticipating the evolution of potential risk situations.

1.2 Plant Species Classification

1.2.1 Static Criteria and Constraints

Since the time of the great naturalists – such as Linnaeus and Buffon, who laid the foundations for the observation of species and their classification [4] – biologists have attempted to clarify these classifications. They have done this through careful observation, based on the shape of individuals (popular classification), their properties (phenotypic classification), or, more recently, based on how they relate genetically (phylogenetic classification) [5].

Reliable species discrimination remains an important issue. Within an ecosystem, we can make a primary distinction based on scale. We speak of bushes for trees measuring up to 7-8 m high. Meanwhile, shrubs are perennials (a perennial plant has a life cycle that exceeds two years, as opposed to annual and biennial plants) and are branched from the base: they also have a small height. Unlike bushes, they do not have a distinct main trunk. Their multiple trunks are usually less than five centimeters big. For their part, herbaceous plants are defined in opposition to woody plants, such as trees or shrubs that produce wood. We show these distinctions in Figure 1.

Considering the small size and the high density of the last two representatives we have described above, the risk of misclassification is significant. This especially true since some species have very similar phenotypes, are closely intertwined with their parasites, or are overlapped with other plants that share their environment. All these criteria are constraints that make it difficult to distinguish species from each other.

1.2.2 Dynamic Criteria

To improve discrimination, this static view of species can be complemented by a dynamic vision of individuals within their ecosystems. Indeed, the study of the dynamics of the natural environment seeks to understand the interactions between species and their environment, as well as the evolution in time of these interactions. This requires relying on knowledge of taxonomy and physiology, as well as on knowledge of climatology, geology and pedology. It is then possible to rely on the phenological characteristics of plants, that is to say, the influence of the seasons and of

Figure 2a. An example of manual mapping methods: an ecologist forester measuring the diameter of trees near the Smithsonian Environmental Research Center (source: K. Bauer/SERC).

Figure 2b. An example of manual mapping methods: Soil coring by the members of the French National Museum of Natural History (source: B. Riera/CNRS-MNHN).

Figure 2c. An example of manual mapping methods: Measuring the linear profile of the ground height with a contact profilometer (source: weru.ksu.edu).

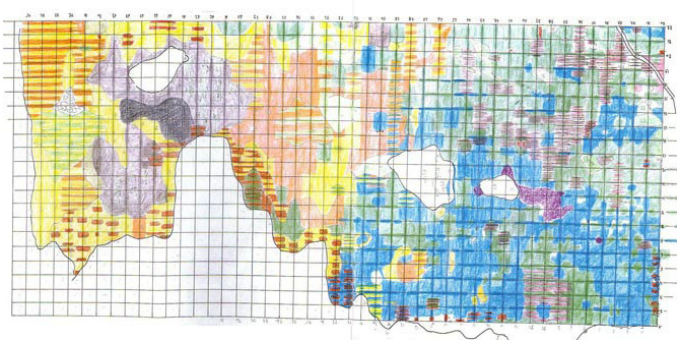

Figure 2d. An example of manual mapping methods: A map locating different phytogeographical groups (source: ONF [9]).

climate variations on plants' cyclical phenomena, such as germination or flowering. Some annual or biennials plants are visible only during part of the year, and in perennials, species looking similar stand out more clearly during flowering. Moreover, as they do not necessarily bloom at the same time, this reduces the risk of confusion.

The dynamic cartography of ecosystems is then a special task, which requires both accurate spatial tracking and a series of instantaneous temporal classifications, adapted to the lifestyle of individuals.

1.3 Mapping Methods of Plant Species

The dynamic evolution of ecosystems is studied by developing repeated land maps that incorporate spatial and temporal parameters of the classification. The location, the extent, the surface biophysical parameters (species, age, health, etc.) and geophysical parameters (soil type, moisture, exposure, etc.) of each group of individuals are identified and annotated. These maps are all representations of the state of the study area at the time of completion of the study.

Such studies, such as those described by Heller and Zavaleta [6], may extend over long periods of up to several decades. In botany, where the species usually have relatively long life expectancies (about 50 years for shrubs, a hundred years or more for trees), the periodicity of dynamic maps is of the order of three to ten years.

It should be noted that many species of weeds are annuals or biennials, and thus have much faster life cycles. We therefore note that in the context of risk prediction, it is necessary that the frequency mapping should be even higher than in the classical studies of ecosystems.

1.3.1 Manual Mapping

In the absence of an alternative technique to grasp this field truth, the dynamic mapping of the living is often done manually, via the annotation of paper charts by a small team of researchers and students (see Figure 2).

As we quickly found out with the botanists of the French National Museum of Natural History (MNHN) (Tropical ecology, UMR 7179, Ecology and Management of Biodiversity Department, CNRS – MNHN), this manual mapping involves tedious logistics. Both human and financial costs rapidly become a limiting factor for the quality and quantity of observations. The scope of the work of analysis and interpretation is therefore reduced, despite the use of statistical techniques and the definition of a representative sample of study sites.

In addition, a sub-meter mapping of a few acres can last several months: the surfaces of the study areas covered are therefore often small. For example, it takes about five weeks for an MNHN team of two botanists to cover two hectares of their study area. Under these conditions, any limitation of resources quickly results in reducing the mapped area, thereby penalizing the statistical quality of the final study.

This extended period of transcription spent in the field is the cause of other problems. First, the accuracy of mapping is affected: the time required for the description of each individual is prohibitive. Botanists then define phytogeographical groups – relatively homogeneous – which they spatially characterize with an accuracy of about 20 cm. These groups are approximations of floristic characteristics of individuals: for example, "Calluna *vulgaris* plants that measure less than 40 cm." However, they do not consider the possible mixing of species within a group, the density of individuals, their specific age, or their state of health.

However, this also raises the reliability of the classification. We discussed the possibility of relying on the phenological characteristics of species to improve the distinction, but this advantage can turn into a disadvantage because of the long mapping period: in a month of work, the same phenological phenomena can change the appearance of plants, and then disturb the viewer. To this must be added the fact that manual mapping is subject to a strong

Figure 3a. An image acquired by aerial remote sensing.

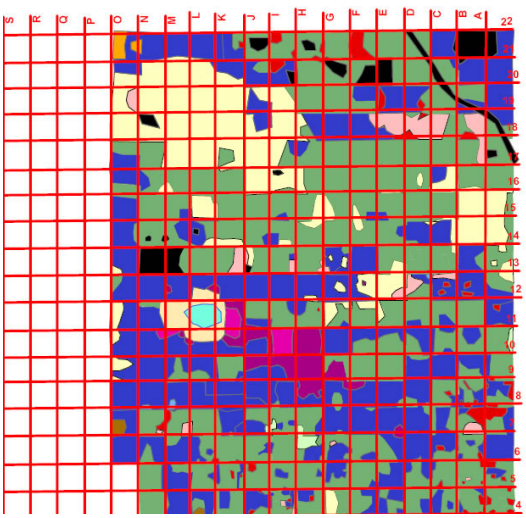

Figure 3b. An example of a map created from the image of Figure 3a.

subjective bias. This increases the degree of uncertainty in the data when comparing maps of the same area of study, made without consultation by different observers. It should also be noted that for lack of sufficient statistical visibility, species underrepresented and/or short-lived cannot be integrated into the mapping at the expense of the analysis of the entire ecosystem.

It is noteworthy that the manual mapping of phytogeographical groups is meticulous work, which must adapt to the natural cycles of species we seek to identify. If a floristic approach, based on individuals, would be much richer and more interesting for botanists, it is often unattainable, given the current resources at their disposal.

1.3.2 Remote-Sensing Mapping

Another way to achieve these maps is to use advanced imaging techniques (see Figure 3). Indeed, we have seen significant benefits in monitoring the dynamics of ecosystems through the use of remote sensing [7]. In the article of Lu [8], we saw more specifically the potential of remote sensing for the assessment of plant biomass above the ground, that is, all the living resources (trees, shrubs, plants, etc.) in a given space.

Remote sensing offers the opportunity for mapping out faster than manual mapping. It thus allows considering several observations of the phenological cycle (flowering, leafing, leaf coloration, etc.) at different times, offering at the same time a much better identification or differentiation of individuals: if calluna and heather are difficult to distinguish with the naked eye, they do not have the same flower or the same time of flowering. Two observations at two epochs carefully chosen may allow easy differentiation, and the identification of certain short-cycle plants (visible only for a few months, such as the crucifers of the rumex acetosella).

It must be said that the limits of this system are generally a mismatch between the scale of measurement in the field and the level of the acquired images. If spatial remote sensing allows observation over large spatial and temporal scales, it generally lacks precision for understanding the complex phenomena involved. It is then usually necessary to certify the data by field surveys: what we commonly call *ground truth*. We can cite the work of [9] and [10], which sought to establish a relationship between the local measurements obtained during field surveys, and characteristics (spectral signature, texture, or volume) of the data acquired by satellites, in order to extrapolate this relationship to the study of much larger areas.

Another critical point concerns the accuracy of the mapping. Indeed, if forest maps can rely in part on aerial or satellite imagery [9, 10], mapping of shrubs and herbaceous plants can usually only be done by manual annotation during field surveys. It is understood that the small size of these plants – between 20 cm and 1 m – and their high density and degree of entanglement do not allow conventional approaches based on the interpretation of remote-sensing images, which are used to count trees.

2. The Extended Ground Truth Concept

In the previous section, we have seen the need for a new concept, incorporating potential benefits of both imaging and field-survey methods. This new concept would significantly improve the extraction of biophysical and geophysical surface parameters in field missions. For this to work, it is necessary to work with data (images) at the scale of individuals.

Our new concept, Extended Ground Truth, can be stated as a methodology for ground-truth data acquisition

Feature	Land records	Classical Remote Sensing
Source of analysis	Instant and volatile	**Perennial images**
Repeatability	Subjective bias	**Systematization possible**
Method of measurement	Manual	**Automated**
Mission time	Limited by the human factor	**Extended by the possibility of delayed analysis**
Schedule	**Adapted to the phenology of species**	Determined by orbital or administrative constraints
Measures	**Direct measurements (size, color, etc.)**	Estimated based on the properties of the sensor
Certitude	**Ground truth**	Interpretation of a signal

Table 1. A comparison of the features of land surveys and classical remote-sensing techniques. In bold, the characteristics we want to keep in Extended Ground Truth.

of biophysical and geophysical parameters at the level of individuals, using advanced imaging techniques.

2.1 What Features to Keep Between Those of Land Records and Those of Classical Remote Sensing?

We examined which features of the two techniques – classical remote sensing and land records – it would be desirable to keep for performing remote sensing at the scale of individuals. These are described in the following sections, and summarized in Table 1.

2.1.1 Durability of Images

In a field survey, information analysis is made on-site, and only the land-cover mapping is carried out. It is therefore no longer possible to retrospectively reanalyze the data sources in the light of new information. With remote sensing, we acquire source images corresponding to a "snapshot" of the scene at a given time, and we then analyze the images to extract the land-cover map. Being able to keep the source images of a study for another study permits reanalyzing them given additional information. Furthermore, if they are geometrically rectified, the source images are stackable. This allows an easier comparison of the dynamic changes from one period to another. With Extended Ground Truth, we want to keep this property. We want to produce images of comparable sources that can be analyzed at leisure, to extract information from the highest level (as surface parameters) of interest to botanists.

2.1.2 Repeatability

The great difficulty in field surveys is to produce homogeneous information. Indeed, the observation conditions change during the mapping (light, tiredness, etc.), or from one study to another (not the same person, not exactly the same instructions, etc.). When working as a team, botanists locate the data each time in an absolute and identical reference, based on a decametric grid positioned using GPS, and allowing a comparison study. However, if another team needs to choose another reading grid, data comparison can be problematic.

Nowadays, the use of photography in land records is not subject to any shooting constraint (generally, oblique photographs are taken by hand, showing the global situation), and photographs are therefore difficult to compare. In remote sensing, the intrinsic rigidity of the images allows stacking the images acquired in different studies, when they are rectified in geometry and acquired at consistent scales. This capability of the repeatability of the acquisition in almost identical conditions is an important advantage of remote sensing, and we seek to keep it when measuring in Extended Ground Truth.

2.1.3 Automatic Analysis

Due to the high repeatability of the acquisition of source images, the conditions of the extraction of the parameters of surfaces are generally similar. The processing of remote-sensing images has become increasingly automated (segmentation, calculation of indices or surface parameters, classification, etc.). Based on imaging, the Extended Ground Truth concept is obviously trying to tap into this arsenal, to give researchers in the field the best tools for their studies.

2.1.4 Mission Time

In addition, we note another methodological change: during land records, the interpretation of the information is performed on-site in the form of paper maps and GPS readings. The information is then digitized in the laboratory. In contrast, the use of imagery allows the digitization of information directly on the ground, and later analysis in the laboratory. As the longest work is generally the analysis, by

allowing later analysis Extended Ground Truth can enable devoting precious time spent in the field to the point. This allows us to study a larger area, or to repeat the acquisition more often (for example, at both morning and evening, which allows the use of other phenological properties), or to reduce costs.

2.1.5 Acquisition Schedule

On the other hand, conventional remote sensing is not a panacea for mapping at the scale of individuals. Gigantic sensors, sometimes located thousands of miles away, are used. They are subject to external constraints (orbital or aerial constraints, cloud cover, etc.), which can be extremely demanding. By definition, a sun-synchronous satellite can never take pictures at a different time than that for which it was provided, and the period between two acquisitions is limited by the satellite's time revisit of the site.

The use of an air carrier (airplane, microlight, etc.) offers greater flexibility than satellite imagery, although traffic in the airspace itself is highly regulated (flight plan, need for an aerodrome and a driver, etc.). However, the main obstacle to the use of airborne imagery is its cost (usually between five and 10 times that of the satellite's).

To find intermediary acquisition vectors that enable both operational flexibility and a reasonable cost, we must turn to extremely-low-altitude remote-sensing tools. These are usually flying machines, robotic or otherwise, which do not exceed a ceiling of 150 m, but allow photographic material as their payload: kites, balloons, aircraft models (manned), or drones (automated). Because of their versatile features and their ability to be directly used from the field study, these tools are close allies of Extended Ground Truth.

2.1.6 Direct Measurements of Characteristics

Remote-sensing analysis, unlike land surveys, does not provide direct measures of individual characteristics, but these measures are inferred from the interpretation of source images. To extract dendrological phenotypic parameters, it is essential to have a complete and sufficiently precise view of individuals. Most of the time, this is not possible with conventional remote sensing. However, with the use of extremely-low-altitude remote-sensing tools, Extended Ground Truth allows high-resolution mapping at the scale of individuals, and thus allows the extraction of these parameters.

2.1.7 Certification

Using imagery to perform ground truth is a big gamble. By definition, remote sensing is indeed a science of interpretation of the physical properties (optical, roughness, etc.) of objects to determine their nature. This is why remote-sensing studies are usually doubled by field studies to define a punctual ground truth, giving a confidence indicator on the analysis carried out by remote sensing. In the case of Extended Ground Truth, the initial idea is to expand opportunities for land records. We therefore had to find a way to abstract this constraint. How can the opportunity be given for experts to certify the results automatically obtained by means of Extended Ground Truth? The answer is by acquiring the images of sources at a scale where visual interpretation is unquestionable, in other words, by taking the images at the scale of the individuals.

2.2 What is New with Extended Ground Truth?

The idea of using images acquired at a smaller scale to serve as ground truth is not new. In fact, [11] showed the interest of photographs taken by hand from a small plane for the interpretation of optical and radar images acquired by satellites. However, if these oblique images allowed the confirmation of their assumptions, they do not allow them to retrieve surface parameters. In addition, no shooting constraint was determined for the acquired images, and these were not used for the production of maps, but only as ground truth. In their case, [12] used low-altitude remote-sensing tools, such as hang gliders and helium balloons, with the same goal. However, again, the images were not sufficiently accurate to be used beyond visual interpretation. These examples are typical of the role previously reserved for imaging in land records.

In a complementary approach, [13] proposed the development of a tool allowing the acquisition of spectral responses from the vegetation to serve as a formalized ground truth for satellite images. Their sensor was carried by a truck crane, so it did not meet the desired criterion of operational flexibility. However, these studies showed the need and the possibilities offered by high-resolution data acquired on the ground for the analysis of results on a larger scale obtained by satellite remote sensing.

The work in [14] and [15] (tethered balloon), [16, 17] (airships), [18] (kites), [19] (automated paragliding), [20] (controlled model airplane), [21] (automated aircraft), [22] (controlled model helicopter), and [23] (automated helicopter) showed spectacular advances in recent years in remote sensing at low altitude. These tools provided a mapping with millimeter or centimeter accuracy, and were therefore ideally suited to mapping at the scale of individuals. However, apart from work in precision agriculture, it is unusual to consider plants smaller than trees at the scale of individuals, and to take into account their biophysical characteristics. This is why we propose a formalization of the concept of Extended Ground Truth that seems to be a promising lead for research on extracting biophysical and geophysical surface parameters in general, and for vegetation mapping at the scale of individuals, in particular.

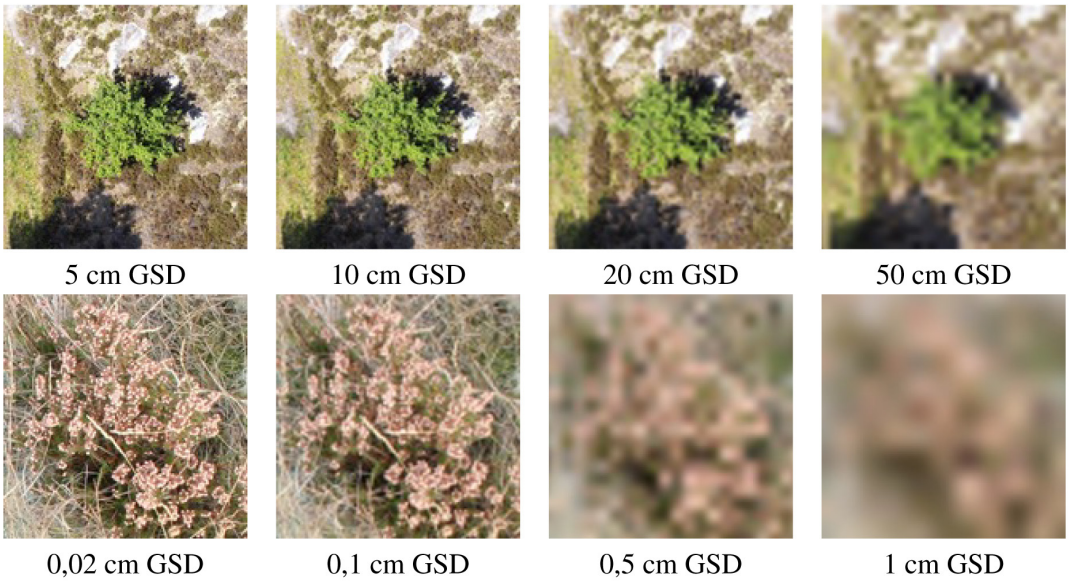

Figure 4. Examples of simulated images of two scenes. The size of the GSD varied during the acquisition, although it is displayed on the same scale. We see that the sample size, which corresponds to the area on the ground for a photo site, determines the size of the smallest identifiable object in the image.

2.3 The Extended Ground Truth Methodology

To produce Extended Ground Truth, it is necessary to take into account a number of technical constraints. In this section, we formalize the concept and describe the different stages of the feasibility study, in order to be able to take images that meet the criteria.

2.3.1 Determining the Size of the Ground-Sample Distance

In order to map at the scale of individuals, we must begin by questioning the size of the individuals we want to observe in the study area. This allows us to define the size of the ground-sample distance (*GSD*, in millimeters) needed for mapping. As we can see in Figure 4, we consider the smallest identifiable object on an image corresponding to a given *GSD* as having a size of about five to 10 times the size of the *GSD*. For example, if we wish to observe mangroves the crown of which is about 30-50 cm in diameter, we need a *GSD* from 50 mm (the limit of distinction: this size allows distinguishing objects with a size of at least 25-50 cm) to 10 mm (very detailed: this size allows distinguishing objects with a size of at least 5-10 cm). If we want to observe the flowers or leaves on the crown, we may consider a more specific *GSD* of 1 mm, for example.

Once we have fixed the interval, the choice of the *GSD* depends of the analysis we want to achieve. This will require more or less detailed views (density evaluation, delineation of parcels, etc.). The choice of the *GSD* also depends on other feasibility constraints that we address in the following sections. For the remainder of the study, we will do the calculations for several typical values of this interval.

2.3.2 Determining the Type of Sensor

It is next necessary to choose the type of sensor that can meet the needs of the mission. The choices are numerous: compact digital or reflex camera, aerial camera, LIDAR, etc. The type of sensor itself (camera, video camera, etc.) depends in particular on the needs for the analysis, and on constraints such as weight and size (the throw weight of the carrier, as we will see later), cost and availability, etc. However, some of the most important criteria in the feasibility study correspond to the optical properties of the sensor. We are mainly interested in maximum exposure time, pixel resolution, width of the optical chamber, and focal length.

2.3.2.1 Estimating the Maximum Flight Speed According to the Constraints of the Sensor

The maximum exposure time of the sensor ($TimeExp_s$ in seconds) will constrain the flight speed to avoid motion blur in the shooting (Figure 5). For a given *GSD* (GSD_{min} , in millimeters), the maximum flight speed ($vmax_{mm/s}$, in millimeters per second) is given by Equation (1):

$$vmax_{mm/s} < \frac{GSD_{mm}}{2TimeExp_s} . \quad (1)$$

Figure 5. (a) An image without motion blur, and (b) an image with motion blur.

We consider that the carrier should not move more than half of a pixel during the acquisition (an empirical estimation validated by our experiments). Note that the exposure time depends on the lighting conditions, and on the aperture of the device.

2.3.2.2 Estimating the Necessary Flight Height According to the Constraints of the Sensor

The resolution (R_{pix} , in pixels), the width of the optical chamber (L_{mm} , in millimeters), and the focal length (f_{mm} , in millimeters) allow us to determine the flight height (H_{mm} , in millimeters) needed to obtain the desired GSD (GSD_{mm} , in millimeters) (Figure 6). This is given by Equation (2):

$$GSD_{mm} = \frac{L_{mm}}{R_{pix} f_{mm}} H_{mm} \Leftrightarrow H_{mm} = \frac{R_{pix} f_{mm}}{L_{mm}} GSD_{mm} . \quad (2)$$

2.3.2.3 Estimating the Scan Swath According to the Constraints of the Sensor

The resolution of the sensor (R_{pix} , in pixels) will allow us to calculate the total width of the surface seen on an image, called the scan swath (F_{mm} , in millimeters). For a given GSD (GSD_{mm} , in millimeters), we have

$$F_{mm} = R_{pix} GSD_{mm} . \quad (3)$$

We will use this to estimate the maximum time we should have between two shots, and also the time of over-flight of the area.

2.3.2.4 Estimating the Overlap Rate Between Two Shots According to the Constraints of the Sensor

From the scan swath (F_{mm} , in millimeters), we can estimate the base (B_{mm} , in millimeters) that corresponds to the distance between two shots (Figure 7). This value will constrain the overlap rate (r_{prct} , percent expressed as a fraction), an important parameter for image mosaicing (which needs an overlap of about 30%), or to create stereo pairs (which needs an overlap of about 60%). This information is grouped into Equation (4):

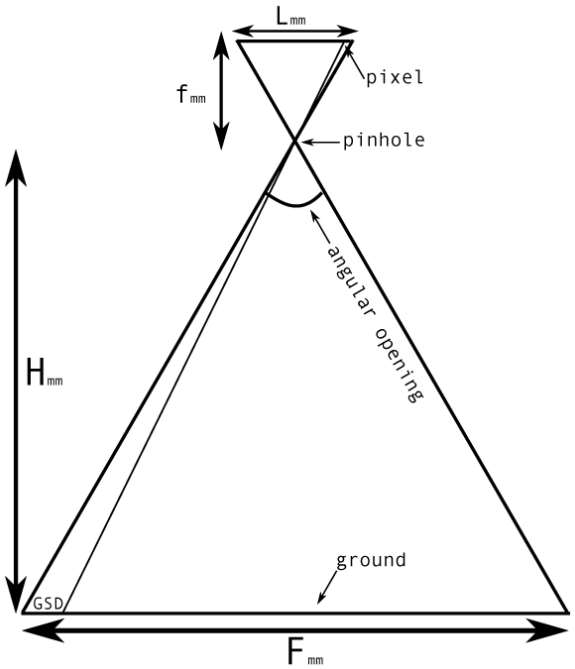

Figure 6. An illustration of the relationships among the scan swath (or the GSD), the parameters of the sensor, and the height of flight.

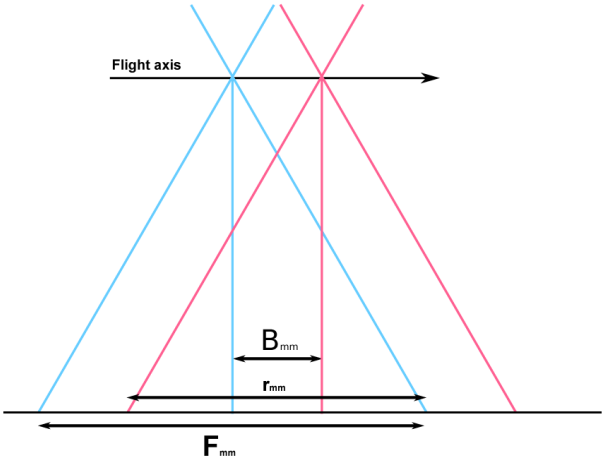

Figure 7. An illustration of the relationships among the scan swath, the base, and the overlap rate.

$$B_{mm} = F_{mm}\left(1 - r_{prct}\right). \quad (4)$$

According to Equation (3), we thus obtain

$$B_{mm} = R_{pix} GSD_{mm}\left(1 - r_{prct}\right). \quad (5)$$

Once the speed of flight is set, this will tell us the maximum time ($tmax_s$, in seconds) between two shots required in order to get the desired overlap rate. It is necessary to check that the sensor is able to perform two consecutive shots in this period.

$$tmax_s = \frac{B_{mm}}{vmax_{mm/s}} \quad (6)$$

$$= \frac{R_{pix} GSD_{mm}\left(1 - rprct\right)}{vmax_{mm/s}}.$$

2.3.3 Determining the Type of Carrier

Constraints obtained from the sensor will help determine the choice of the carrier, in terms of the throw weight, the speed of flight, as well as the flying height. If the carrier does not meet these constraints, we must find another one that fits best, look for another sensor, or review the requirements about the *GSD* until we find a satisfactory solution.

2.3.4 Validation of the Choices: Time and Cost of the Mission

Finally, we estimate the coverage and therefore the required flyby time to complete the mission, and therefore its cost.

For the case of a rectangular area with a width less than the width of the scan swath ($l_m < F_m$, in meters) and a length (d_m , in meters), and given the speed of flight ($v_{m/s}$, in meters per second), the time (t_s , in seconds) to map this area is given by the classical formula

$$t_s = \frac{d_m}{v_{m/s}}. \quad (7)$$

However, if the area is larger than the width of the scan swath, the overlap rate must be taken into account. For example, if the width of the over-flown area is twice the width of the scan swath, it will take three flybys, and thus about three times the time calculated with the above formula (Figure 8). If we denote the width of the area by l_m , the scan swath by F_m , and the needed overlap rate by r_{prct} , we can deduce the following formula from Equation (7):

$$t_s \cong \frac{d_m \left\lceil \frac{l_m}{F_m}\left(1 + r_{prct}\right) \right\rceil}{v_{m/s}}. \quad (8)$$

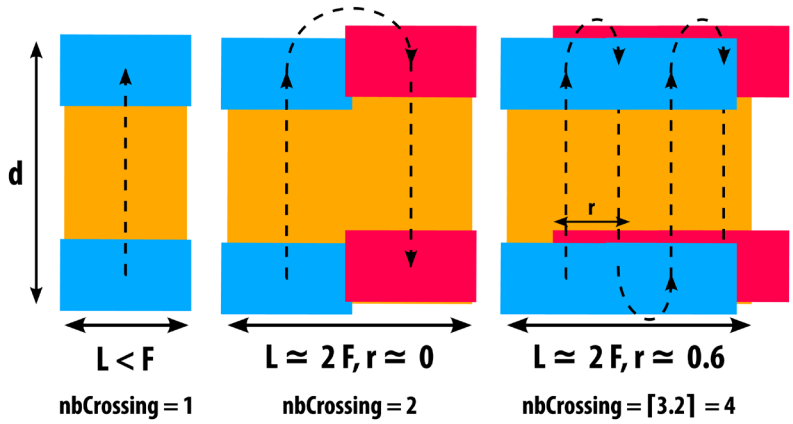

Figure 8. An illustration of the calculation of the flyby time based on the overlap rate.

Figure 9a. The location of the Mare aux Joncs area (source: Google Maps).

Figure 9b. What surrounds the Mare aux Joncs area (the study area is delimited by the red frame) (source: Google Maps).

Figure 9c. The study area (source: Google Maps).

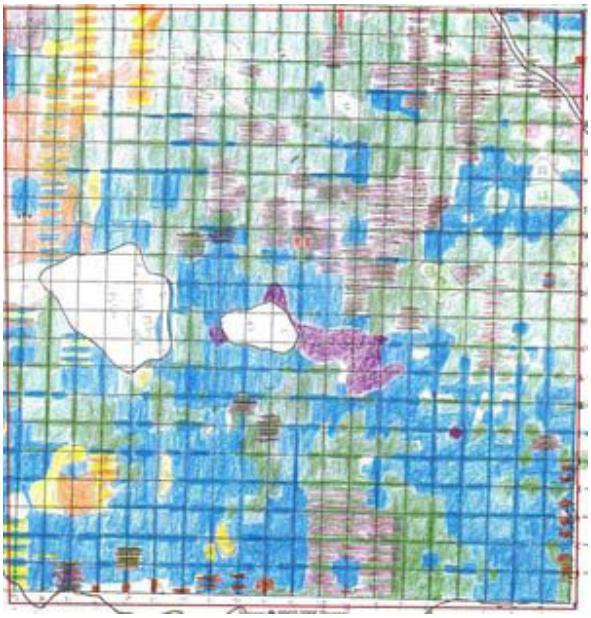

Figure 9d. A manual map of the study area (source: ONF).

The ceiling in the numerator corresponds to the fact that the number of passages (calculated from the width of the area, the width of the scan swath, and the overlap rate) is necessarily an integer (no halfway is possible). In the case of a rectangular field, we will consider the bounding rectangle.

We could add that the calculated time is a minimum time. We must account for the time required for flipping the carrier, and for performing the passages to reinforce the geometric constraints (perpendicular to the previous flights). We also have to take into consideration the constraints of autonomy, and the time to return to the ground station to change batteries.

Again, if the result is not satisfactory, we must return to the previous step and adjust the settings accordingly.

2.3.5 General Remarks

The process of selecting the sensors and carrier adapted to each mission is an iterative process. It seeks to minimize the various constraints of low-altitude remote sensing (the theoretical constraints, such as those we just developed, as well as constraints of feasibility, costs, or availability, etc.). Our experience shows that there is no single solution applicable in all circumstances, but there is a methodology to roll out whenever necessary.

3. A Study Case: The Trois-Pignons Forest Area

In the context of this article, we present our collaboration with a team from the French National Museum of Natural History (Tropical Ecology, UMR 7179, Ecology and Management of Biodiversity Department, CNRS – MNHN). The objective was to study the evolution of the dynamics of vegetation on the Mare aux Joncs test area, located in the Trois-Pignons forest (France, see Figure 9). This area of four hectares stands on the boundary between heath-land and forest. It is mainly populated by shrubs (< 80 cm) and grasses, as well as isolated trees producing shoots.

Until this study, the mapping of this area was mainly conducted by manual land records, complemented by aerial ortho-images provided by the French National Institute for Geographic Information and Forestry (IGN). The aim of our work was to validate the interest of low-altitude acquisitions to obtain Extended Ground Truth.

To acquire the data, we needed an acquisition system composed of a carrier and optical sensors. Based on the presented methodology, we will see the reasoning that led us to the following choices: a micro-quadricopter, allowing stationary or slow flight, with a payload capacity of the order of kilograms, to be able to carry one or more sensor devices, such as cameras. We will describe this system in more detail in the following sections.

Figure 10a The Faucon Noir UAS.

Figure 10b. The Faucon Noir UAS in flight.

3.1 The Low-Altitude Remote Sensing Tool: Faucon Noir, a Light Homemade UAS for Centimetric Mapping

3.1.1 Choice of the System

In their manual mapping, the botanists of the French National Museum of Natural History consider only individuals greater than 10 cm in diameter. However, formal identification of the species of these individuals requires recognizing structural elements of only a few centimeters. We therefore estimated *a priori* that we needed a *GSD* better than 1 cm. Considering an average brightness and a standard diaphragm aperture, we set the exposure time to between 1/400 s to 1/800 s. Equation (1) gave us a maximum flight speed of the order of 7 km/h to 15 km/h, which eliminated most of the fixed-wing carriers that required a higher speed to sustain flight. Moreover, the desire of an important maneuverability to cover the whole study area in a semi-automatic mode, and the need for a strong resistance to wind gusts – up to 25 km/h in the area – eliminated carriers such as kites and balloons.

That left the vertical takeoff and landing (VTOL) vehicles: carriers such as helicopters (with a main rotor and a variable pitch), or multi-rotor aircraft (with multiple rotors and a fixed pitch). The VTOL carrier had the advantage of performing stationary flight or, with a speed as slow as you want, possessed a great maneuverability. They were easy to deploy (since they did not require a landing strip), but they generally have a limited endurance (they consume a lot of power to keep themselves in the air).

Although the carrying capacity of VTOL carriers does not reach the capacity of fixed-wing carriers or of tethered carriers, multi-rotors are distinguished from helicopters by their increased capacity to carry material. That made them very attractive to us. Moreover, with their short propellers, they were easier and safer to handle. However, unlike helicopters, which provide mechanical stability with the

Figure 10c. The Faucon Noir UAS in flight, equipped with one of its mapping payloads.

Size (without landing gear)	70 × 70 × 15 cm + 35 cm with landing gear
Weight (with batteries)	1.6 kg
Maximum weight available for payload	1 kg
Battery	Lithium Polymer 11.1 V 8400 mAh
Maximum power	1 kW
Endurance (no payload)	25 minutes
Endurance (with payload)	20 minutes
Frequency control	72 MHz
Frequency ground station	2.5 GHz
Maximum height (visual flight rule)	80 m
Maximum height (automatic mode)	150 m

Table 2. Main characteristics of our Faucon Noir UAS.

flybar and their long propellers, multi-rotors carriers are inherently unstable, which is generally offset by an active electronic control.

3.1.2 Our System

At the time of this study, there were not many multi-rotor systems commercially available, and none allowed carrying 1 kg of material. We therefore built our own prototype to meet the aforementioned constraints: a quad-rotor carrier (Figure 10), called Faucon Noir [24]. As usual for autonomous robotics, the system architecture was quite complex. There was a low-level assistant board (based on a real-time microcontroller chip) that ensured sustaining flight and communication with the pilot. There was a high-level computer that did the complex navigation, based on GPS data, and was also used as a flight-data recorder.

The low-level assistant was critical, as it controlled the attitude and motion of the UAV in real time and at high frequencies. It was developed with the greatest care. A malfunction of this card always meant a serious accident. Developed as flexible systems, other boards could be plugged in to add important functionalities, such as altitude control or full payload control (acquisition, orientation, and data recording). At the time of the study, our prototype had only an attitude control, a full payload control, and an altitude-measuring unit. It achieved only the minimal requirements for the mission. Nowadays, full attitude, altitude, and position controls are available on most commercial multi-rotor unmanned aircraft system (UAS) at a reasonable cost, strengthening the operational capacity of these tools. The flying robot was completed by a set of software tools running on the ground-station computer. This software allowed real-time checking of the state of the machine, provided a visual check of what was seen from the onboard cameras, and allowed acquisition control. The main characteristics of our Faucon Noir UAS are summarized in Table 2.

3.2 The Mapping Payload

3.2.1 The Choice of the Sensors

Considering the flight speed of our device, the *GSD* of 1 cm maximum we chose imposed a shooting period within six seconds (minimum speed), and three seconds (maximal speed) for an overlap rate to perform stereo-restitution (60%). This constraint was achievable for most commercial digital cameras. On the other hand, from an operational point of view, the instability of platforms such as a micro-unmanned aerial system make the reliability of

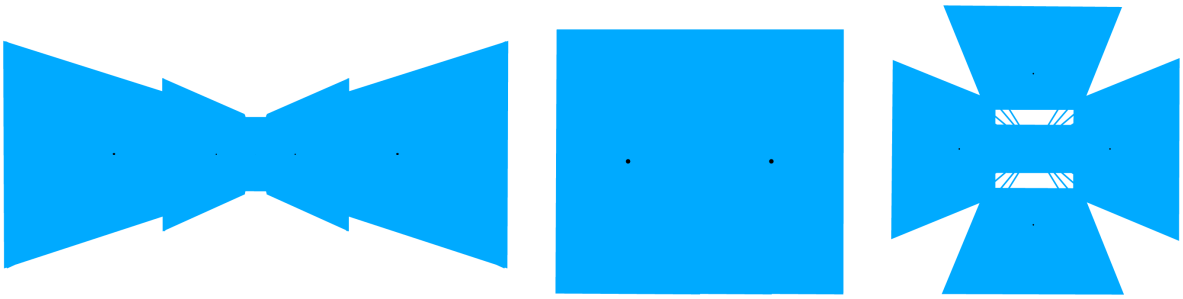

Figure 11. Representations of the scan swath for the three types of multi-camera systems cited: (l) the "fans" type; (c) the "block" type; (r) the "Maltese-cross" type.

the overlap rate difficult. We therefore decided to develop a dedicated mapping payload. Equipped with multiple cameras, it allowed simultaneously taking shots, and thus ensured obtaining synchronized stereo pairs.

We can distinguish three types of multiple-camera systems [25] (Figure11):

- The "fans" systems, which include several cameras aligned perpendicular to the axis of flight. They thus have strong incidence angles, and therefore strong geometrical deformations.
- The "block" systems, combining cameras having very low incidence angles, thus having little deformation.
- The "Maltese-cross" systems, consisting of a vertical camera surrounded by several oblique cameras. This type of system is particularly desirable for defense and security applications [26], as well as for mapping land use [27], due to the ease of visual photo interpretation of oblique images.

Our payload consisted of three devices aligned along the line of flight. The orientation of the front and rear cameras was adjustable in flight. This allowed us to get the "Maltese-cross" or "block" types of configurations, according to the needs of the mission (Figure 12).

The camera must have good image quality and support manual settings, while remaining as small and light as possible. References [28-30] showed that the quality of images produced by non-professional digital cameras was satisfactory for remote-sensing applications. Optical distortion due to non-professional lenses can be considered acceptable with fixed lens systems if one takes the trouble to perform a calibration before the flight. We chose three compact digital cameras weighing less than 200 g, thereby complying with the constraint of a payload less than 1 kg.

3.2.2 The Control of the Payload

Controlling a camera covers operations such as switching on, triggering the acquisition, and, in our case, dating and validating the shots. Another point for geo-localizing the data concerns the synchronization of shots between the devices themselves, and with the other sensors of the system. This was all the more important in that quad-rotor carriers can very quickly change position.

Generally, commercially available systems only deal with the triggering: the devices must be switched on manually, and users must settle for the dating inside the unit. The automated triggering systems that existed at the time of our study (mechanical, IR, etc.) did not meet our criteria. In our tests with an infrared remote control, we realized that the frequency of shooting was very low, the timing was unfortunate, and the order of shooting could be ignored if the camera was not ready. We thus chose a solution that was intrusive. We connected a homemade control card directly to the internal electronics of the camera. Our control card used the ability of a microcontroller to relay, analyze the signals from the device, and communicate with the rest of the system. It electronically triggered simultaneous shots and dated them when the acquisition signal was issued, all with an accuracy of about 20 milliseconds. The digital camera then became a fully controllable device.

3.3 Data Acquired and Results

Several hundreds of pictures were acquired with the system over the Mare aux Joncs study area. Many of them were blurred, due to the strong wind and the fact that our unmanned aircraft system was still under development at the time of the mission. The scale constraint was also a difficult goal to achieve with a quadri-copter without automatic height control (as can be found nowadays in most rotary or fixed wing unmanned aircraft systems). The automatic processing of the data was thus not feasible at that time. For the same reason, the 1 cm *GSD* constraint was not obtained for the whole sequence. Nevertheless, an automatic mosaicing algorithm was applied to a subset of the data with good results (Figure 13). This produced perfectly usable land-cover maps (geolocated orthoimages stackable on maps) for the identification of species.

Manual cartography was done during the test campaign. A second cartography was produced based on the sole observation of the image data, to allow comparison of the efficiency of the Extended Ground Truth methodology.

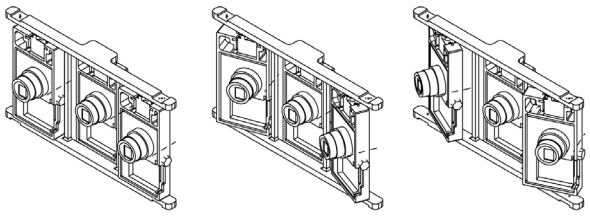

Figure 12a. Our tri-camera system: an illustration of the possible orientations of the cameras inside the system.

Figure 12b. The tri-camera system as built.

Figure 13a. A mosaic of the stackable orthoimages acquired for the area.

Figure 13b. An enlargement of the upper-right-hand corner of the mosaic shown in Figure 13a.

Reference [31] showed that compared to classical airplane images, the images acquired with a 5 cm *GSD* allowed the identification of trees, bushes, shrubs, and herbaceous plants. However, it was still not sufficient for close relative species of shrubs (indicating the need for lower acquisition) with a precision similar to manual cartography. The PhD thesis of the author of [31] concluded with strong interest in this method for ecosystem studies and general biodiversity management.

On our side, this test mission gave us satisfying elements showing that Extended Ground Truth had a concrete interest to enlarge the scope of field records. Obviously, a more reliable version of our unmanned aircraft system would allow us to perform better data acquisition, and to develop the full potential of automating the process. From an operational point of view, making several acquisitions of the same scene at different scales (1 cm *GSD* and 10 cm *GSD*, for example) could allow a stronger geo-localization of the images.

The oblique images produced (Maltese-cross mode) were used for visual interpretation (Figure 14). The stereo images (block mode) were used in the PhD thesis of [32] (Figure 15). This proved the feasibility of automatic extraction of the surface parameters (Figure 16), as ground roughness or dendrometric parameters, with low-altitude stereo couples.

Figure 14. A mosaic created with the oblique images.

4. Conclusion

In this article, we have presented the concept of *Extended Ground Truth*, which allows using the efficient tools of imagery while preserving the certification of the data (ground truth) usually provided by land records. To obtain data compatible with Extended Ground Truth, we developed the methodology that allows fixing technical choices according to the mission criteria. We have seen that this process is iterative, and that there is no universal solution.

We used this methodology to map ecosystems at the level of individuals in the study area of the Mare aux Joncs, with an acquisition system we developed. One of the background objectives of this study was to survey the invasion of the forest on the moor, a characteristic and thus protected area of the region. According to experts, the first results we obtained were very encouraging. We showed that the Extended Ground Truth methodology and the tools we used offer the possibility for precisely distinguishing plant species, even if they are very small. They thus make it possible to classify and produce precise and stackable maps, which could be reanalyzed at leisure.

Automatic recovery of ground truth greatly shortened the duration of the study. Although image analysis has so far

Figure 15. An example of an acquired stereo couple.

Figures 16a, 16b. Two views of the points cloud extracted from the stereo couple (source: Petitpas).

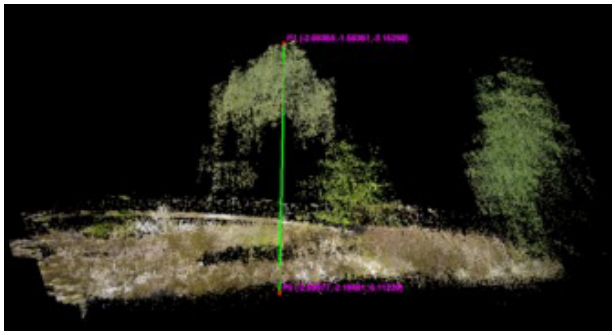

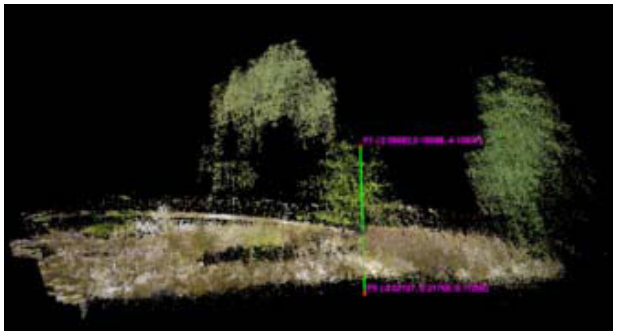

Figures 16c, 16d. Two examples of measures that have been tested with the cloud point (source: Petitpas).

been done mostly manually in our test mission, it is possible to consider the use of automatic classification algorithms. In addition, we explained that this type of mission, unlike conventional missions, is less subject to weather constraints or even geographical constraints (such as hard-to-reach areas, such as volcanic areas), because the system is very easy to deploy and quick to use. Accordingly, missions can be programmed almost on demand. As a result, they are more adapted to the phenological cycles of plants.

The classification accuracy, the speed of acquisition and analysis, and the ability to easily perform repeated acquisitions are three factors that allow us to consider the use of these methods and tools in studies of pest plants. Indeed, to counter these invasions, we need to monitor the evolution of species in an area and to dynamically map them. This must be done in order to detect abnormal proliferation of one of these species as soon as possible, even though their individuals may still be at an early stage in their evolution. The type of map produced with the Extended Ground Truth Methodology can therefore be one of the critical pieces of data used to prevent the emergence of such risk situations.

5. References

1. Universalis, "Encyclopaedia Universalis Version Électronique," 2012.

2. H. Perrier de la Bâthie, "Les Pestes Végétales à Madagascar," *Revue de Botanique Appliquée et d'Agriculture Coloniale*, **8**, 77, 1928, pp. 36-9.

3. R. Lavergne, "Les Pestes Végétales de l'île de la Réunion," *Info-Nature*, **16**, 1978, pp. 9-60.

4. J. McNeill, F. R. Barrie, H. M. Burdet, V. Demoulin, D. L. Hawksworth, K. Marhold, D. H. Nicolson, J. Prado, P. C. Silva, J. E. Skog, et al., "International Code of Botanical Nomenclature (Vienna Code)," 2006.

5. T. F. Stuessy, *Plant Taxonomy: The Systematic Evaluation of Comparative Data*, Columbia, Columbia University Press, 2009.

6. N. E. Heller and E. S. Zavaleta, "Biodiversity Management in the Face of Climate Change: A Review of 22 Years of Recommendations," *Biological Conservation*, **142**, 1, 2009, pp. 14-32.

7. J. R. Jensen, *Remote Sensing of the Environment: An Earth Resource Perspective*, Upper Saddle River, NJ, Pearson Prentice Hall, 2007.

8. D. Lu, "The Potential and Challenge of Remote Sensing-Based Biomass Estimation," *International Journal of Remote Sensing*, **27**, 7, 2006, pp. 1297-1328.

9. R. A. Houghton, D. Butman, A. G. Bunn, O. N. Krankina, P. Schlesinger, and T. A. Stone, "Mapping Russian Forest Biomass with Data from Satellites and Forest Inventories," *Environmental Research Letters*, **2**, 2007, pp. 045032.

10. P. Muukkonen and J. Heiskanen, "Biomass Estimation Over a Large Area Based on Standwise Forest Inventory Data and ASTER and MODIS Satellite Data: A Possibility to Verify Carbon Inventories," *Remote Sensing of Environment*, **107**, 4, 2007, pp. 617-624.

11. H. D. V. Böhmand F. Siegert, "Remote Sensing Verification by Aerial Surveys and Ground Truth Campaigns 1997 and 1998 in Central Kalimantan, Indonesia-Peat Swamp Forest, Mega-Rice-Project and Fires," Workshop on Tropical Forest and Remote Sensing, 1999.

12. J. Nogami, D. Phuon, and M. Kusanagi, "Field Observation Using Flying Platforms for Remote Sensing Education," Asian Conference of Remote Sensing, 2002.

13. Y. Minekawa, T. Edanaga, K. Uto, Y. Kosugi, and K. Oda, "Development of a Low-Altitude Hyperspectral Imaging System for Measuring Ground Truth in Agricultural Fields," IEEE International Geoscience and Remote Sensing Symposium, IGARSS 2006, pp. 2052-2055.

14. Troy Arnold Jensen, *Using a Remotely Controlled Platform to Acquire Low-Altitude Imagery for Grain Crop Mapping*, PhD thesis, Thèse de doctorat, soutenue en Novembre 2008, University of Southern Queensland, 2008.

15. B. Planer-Friedrich, J. Becker, B. Brimer, and B. J. Merkel, "Low-Cost Aerial Photography for High-Resolution Mapping of Hydrothermal Areas in Yellowstone National Park," *International Journal of Remote Sensing*, **29**, 6, 2008, pp. 1781-1794.

16. S. Lacroix, "Ballons Dirigeables Autonomes," 2007.

17. E. Hygounenc, I. K. Jung, P. Soueres, and S. Lacroix, "The Autonomous Blimp Project of LAAS-CNRS: Achievements in Flight Control and Terrain Mapping," *International Journal of Robotics Research*, **23**, 4-5, 2004, pp. 473.

18. I. Marzolff, J. B. Ries, and K. D. Albert, "Kite Aerial Photography for Gully Monitoring in Sahelian Landscapes," Proceedings of the Second Workshop of the EARSeL Special Interest Group on Remote Sensing for Developing Countries, 2002, pp. 18-20.

19. H. P. Thamm and M. Judex, "The "Low Cost Drone" – An Interesting Tool for Process Monitoring in a High Spatial and Temporal Resolution," ISPRS Mid-Term Symposium, 2006, pp. 8-11.

20. J. B. Vioix, *Conception et Réalisation d'un Dispositif d'Imagerie Multispectrale Embarqué: Du Capteur aux Traitements pour la Détection d'Adventices*, PhD thesis, Thèse de doctorat, Université de Bourgogne, 2004.

21. A. S. Laliberte, A. Rango, and J. E. Herrick, "Unmanned Aerial Vehicles for Rangeland Mapping and Monitoring: A Comparison of Two Systems," The American Society for Photogrammetry and Remote Sensing Annual Conference, Tampa, FL, 2007.

22. K. C. Swain, S. J. Thomson, and H. P. W. Jayasuriya, "Adoption of an Unmanned Helicopter for Low-Altitude Remote Sensing to Estimate Yield and Total Biomass of a Rice Crop," *Transactions of the ASABE*, **53**, 1, 2010, pp. 21-27.

23. A. Rango, A. Laliberte, C. Steele, J. E. Herrick, B. Bestelmeyer, T. Schmugge, A. Roanhorse, and V. Jenkins, "Using Unmanned Aerial Vehicles for Rangelands: Current Applications and Future Potentials," *Environmental Practice*, **8**, 3, 2006, pp. 159-168.

24. A. Gademer, B. Petitpas, S. Mobaied, L. Beaudoin, B. Riera, M. Roux, and J. P. Rudant, "Developing a Low Cost Vertical Take Off and Landing Unmanned Aerial System for Centimetric Monitoring of Biodiversity – The Fontainebleau Case," IEEE International Geoscience and Remote Sensing Symposium, IGARSS 2010, 2010, pp. 600-603.

25. Gordon Petrie, "Systematic Oblique Aerial Photography Using Multiple Digital Cameras," VIII International Scientific and Technical Conference "From Imagery to Map: Digital Photogrammetric Technologies," University of Glasgow, September 15-18, 2008, Porec, Croatia.

26. Gordon Petrie, "Systematic Oblique Aerial Photography Using Multiple Digital Frame Cameras," *Photogrammetric Engineering and Remote Sensing*, Février 2009, pp. 102-107.

27. M. Lemmens, C. Lemmen, M. Wubbe, et al., "Pictometry: Potentials for Land Administration," 2008.

28. M. R. Shortis, C. J. Bellman, S. Robson, G. J. Johnston, and G. W. Johnson, "Stability of Zoom and Fixed Lenses Used with Digital SLR Cameras," The International Archives of Photogrammetry, Remote Sensing and Spatial Information Sciences, 2006.

29. A. Habib and M. Morgan, "Stability Analysis and Geometric Calibration of Off-the-Shelf Digital Cameras," *Photogrammetric Engineering and Remote Sensing*, **71**, 6, 2005, pp. 733-741.

30. F. Remondino and C. Fraser, "Digital Camera Calibration Methods: Considerations and Comparisons," *International Archives of Photogrammetry, Remote Sensing and Spatial Information Sciences*, **36**, 5, 2006, pp. 266-272.

31. Samira Mobaied, The Spatiotemporal Dynamics of Vegetation and the Distribution of Biodiversity in Forest-Heathland Interfaces. Implications for Conservation Management of Nature Reserves, Thèse, Muséum National d'Histoire Naturelle, 2011.

32. Benoît Petitpas, Extraction de Paramètres Bio-Géo-Physiques de Surfaces 3D Reconstruites par Multi-Stéréo-Restitution d'Images Prises sans Contraintes, Thèse, Université Paris-Est de Marne-la-Vallée, 2011.

Two-Tier Femto-Macro Wireless Networks : Technical Issues and Future Trends

J. Zhang
Z. Xiao
X. Zhang
E. Liu

Abstract

Femto/small cells have been considered a promising technology in wireless communications for extending indoor-service coverage and for improving overall network capacity. Two-tier networks – where the current cellular networks, i.e., macrocells, overlap with a large number of randomly distributed femtocells – can potentially bring significant benefits to spectral utilization and system enhancement. In this article, we provide an overview of two-tier femto-macro cellular networks, together with insight into recent research activities and results. We focus on the following technical topics relating to two-tier femtocell-macrocell networks: spectrum allocation, interference management, and access control. Other key issues, such as backhaul, user mobility, and energy efficiency, are also discussed. Finally, we describe developing trends relating to femtocells, and conclude with describing possible future research directions.

1. Introduction

Mobile and wireless communications have undergone sustained and rapid growth in the first decade of this century. Due to the developments of new standards, such as the Third Generation Partnership Project (3GPP) and Long-Term Evolution (LTE), macrocellular networks have significantly improved the wide-range network coverage and mobile broadband communications. The increasing demand for higher data rates in the local area stems from the fact that over 60% of voice and 80% of data service occur in indoor scenarios [1]. The current macrocells are unable to provide sufficient wireless coverage and data throughput for the indoor environment, due to the wireless-signal attenuation incurred by long-distance propagation and blocking by obstacles. The "micromation" of cellular networks is one recognized means of alleviating this problem, through the utilization of microcells and picocells. However, this brings high operating expenses (OPEX) and capital costs (CAPEX) for operators [2]. Achieving higher data rates and better signal quality for indoor environments in a cost-effective way is therefore one of the major challenges facing wireless and mobile communications.

As an emerging technology for high-data-rate wireless provision, femtocells are small in size, and are user-installed base stations connecting to the Internet and the cellular network via a cable modem or digital subscriber line (DSL). They provide enhanced cellular services in indoor scenarios, such as residences or enterprises [3]. The deployment has been extended to outdoor hotspot scenarios. Femtocells first appeared in 2006, and were initially regarded as low-power and short-range access points, such as in the definition of *Home NodeBs* (HNBs) from 3GPP. The Femto Forum, which was founded in 2007 to support the development of femto technologies, has obtained support from more than 100 companies, including operators, suppliers, and content providers. In 2008, 3GPP LTE Release 8 proposed the design of Home Node-B, and remarked that femtocells had become a mainstream radio-access technology [4].

As an embodiment of small size and low-power base stations that have been deemed to be one of the revolutionary directions for future cellular wireless systems, femtocells have continuously attracted increasing attention from both industry and academia in recent years. The deployment of femtocell access points (FAPs) offers high-frequency spectrum utilization in terms of spatial spectral efficiency (SSE) or area spectral efficiency (ASE), and thus provides capacity enhancement for present and future cellular networks [5]. In the case of two-tier networks, where an

J. Zhang is with the Department of Electronic and Electrical Engineering, University of Sheffield, Sheffield, S13JD, UK.
Z. Xiao is with the College of Information Science and Engineering, Hunan University, Changsha 410082, China (CIE); E-mail: zhu.xiao.work@gmail.com.
X. Zhang and E. Liu are with the Institute for Research in Applicable Computing, University of Bedfordshire, Luton, LU13JU, UK.

This is an invited contribution from Commission C.

underlying layer of femtocells is deployed in the macrocells, there are prospective benefits to both operators and subscribers [6]. This enables existing macrocells to increase the system throughput, and to reduce the churn rate with a low operational cost, owing to self-deployment of femtocells by consumers. Mobile subscribers are able to achieve higher data rates since they are served by the femtocells, which provide improved link quality and better services.

The introduction of femtocells also gives rise to technical challenges in two-tier networks. Plenty of previous works in the literature have focused on spectrum reuse and cross-tier interference (CTI). There are usually two ways to allocate spectrum between the femtocells and macrocells: via dedicated channel and via co-channel. Femtocells using dedicated channels can prevent cross-tier interference. However, when frequency planning, spectral efficiency, and spectrum scarcity are taken into consideration, this becomes a suboptimum choice for mobile operators. Co-channel spectrum sharing gives an effective way to maximize the area spectral efficiency, which is a preferable option in two-tier networks. As advocated in the preceding works, e.g., in references [7, 8], the feasibility of co-channel deployment with femtocells underlain in a macrocell has been proven by system-level simulations and financial analysis. However, this method is accompanied by interference. It is noted that present cellular networks are becoming increasingly vulnerable to interference, as more radio resources need to be shared to achieve higher data speeds, therefore reducing the interference margin. Consequently, cross-tier interference is regarded as one of the major issues in femto-macro two-tier networks [9], particularly when femtocells are densely deployed in a macrocell. In general, the optimal sharing of radio spectrum is irresistible for both operators and users, and calls for innovative interference-management techniques.

Access control is another key factor for supporting user mobility and to reduce turnover. Several policies have been proposed for deciding whether a mobile user can connect a femtocell access point [10]: (1) open access (OA), where all users can access any femtocell access points without restriction; (2) closed access (CA), where only registered users have the right to connect to the femtocells; and (3) hybrid access, where a portion of the femtocell resources can be accessed by unregistered users, while the rest of the resources are exclusively for registered users. The first two types of access are referred to as open-subscriber-group (OSG) and closed-subscriber-group (CSG) by 3GPP, respectively. The third type of access is a mixed-access mechanism, which is referred to as closed-subscriber-group open. Access control offers a means of alleviating the interference and obtaining the required spectral resources in the handover process, and plays an important role in accomplishing those goals in two-tier networks.

By employing the backhaul connectivity, femtocells can build up broadband communications with macrocells with comparatively lower energy consumption. Due to the possibility of self deployment by femtocell access-point owners, network operators do not need to increase the cost of network expansion and base-station investment. Macrocells are the primary tier in current cellular networks, and they provide the wide-range coverage. Femtocells must hence utilize the wireless spectrum without affecting the macrocell's operation. This is to maximize the joint macrocell and femtocell system capacity.

In this article, we provide an overview of technologies and solutions used in femto-macro two-tier networks. We first look into well-accepted technical challenges, namely spectrum-resource allocation, cross-tier interference management, and mobility management. We then analyze issues that emerge from the implementation, such as bottlenecks in backhaul, mobility, and energy efficiency. Lastly, we identify some future trends in research and deployments.

The rest of the paper is organized as follows. In Section 2, we present spectrum allocation and approaches. In Section 3, we start by describing cross-tier interference scenarios, and then analyze the existing solutions for interference mitigation. In Section 4, we discuss access control and handover. Section 5 studies backhaul, mobility, and energy efficiency. Section 6 poses future trends and research directions. The conclusion is given in Section 7.

2. Spectrum Allocation in Two-Tier Networks

2.1 Hybrid Spectrum Partition

Femtocells are usually overlaid with macrocells, and operate within the same frequency band. Spectrum allocation based on dedicated channels, such as fractional frequency reuse or soft frequency reuse (FFR or SFR) [11], is a preferable choice for avoiding interference, but with comparable low spectrum efficiency. In order to improve the spectral utilization in two-tier networks, a co-channel assignment mechanism should be employed. This provides more spectrum resources for femtocells so as to improve the system capacity, especially in their own coverage area. However, such behavior may bring cross-tier interference. On the other hand, hybrid spectrum allocation (HSA) is able to achieve the tradeoff between sharing frequency resources and reducing interference. As shown in Figure 1, B_{Mac} and B_{Fem} are used to meet the basic requirements of each tier. Normally, the macrocell has priority for using the whole spectrum, because it serves a wide-ranging area, and accommodates user mobility. Assigning dedicated channels to femtocells is not feasible in some cases, because this could impose restrictions on the capacity of the macrocell. In this case, the co-channel deployment for femtocells allows efficient spatial frequency reuse. The parameter B_{Co-Ch} is a dynamic partition in the co-channel scenario. Once B_{Co-Ch} reaches the value of the entire bandwidth, it leads to universal spectrum reuse in two-tier networks.

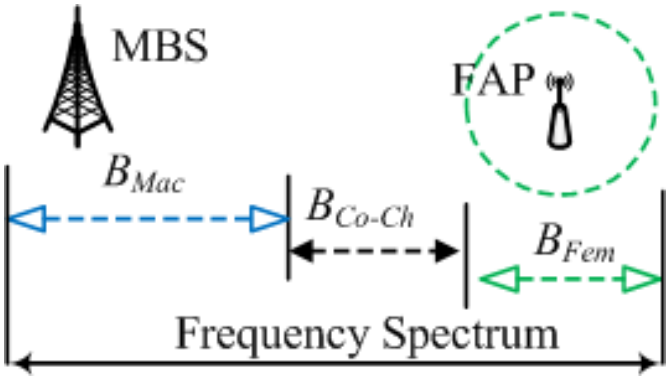

Figure 1. Hybrid spectrum allocation.

2.2 Spectrum-Allocation Approaches

Hybrid spectrum-allocation approaches for two-tier networks use both the dedicated channel and co-channel: they provide a means of dynamic spectrum allocation in two-tier networks. Many previous research works have addressed this, and they have adopted a range of approaches [11-15]. For the LTE standard, the user equipment (UE) is expected to report the channel information to its attaching multicast/broadcast service (MBS) or femtocell access points. When there is lack of cooperation between the MBS and femtocell access points, a rational spectrum allocation can still be achieved autonomously by using queuing theory based on the channel-quality information, as proposed in [12]. In [13], a distributed system configuration of spectrum resource allocation was proposed, where each femtocell adaptively allocated the number of sub-channels according to their locations, so as to reduce interference. In [14], the authors proposed an optimal frequency-division multiple-access (FDMA) method for two-tier networks, which is also suitable when OFDMA is employed. This method used orthogonality to ensure data rate and quality of service (QoS) for both the macrocells and femtocells, by considering the inter-cell interference and the generic channel environment. It can be concluded that the dynamic spectrum allocation in two-tier networks relies mainly on the relevant system information, wherein the interference is the major factor.

2.3 Efficiency of Spectrum Allocation

The coverage of a macrocell can be roughly divided into the inner region and the outer region, according to the distance from UEs to the MBS [15]. One method often employed to determine the regions is based on using the signal-to-noise-plus-interference ratio (SINR) at the UEs. For the sake of simplicity, the received power of the reference signal from the macrocell can be adopted to set up the regions. Let (Th_1, Th_2) denote two adaptive thresholds, and let $P_{rx,M}$ be the macrocell downlink power that the UE receives. The regional classification criterion is (1) inner region when $P_{rx,M} \geq Th_2$, (2) middle region when $Th_1 < P_{rx,M} < Th_2$, and (3) outer region when $P_{rx,M} \leq Th_1$. If a femtocell access point is inside the inner region – which means the interference is significant – the femtocell access points and MBS are assigned with individually dedicated channels, and thus the spectrum efficiency is low. When a femtocell access points is located in the outer region, co-channel operation can be employed, because interference is negligible. In the middle region, hybrid spectrum allocation can be used. The thresholds can be set depending on two aspects: one aspect is the interference caused by femtocells at the macrocell, and the other aspect is how much interference from the macrocell the femtocell can tolerate. Co-channel deployment of femtocells overlaid in a macrocellular network ensures a low impact on the macrocell's performance when suitable interference-mitigation approaches are employed for the femtocell links. Interference management is therefore indispensable for enhancing the overall spectral efficiency in two-tier networks. We discuss this in the next section.

The spatial spectral efficiency or area spectral efficiency (SSE/ASE) can be defined as [15]

$$\eta_{\text{ASE}} = \left(C_M + \sum_{i=1}^{N_f} C_{F,i}\right) \Big/ B_{tot}\ , \qquad (1)$$

where C_M represents the throughput of the macrocell, $C_{F,i}$ represents the ith femtocell's throughput, N_F denotes the number of femtocell access points that are embedded in the macrocell's coverage, and B_{tot} represents the total authorized frequency band within the coverage range. In order to evaluate the resource-allocation algorithm, there are other important parameters, i.e., quality of service, or utility function, which is based on the fairness [16]. Further analysis of the fairness issue will be given later.

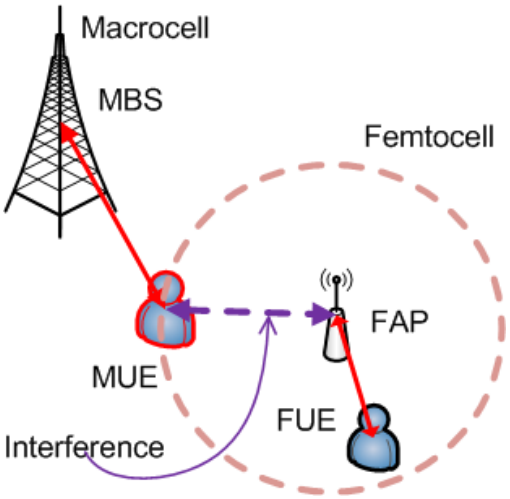

Figure 2a. A typical cross-tier interference scenario: Cross-Tier Interference I.

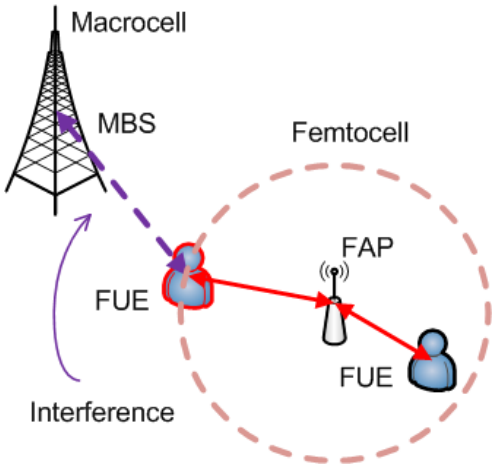

Figure 2b. A typical cross-tier interference scenario: Cross-Tier Interference II.

3. Cross-Tier Interference Management

When a femtocell access points is installed in the coverage area of a macrocell, femtocells and macrocells affect each other. Since current cellular networks are vulnerable to interference; the study of such issues is extremely important. In addition, we foresee that a high density of femtocell access points will be deployed due to the continuing demand for high-speed wireless services. This makes the interference situation more complex. Various interference scenarios and mitigation approaches are presented in this section.

3.1 Cross-Tier Interference Scenarios

Cross-tier interference (CTI) mainly stems from the uncoordinated planning of femtocell access points that share the frequency band with macrocells. Cross-tier interference is mutual in two-tier networks, where either macrocells or femtocells can be the victim or the aggressor. Two typical cross-tier interference scenarios are shown in Figures 2a and 2b. In the first cross-tier interference scenario, if the macrocell user equipment (MUE) is approaching the coverage area of the femtocell, it will be a victim of the cross-tier interference due to signal leakage from the femtocell's downlink. This can also create uplink interference at the femtocell access points' receiver. This interference occurs under three cases: (1) when the wireless signal from the MBS is blocked by obstacles, such as buildings; (2) when the macrocell user equipment is inside the coverage area of the femtocell access points; and (3) when the macrocell user equipment is at the coverage edge of the macrocell, and close to a femtocell access point. In these cases, the macrocell user equipment would increase the transmitted power to ensure the uplink quality with MBS. This would therefore affect the uplink of nearby femtocells. In the second cross-tier interference scenario, when the femtocell user equipment (FUE) is at the edge of the femtocell's coverage, it may create interference to the MBS. For example, suppose a piece of femtocell user equipment is located beside a window with line-of-sight to an MBS deployed at the rooftop across the street. This femtocell user equipment would have to increase the transmitted power to communicate with femtocell access points, and thus give rise to interference at the MBS. The macrocell downlink also causes interference at the femtocell user equipment's receiver, in this scenario.

Interference issues in two-tier networks include other scenarios, which were described in [17], such as the inter-femtocell interference and the interference between femtocells and neighboring macrocells. All the interference scenarios in [17] are important to tackle. In this article, we mainly focus on the solutions of cross-tier interference, which are related to the second set of typical scenarios.

3.2 Cross-Tier Interference Mitigation

Since the macrocell is considered to be the primary tier in two-tier networks, femtocells are required to apply mitigation strategies, such as power control, so as to maintain reliable underlay operation in the macrocell. Femtocells always try to achieve a compromise between protecting their own system performance against interference from macrocells, whilst preventing the macrocell performance from degrading.

3.2.1 Cross-Tier Interference I

In the vicinity of a femtocell, the macrocell coverage hole can be easily created by signals leaking from the femtocell's access points. This is normally more significant in co-channel deployment than in the case when the femtocell has dedicated channels. The general solution is to implement femtocell (aggressor) downlink power degradation to suppress the interference to the macrocell user equipment (victim). To avoid affecting the link quality of the femtocell downlink, the power adjustment should be done with an acceptable SINR at the femtocell user equipment. In [18], the authors derived the penalty function to make sure the cross-tier interference to the macrocell remains at a tolerable level, while in the meantime ensuring the femtocell user equipment has a fair enough receiving power to assure its own link quality. Recently, intercell interference coordination (ICIC), and its enhanced version, eICIC, offer alternative options to alleviating cross-tier interference [19]. The basic idea of intercell interference coordination is to keep the interference under control by radio resource management (RRM) methods. This makes use of almost-blank subframes (ABSFs) in the temporal or spectral domain to avoid cross-tier interference. This is able to maximize the spectrum utilization, especially for the cell-edge area, and thus eliminate the cell boundary. Efficient ways of exchanging information – e.g., the resource usage status and traffic load situation – need to be taken into account between femtocells and macrocells. Considering the macrocell user equipment as an aggressor, adaptive uplink attenuation for femtocell access points is a commonly accepted method for alleviating the uplink interference caused by macrocell user equipment [20]. However, this could harm the quality of the femtocell uplink. Another solution is for the femtocell user equipment to increase its transmitting power to overcome the uplink interference from macrocell user equipment. However, this shortens battery life, and may cause interference at MBS (the second cross-tier interference).

3.2.2 Cross-Tier Interference II

The second category of cross-tier interference is particularly important when the femtocell access points are deployed to be close to a macrocell. Considering the MBS as the victim in this case, the interference caused by femtocell user equipment can be mitigated by transmitting power control. In reference [21], open-loop and closed-loop power-adaptation schemes were designed. In these, the femtocell user equipment adjusts its maximum transmitted power according to a fixed interference threshold (open loop) and an adaptive interference threshold (closed loop), in order to reduce the cross-tier interference at the MBS. For the interference at femtocell user equipment that is caused by the MBS, the use of intercell interference coordination could be a solution [19]. By means of a spatial interference avoidance strategy, directional antennas can also be employed to reduce the interference from the MBS, as well as to mitigate the interference at the MBS [22].

From the femtocells' perspective, the dynamic transmitted power range and the adaptive link attenuation for the femtocell user equipment and femtocell access points are effective ways of suppressing interference at the MBS (macrocell user equipment). This also prevents femtocell user equipment and femtocell access points from suffering the interference caused by the MBS (macrocell user equipment). The ideas based on spectrum allocation are also introduced to manage the level of cross-tier interference. A universal frequency-reuse scheme for interference avoidance was proposed in [23]. There, the results from moderately loaded networks showed that the network capacity is increased compared to spectrum separation. The issue is that this requires careful frequency planning, especially for large-scale deployment of femtocell access points with high user density.

Handover in two-tier networks is another cross-tier interference-mitigation option, when open access is adopted [15]. In some situations, the aggressor is regarded as an interferer when it is moving around towards the coverage boundary, rather than entering the coverage area. This incurs unnecessary handover. Moreover, handover is not applicable if the networks are working under closed-subscriber-group mode, or the system is fully loaded.

In a word, most of the attempts at solving the interference issue aim at achieving coexistence of the macro and femto tiers. This is done by seeking a balance among utilizing various radio resources in two-tier networks, such as frequency spectrum, transmitted power, and access approaches.

4. Access Control and Handover

Random access and mobility are conspicuous features in mobile communication networks. For a two-tier network, macrocells overlapped by femtocells presents a more complicated random access and mobility challenge, compared to single-tier networks [24]. This section outlines the studies of access-control and handover issues in this respect.

4.1 Access Approaches

For two-tier networks, the restricted access control associated with femtocells can lead to strong interference in both the uplink and downlink, since users may not hand over to the nearest cells. How should users access femtocells? The operators prefer open access (OA), since this is expected to be a low-cost way to achieve network expansion, while femtocell access-point owners would prefer closed access (CA), so as to guarantee their own capacity and throughput. For the uplink, the choice of access methods depends on

the multiple access schemes employed in the network. Open access would match well in CDMA femtocells, since this benefits from alleviating the near-far effect, whereas when OFDMA or TDMA is employed, the user density becomes a major factor. Open access and closed access are suitable for medium and high user densities, respectively [25]. Unlike the uplink, the downlink requirements for the femtocell user equipment and macrocell user equipment are contradictory. Macrocell user equipment would like to access femtocell access points without any permission, while femtocell user equipment tends to be served privately by the femtocell access points. Hybrid access could hence be a compromise [10, 26], in which the unregistered macrocell user equipment is allowed to access the femtocell access points, but only for limited usage of resources, and the rest are under the closed-subscriber-group manner.

4.2 Tier Selection

Femtocells are able to accommodate most of the system load for indoor environments, which enables two-tier networks to greatly benefit from joint femto-macro deployments [2, 6]. When users are at the boundary of the two-tier network, there are two methods to determine which tier the user should access. The first method is based on the strength of a pilot signal that the user equipment receives from the femtocell access points and MBS. The other method is based on system load.

Users sense the pilot signal from the MBS and femtocell access points, and then access the tier that has the higher power. The fact that the pilot signal is decreasing linearly implies that the number of served users is being reduced. The tier selection is made according to the system load.

Femtocells serving fewer users do not mean more users can access the resource, since it depends on the data requirements of the individual users. System-load-based tier selection takes into account both criteria: the traffic demand of users, and the available resources in the macrocell or femtocell. The combination of these two methods is able to avoid misjudgments when the cell is capable of providing a good link quality but is nearly fully loaded, or conversely, has poor link quality but there are spare radio resources.

4.3 Multiple Femtocell Access Points Inbound Handover

In order to support the user's mobility, cross-tier handover is used to ensure service continuity for a UE. The provision of seamless handover by a femtocell is one of the biggest advantages over Wi-Fi. According to the technical realization, the operation of a UE switching from femtocell to macrocell is straightforward [10]. The discussion therefore focuses on the handover from macrocell to femtocell, which is often referred to as inbound handover [24]. The major challenge is the uncertain number of self-deployed femtocell access points, which results in the lack of maneuverability of having a record of the physical cell identity (PCI) list for all femtocell access points stored in the MBS. The inbound handover scenario when multiple femtocell access points are deployed in macrocells is discussed in the following.

When a UE detects a femtocell and reports the measurement to macrocell, the macrocell may not be able to decide to which cell to hand over, due to the ad hoc nature of the femtocell access points' deployment. A similar situation can occur for inter-femtocell handover. This is regarded as a physical-cell-identity confusion or collision. It can be divided into three cases, as shown in Figure 3: (1) in the

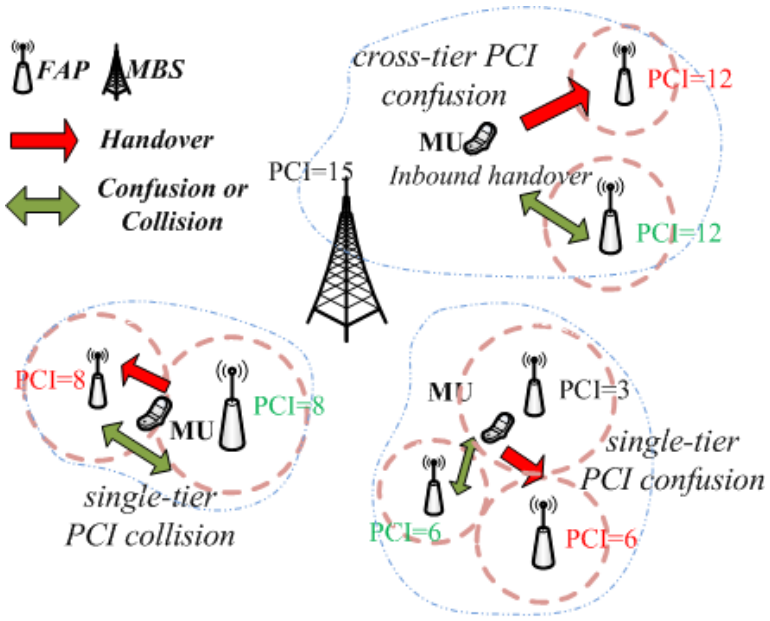

Figure 3. Physical cell identity confusion and collision.

top right case, when a UE tends to inbound handover from macrocell to femtocell, the cross-tier physical-cell-identity confusion occurs; (2) in the case shown on the left, when two neighboring femtocells share the same physical-cell identity, the inter-femtocell physical-cell-identity collision could happen; and (3) in the bottom case, when a UE moves from one femtocell access point to another, inter-femtocell physical-cell-identity confusion is likely to occur.

In the 3GPP standard, femtocells broadcast their closed-subscriber-group identities, which include a closed-subscriber-group indicator and a physical-cell identity ID number. The closed-subscriber-group indicator is used to identify whether the femtocell is open, closed, or hybrid. The physical-cell identity ID is used to decide whether it is physical-cell-identity confusion or collision. It is challenging to uniquely identify each femtocell, due to the limited number of physical-cell identities (e.g., a maximum of 504 unique numbers in LTE). To resolve this problem, cell global identity (CGI) was proposed in 3GPP Release 9, since cell global identity is the unique ID for each femtocell access point. When a macrocell user equipment moves close to the vicinity of the femtocells, the general procedure of inbound handover for an LTE femtocell can be summarized as follows [24, 27]:

1. The macrocell user equipment reads the closed-subscriber-group indicator from the femtocell access point to decide whether it is allowed to access.

2. The tier selection is implemented as described above, and it is decided whether the femto tier is more suitable for accessing. In most cases, the UE prefers to access a femtocell if it is registered to one or more closed-subscriber-group femtocell access points, since often a femtocell can provide better link quality and more radio resources.

3. The physical cell identity is read to determine whether there is confusion or collision. If there is no confusion, it completes the inbound handover; otherwise, it has to read the cell global identity.

For a rapid-moving mobile user, such behavior creates a distinguishable measurement gap for obtaining system information, thus resulting in service interruption and call dropping. For example, in LTE, such a measurement exceeds 160 ms [28]. This procedure also results in rapid depletion of the UE's battery.

5. Backhaul, Mobility Prediction, and Energy Efficiency

5.1 Backhaul Connection

In mobile communication networks, backhaul is used for connecting the base station and radio controller. Macro-cellular operators use expensive (or typically, leased) T1/E1 lines to backhaul the data traffic from the MBS, which costs 20-40% of operational expenditures (OPEX) [29]. Femtocell networks need to include the connectivity between the femtocell and macrocell networks to support such mobility and service continuity. xDSL, which is a family of digital-subscriber-line (DSL) technologies, is more likely to be used by femtocells to implement the backhaul connection. This is regarded as a cost-effective way of improving indoor coverage and reducing operating costs. However, it leads to restricted backhaul bandwidth, and faces difficulties in maintaining quality of service and security.

Femtocells expect to obtain sufficient bandwidth for backhauling traffic, particularly for the users that have high-speed data requirements, or in a home with high-bandwidth applications. In order to increase the user experience and ensure the quality of service, it is necessary to establish a service-level agreement between Internet service providers (ISPs) and femtocells [30]. This can be done by designing the xDSL bandwidth-reservation mechanism for upcoming femtocell data requirements.

Due to the lack of dedicated backhaul that provides a sufficient quality of service in two-tier networks, the data link between femtocells and femto gateways suffers greatly from delay and packet loss [2]. For the high-user-mobility scenario, this results in taking a long time to read the cell global identity, and affects the smoothness of cross-tier handover. The information exchange is processed via backhaul, and delay will cause the resource-block allocation to be ineffective. The Global Positioning System (GPS) can be used for time synchronization and to obtain location information among MBSs. However, it is not suitable for indoor femtocells, due to the high attenuation of the GPS signal through the buildings. A master-slave structure, IEEE 1588 Precision Timing Protocol (PTP), is considered as an alternative synchronization scheme [6], in which a master clock in the two-tier network provides the timing reference to the slave clocks for femtocell access points. The timing signal is transmitted over xDSL backhaul. This method is subject to the asymmetric bandwidth of xDSL, and significant traffic load may take place at the master clock, and quality of service has to be compromised.

Femtocells use public Internet as the backhaul to connect to the core network, which creates issues of data security. These incur the risk of exposing the mobile core to security threats, possible compromises of user privacy, and the potential for other network attacks. In both 3GPP (UMTS) and 3GPP2 (CDMA) femtocell architectures, the security gateway (GW) allows owners and operators to turn off the femtocell access points so as to prevent femtocells from network attacks and security threats when there is a non-dedicated backhaul connection employed [24, 27]. A gateway should support multi-mode femtocell deployments to provision flexibility for operators in choosing a suitable model that would meet the network demands.

Currently, the backhaul connection still remains one of the bottlenecks in two-tier networks. Researchers have tried to seek different forms of backhaul connection, such as wireless over cable (WoC), to replace xDSL [31]. It has also been suggested that DSL needs to be upgraded to carrier-grade Ethernet, or replaced by passive-optical-network (PON) technology, to solve the backhaul issue. The future alterative solution tends to be a mixture of both wireless and fixed wired backhaul technologies.

5.2 Mobility Prediction

The performance of mobile networks largely relies on the intensity of the received signals and interference, wherein the spatial locations of the participators play one of the crucial roles. The radio signals usually undergo various forms of attenuation and interference, which are often related to the locations of receivers and emitters.

As previously mentioned, randomly deployed femtocell access points and the frequent movement of UEs are the major factors that cause the geographic location keep changing in two-tier networks. The location of the femtocells and UEs in two-tier networks can be modeled as being random, following, for example, a spatial Poisson point process (SPPP) [13, 23]. Due to the independent property among the nodes, it is possible to obtain good results with analytical tractability. However, this fails to represent the mobility patterns of UEs, due to ignoring the relevance of their positions. Mobility prediction offers an option to predict future locations of the moving trajectory of UEs, considering the relevance among the locations of the UEs. In [32], the authors proposed a caching mechanism for available spectrum allocation in two-tier networks. This was based on three different user-mobility models, to consider one-dimensional, two-dimensional, and forward/backward movement, with respective probability distributions.

The moving probability distribution was studied in [33] to describe the possibility that a UE stays in the coverage of a femtocell access point or MBS, or moves across tiers. An incoming call mechanism was designed to resolve the rapid handover. This takes into account of the variation of the UE's velocity and accelerated velocity, where the assistance of GPS or a relative localization algorithm is required for obtaining the UE's position information. For future mobile communications, the UE should periodically update its location to the base station. Based on the current position and velocity of the user, the next possible direction and speed of user movement can be predicted. Considering that the next move probability is related to the present status, a Markov process was employed in [34] to predict the heading location of the UE, as well as to estimate the target MBS or femtocell access points that the UE may access. In general, mobility prediction helps to ensure seamless and reliable voice/data service, as well as reasonable radio-resource allocation, by pre-determining a network's geometrical configuration.

5.3 Energy Efficiency in the Deployment of Femtocells

Reduced cell sizes and transmitting distances have contributed to massive gains for mobile communication networks, resulting in achieving high spatial reuse of spectrum. This also transfers the energy-consumption issue from the transmitted power to the processing power [35]. Microcells, picocells, and femtocells are three typical embodiments that are in accord with the small-cell trend, wherein a femtocell can reduce the deployment cost due to its natural self-installation. Moreover, the overlay deployment of femtocells with macrocells can significantly decrease the overall network power consumption. As presented in [36], when the femtocell employment rate is maintained between 20% and 60%, the overall energy consumption can be reduced. Meanwhile, high quality of service can be obtained due to the fact that more UEs are served by femtocell access points. Energy-saving mechanisms for femtocells also rely on the UEs' activity. When a femtocell user equipment has no call request, its serving femtocell access points can set *idle* mode to suspend the transmission and take back the associated hardware-processing unit. This could be more energy efficient for femtocells. Network-based and UE-driven activity-detection approaches were proposed in [37]. When there are no active calls in a femtocell's coverage area, the femtocell access points can be switched off. This leads to an average of a 37% reduction of the femtocell's power consumption. When most of the active UEs are located at the edge of two adjacent femtocells, the energy-saving strategy can also be adopted by properly expanding the coverage of one femtocell access point, while switching off the other one.

Energy efficiency can be evaluated by bit-energy consumption, namely, in Joules per unit data bit communicated in a certain bandwidth. A green factor given in [38] took into account the spatial spectral efficiency and unit band energy efficiency for two-tier networks. The overall energy efficiency can be obtained by maximizing the *GF*:

$$\max GF = \frac{B_{tot}\left[rT_M + (1-r)N_f r_f T_F\left(r_f, N_f\right)\right]}{P_{sys}}, \qquad (2)$$

where r is the spectrum-allocation factor between femtocell and macrocell. Recalling the description in the spectrum-allocation section, we have

$$\left(B_{Mac} + B_{Co-Ch}\right)/\left(B_{Fem} + B_{Co-ch}\right) = r\,.$$

r_f represents the ratio of the spectrum usage in the femtocell. T_M and T_F respectively represent the throughputs of the macrocell and femtocell $\left[\text{b/s/Hz}\right]$. N_f is the number of femtocell access points. $P_{sys} = P_M + N_f P_F$ represents the

total downlink energy consumption in a two-tier network. The analysis shows that maximizing the spatial spectral efficiency is one of the ways to maximize energy efficiency.

6. Future Trends in Research

Since its appearance, the understanding of femtocells has been developing all the time. Some different views turn out as more effort is expended on research of the femtocell. In the earlier stages, femtocells were designed to improve indoor wireless service, because the macro-cellular networks were unable to provide sufficient indoor coverage and throughput. Two-tier networks are thus formed when the femtocells join in. It is worth noting that the macro tier dominates, which means that the macro tier has the priority to use the radio resources. Unfairness is hence generated between femtocells and macrocells. Recently, this view has changed. Since the femtocell is playing a key role in tackling the quickly increasing data demand from indoor environments, it should be treated equally to share the radio resources with the macrocell in two-tier networks. Large-scale deployment of femtocells is another developing trend. This also brings challenges, such as self-organization and -optimization for the growing needs of network management. This section will discuss these future developing trends. We then address relevant research directions.

6.1 Fairness in Two-Tier Networks

Fairness is an important metric of resource allocation in two-tier networks. The common metrics of fairness evaluation, such as Jain's Fairness Index (JFI), are independent of the system size, but fail to capture the proportional fairness. Considering that the multi-tier networks, such as picocells, relay, and femtocells, are embedded in macrocells, this turns out to be a multi-dimensional resource-allocation fairness issue. The multilayer network fairness can be written as [39]

$$f_{MFI}(c)=\frac{\left(\sum_{i=1}^{T}\sum_{j=1}^{N_{N,i}}\sum_{k=1}^{N_{U,i,j}}N_{U,i,j}C_{i,j,k}\right)^2}{N_{Tot}\sum_{i=1}^{T}\sum_{j=1}^{N_{N,i}}\sum_{k=1}^{N_{U,i,j}}N_{U,i,j}^2C_{i,j,k}^2} \qquad (3)$$

where $N_{Tot}=\sum_{i=1}^{T}\sum_{j=1}^{N_{N,i}}N_{U,i,j}$ represents the total number of users in a multi-tier network. $C_{i,j,k}$ denotes the *k*th user's capacity of the *i*th tier in the *j*th network. $N_{U,i,j}$ represents the number of users of the *i*th tier in the *j*th network. Jain's Fairness Index is a general description of the fairness of the system, and Equation (3) is used to describe the fairness for each individual tier.

When considering femto-macro two-tier networks, the lower bound of Equation (3) is $1/N_{Tot}$. This can be deemed as a kind of equitable distribution among users, and it also weakens the inequality between macrocell and femtocell. Normally, the macrocell is considered to be the primary tier, and has priority to obtain radio resources to guarantee its requirements. Recent studies have shown that it should not be a pure master-slave relationship between macrocell and femtocell. The principle of resource allocation that follows the user's demands could better reflect fairness in two-tier networks [40]. In fact, the concept of the femtocell was initiated as a promising technology that is able to satisfy the rapidly increasing demand of indoor wireless service. This is still the main function for femtocells at the present stage. Hence, which tier the UEs belong to should not be the prime consideration for meeting quality of service or other requirements. Although femtocells are regarded as supplementary to macrocellular networks, they should also have equal opportunity to obtain the radio resourc

In addition, besides fairness, users attempt to maximize their own utilization of available radio resources. This may occasionally result in harming the other users unwittingly or purposely, for example, to hide private traffic information that might cause unfair resource allocation. This is considered to be the users' selfish characteristics. This may somehow lead to inefficiency by the uncooperative manner wherein an optimal solution for resource utilization is missing. To obtain the truth-revealing dominant-strategy equilibrium in the game of selfishness and fairness, the authors in [41] proposed an inventive scheme to encourage the selfish user to truly report its data-transmission requirements. The two-tier networks are then able to reach the Pareto efficiency and proportional fair resource allocation.

6.2 Self-Organizing and Self-Optimizing for Large-Scale Femtocell Deployment

The femtocell was known as the home base station, because it was initially proposed to solve the coverage problems for multimedia applications at home. In the beginning, the installation of femtocell access points was usually regarded as a personal activity by the owners, who would like to obtain better indoor service. It turns out differently, nowadays. Not only deployed by the end-user, various deployments of the femtocell arise, such as being owned by the operator, or being jointly installed by the end-user and the operator [42]. Moreover, with the higher data requirements of wireless services, large-scale deployment of femtocells has been foreseen in the future mobile-communications system. Since there is a lack of an administrative entity for handling a number of femtocell access points that are densely deployed under an ad hoc manner, it is not acceptable to design a sophisticated management for two-tier networks. Therefore, self-organizing femtocells are regarded as key leverage to reduce the complexity and cost of network management [43]. In order to maintain the scalability and reliability of a femtocell network, self-optimizing needs to be conducted to implement

reasonable load sharing, rational coverage, and power adjustment among femtocells [44]. The characteristics of self-organizing and self-optimizing for femtocells contribute to autonomy for network management and operation, with "zero-touch" by the end-user. This also brings challenges to coordination in two-tier networks.

6.3 Intra-Tier and Inter-Tier Coordination

Due to the lower power cost of femtocells, they provide a solution for enhanced overall system capacity for macrocells, which consume more power. This is also considered as an embodiment of networks with different characteristics [45], which are well known as heterogeneous networks (HetNets). In such a scenario, the heterogeneity of participants should be fully exploited, in order to increase network availability and usability. This also needs working between femtocells and macrocells to provide interoperability for cross-tier radio management.

The critical issue is how to implement intra-tier and inter-tier coordination in two-tier networks. Due to the absence of existing coordination between femtocell access points and MBSs, centralized cooperation, e.g., to mitigate cross-tier interference, is infeasible in the near future. On the other hand, distributed cooperation is more suitable in cellular networks, considering that mobile-network activities are constantly changing. However, the well-known inefficiency issue might arise in a decentralized way when each femtocell tries to optimize its own utility of radio resources. Cooperation among femtocells and macrocells is also required in inter-cell interference coordination [19], whereas the technical challenge is to achieve effective and reliable information exchange. This also restricts the application of coordinated multi-point transmission/reception (CoMP) in two-tier networks [46].

According to the state of the art of coordination approaches, the information exchange between macrocells and femtocells still remains a bottleneck. Solutions such as a dedicated interface between femtocell and macrocells – such as an X2 interface between eNodeBs in LTE – is impractical in femtocell networks. A mixed approach with wired and wireless could be an alternative, such as a combination of relay and PON to achieve a two-tier network of collaboration.

6.4 Outdoor Femtocells and Mobile Femtocells

When the femtocell was first proposed, it was accepted that femtocells are suitable for residential deployments, and other technologies, such as a distributed antenna system (DAS) or relay, are appropriate for large indoor environments such as shopping malls. In recent years, the researchers have gradually changed their minds. Researchers also predicted that femtocells would not be limited by home applications [2, 8], and this has proven to be true. Femtocells have been extended to large indoor areas, such as enterprise applications, as well as outdoor environments [47]. By using multi-antenna technology, femtocells take advantage of both high spectral utilization and spatial diversity [48]. In [49], the authors proposed a hybrid scheme of femtocells and a distributed antenna system (DAS) to provide indoor coverage for a multistory building in the urban environment. In [50], the authors demonstrated the feasibility of a low-cost, flexible configured dipole antenna, installed in street furniture, which can be deployed in outdoor femtocells to enhance outdoor coverage. Recently, attention has been paid to mobile femtocells, which means the locations of the femtocell access points are not fixed. For example, femtocells can be employed as mobile access devices in transportation services such as buses, trains, and airplanes.

6.5 Docitive Femtocells

Recently, a natural evolution of autonomous spectrum utilization has considered femtocells incorporating cognitive radio, which senses a spectrum hole and makes decisions on opportunistic access [51]. From the macrocell's perspective, this does not need many extra processes when more UEs are encouraged to take part in the decision making to alleviate the burden from the MBS. Cognitive femtocells inherit the knowledge learned from the surrounding environment as one of the input factors to the two-tier network management, thus facilitating higher capacity and intelligent coverage. However, the complexity of optimal decision making is high. A new paradigm, docitive radio (from the Latin "docere," meaning "to teach") femtocell was proposed in [52, 53]. This is designed to reduce the cognitive complexity, accelerate the learning process, and lead to more reliable decisions.

6.6 Virtual Femtocells

In the same period of steady femtocell development, researchers have proposed a mobile virtual network operators (MVNO) concept, in order to save the operator's operating expenses and to provide a refined business chain. The mobile virtual network operators and femtocell concepts are both under rapid development, due to the diversifying demands of the mobile communications businesses. They are also considered to be kernel technologies in the next-generation mobile cellular network.

In fact, because a femtocell is easy to deploy, it is suitable for mobile virtual network operators [54]. Therefore, using femtocells to achieve mobile virtual network operators wireless services is an important growth point. In this mobile Femtocell virtualization, it can be extended to be a new access method, e.g., using network-prefix division multiple accesses (NDMA) to quickly access the Internet [55], and to meet various business requirements of different users. This has been considered as a hot topic in the future mobile Internet development.

7. Conclusion

In the first decade of the new century, femtocells have received wide recognition and greater attention by industry and operators. Particularly in recent years, the femtocell has been considered a promising technology in wireless communications for extending indoor service coverage and enhancing overall network capacity. Heterogeneous networks, consisting of cells with different sizes, from macro to femto cells, will play a crucial role in the next-generation broadband wireless network. In this article, the two-tier heterogeneous network was considered, where the current cellular networks, i.e., macrocells, are overlapped with a large number of randomly distributed femtocells. This network infrastructure can potentially bring significant benefits, and can increase the network's capacity significantly to meet the explosive traffic demand of users, with limited capital/operating expenditures and spectrum constraints. In this article, we have presented the technical issues in femto-macro two-tier networks. These included resource allocation, cross-tier interference management, access control, and backhaul. We have also discussed the perspectives of femtocell research and summarized the further research directions.

8. Acknowledgement

This work was supported by the EU-FP7 IAPP@ RANPLAN under grant No. 218309 and EU-FP7 iPLAN under grant No. 230745.

9. References

1. S. Carlaw, "Ipr and the Potential Effect on Femtocell Markets," FemtoCells Europe, ABIresearch, 2008.

2. J. Zhang, G. de la Roche, et al., *Femtocells – Technologies and Deployment*, New York, Wiley, 2010.

3. Jia Liu, Tianyou Kou, Qian Chen and H. D. Sherali, "Femtocell Base Station Deployment in Commercial Buildings: A Global Optimization Approach," *IEEE Journal on Selected Areas in Communications*, **30**, 3, March 2012, pp. 652-663.

4. D. Knisely, T. Yoshizawa and F. Favichia, "Standardization of femtocells in 3GPP," *IEEE Communications Magazine*, **47**, 9, September 2009, pp. 68-75.

5. J. G. Andrews, H. Claussen, M. Dohler, S. Rangan and M. C. Reed, "Femtocells: Past, Present, and Future," *IEEE Journal on Selected Areas in Communications*, **30**, 3, April 2012, pp. 497-508.

6. V. Chandrasekhar, J. Andrews and A. Gatherer. "Femtocell Networks: A Survey," *IEEE Communications magazine*, **46**, 9, September 2008, pp. 59-67.

7. H. Claussen, L. T. W. Ho and L. G. Samuel, "Financial Analysis of a Pico-Cellular Home Network Deployment," 2007 IEEE International Conference on Communications, ICC. June 24-28, 2007, Glasgow, pp. 5604-5609.

8. H. Claussen, "Performance of Macro- and Co-Channel Femtocells in a Hierarchical Cell Structure," 18th IEEE International Symposium on Personal, Indoor and Mobile Radio Communications, PIMRC2007, September 3-7, 2007, Athens, pp. 1-5.

9. R. Y. Kim, J. S. Kwak and K. Etemad, "WiMAX Femtocell: Requirements, Challenges, and Solutions," *IEEE Communications Magazine*, **9**, 47, September 2009, pp. 84-91.

10. G. De la Roche, A. Valcarce, D. Lopez-Perez and Jie Zhang, "Access Control Mechanisms for Femtocells," *IEEE Communications Magazine*, **48**, 1, January 2010, pp. 33-39.

11. H. C. Lee, D. C. Oh and Y. H. Lee, "Mitigation of Inter-Femtocell Interference with Adaptive Fractional Frequency Reuse," 2010 IEEE International Conference on Communications, ICC, May 23-27, 2010, Cape Town, pp. 1-5.

12. M. Andrews, V. Capdevielle, A. Feki and P. Gupta, "Autonomous Spectrum Sharing for Mixed LTE Femto and Macro Cells Deployments," IEEE Conference on Computer Communications Workshops, INFOCOM2010, March 15-19, 2010, San Diego, CA, pp. 1-5

13. Xiaoli Chu, Yuhua Wu, L. Benmesbah and W. K. Ling, "Resource Allocation in Hybrid Macro/Femto Networks," IEEE Wireless Communication and Networking Conference, WCNC 2010, April 18-21, 2010, Sydney, NSW, pp. 1-5

14. V. Chandrasekhar and J. Andrews, "Spectrum Allocation in Tiered Cellular Networks," *IEEE Transaction on Communications*, **57**, 10, October 2009, pp. 3069-3068.

15. I. Guvenc, M. R. Jeong, F. Watanabe and H. Inamura, "A Hybrid Frequency Assignment for Femtocells and Coverage Area Analysis for Co-Channel Operation," *IEEE Communications Letters*, **12**, 12, December 2008, pp. 880-882.

16. F. M. Yang, W. M. Chen, T. K. Cheng and J. C. Wu, "A Study of QoS Guarantee and Fairness Based on Cross-Layer Channel State in Worldwide Interoperability for Microwave Access," *International Journal of Communication Systems*, **25**, 7, July 2012, pp. 926-942.

17. Interference Management in UMIS Femtocells, Smallcell Forum, White Paper, February 2010, http://smallcellforum.org/smallcellforum/resources-white-papers Index Number: 009.

18. Z. Shi, M. C. Reed and M. Zhao, "On Uplink Interference Scenarios in Two-Tier Macro and Femto Co-Existing UMTS Networks," *EURASIP Journal on Wireless Communications and Networking*, **2010**, Article ID 240745, 2010, pp. 1-8.

19. D Lopez-Perez, I. Guvenc, G. De La Roche, M. Kountouris, T. Quek and J. Zhang, "Enhanced Intercell Interference Coordination Challenges in Heterogeneous Networks," *IEEE Communications Magazine*, **18**, 3, June 2011, pp. 22-30.

20. M. Yavuz, F. Meshkati, S. Nanda, A. Pokhariyal, et al., "Interference Management and Performance Analysis of UMTS/HSPA + Femtocells," *IEEE Communications Magazine*, **47**, 9, September 2009, pp. 102-109.

21. H. S. Jo, C. Mun and J. Moon. "Interference Mitigation Using Uplink Power Control for Two-Tier Femtocell Networks," *IEEE Transaction on Wireless Communications*, **8**, 10, October 2009, pp. 4906-4910.

22. S. Park, W. Seo and S. Choi. "A Beamforming Codebook Restriction for Cross-Tier Interference Coordination in Two-Tier Femtocell Networks," *IEEE Transaction on Vehicular Technology*, **60**, 4, April 2011, pp. 1651-1663.

23. V. Chandrasekhar and J. Andrews, "Uplink Capacity and Interference Avoidance for Two-Tier Femtocell Networks," *IEEE Transaction on Wireless Communications*, **8**, 7, July 2009, pp. 3498-3509.

24. A. Golaup, M. Mustapha and L. B. Patanapongpibul, "Femtocell Access Control Strategy in UMTS and LTE," *IEEE Communications Magazine*, **47**, 9, September 2009, pp. 117-123.

25. P. Xia, V. Chandrasekhar, and J. G. Andrews. "Open vs. Closed Access Femtocells in the Uplink," *IEEE Transaction on Wireless Communications*, **9**, 12, December 2010, pp. 3798-3809.

26. H. S. Jo, P. Xia and J. G. Andrews. "Open, Closed, and Shared Access Femtocells in the Downlink," *EURASIP Journal on Wireless Communications and Networking*. **2012**. December 2012: 363.

27. A. Damnjanovic, J. Montojo and Y. Wei, "A Survey on 3GPP Heterogeneous Networks," *IEEE Wireless Communications Magazine*, **18**, 3, March 2011, pp. 10-21.

28. RP-100222 for Rel-9 WI Home NodeB and Home eNB Enhancements; 3GPP TSG RAN meeting #47.

29. O. Tipmongkolsilp, S. Zaghloul and A. Jukan, "The Evolution of Cellular Backhaul Technologies: Current Issues and Future Trends," *IEEE Communications Surveys and Tutorials*, **13**, 1, 2011, pp. 97-113.

30. M. Z. Chowdhury, S. Choi and Y. M. Jang, "Dynamic SLA Negotiation Using Bandwidth Broker for Femtocell Networks," First International Conference on Ubiquitous and Future Networks, ICUFN2009, June 7-9, 2009, Hong Kong, pp. 12-15.

31. J. Gambini and U. Spagnolini, "Radio Over Telephone Lines in Femtocell Systems," 21st IEEE International Symposium on Personal, Indoor and Mobile Radio Communications, PIMRC2010, September 26-30, 2010, Istanbul, pp. 1544-1549.

32. H. Y. Lee and Y. Lin. "A Cache Scheme for Femtocell Reselection," *IEEE Communications Letters*, **14**, 1, January 2010, pp. 27-29.

33. C. J. Huang, P. Chen, C. T. Guan, "A Probabilistic Mobility Prediction Based Resource Management Scheme for WiMAX Femtocells," 2010 International Conference on Measuring Technology and Mechatronics Automation, ICMTMA, March 13-14, 2010, Changsha City, **1**, pp. 295-300.

34. H. Abu-Ghazaleh and A. S. Alfa, "Application of Mobility Prediction in Wireless Networks Using Markov Renewal Theory," *IEEE Transactions on Vehicular Technology*, **59**, 2, February 2010, pp. 788-802.

35. C. Han, T. Harrold, S. Armour and I. Krikidis, "Green Radio: Radio Techniques to Enable Energy-Efficient Wireless Networks," *IEEE Communications Magazine*, **49**, 6, June 2010, pp. 46-54.

36. Y. Hou, D. I. Laurenson, "Energy Efficiency of High QoS Heterogeneous Wireless Communication Network," 72nd IEEE Vehicular Technology Conference, VTC 2010-Fall, September 6-9, 2010, Ottawa, ON, pp. 1-5.

37. I. Ashraf, L. T. W. Ho and H. Claussen, "Improving Energy Efficiency of Femtocell Base Stations via User Activity Detection," IEEE Wireless Communication and Networking Conference, WCNC 2010, April 18-21, 2010, Sydney, NSW, pp. 1-5.

38. W. Cheng, H. Zhang and L. Zhao, et al. "Energy Efficient Spectrum Allocation for Green Radio in Two-Tier Cellular Networks," IEEE Global Telecommunications Conference, GLOBECOM2010, December 6-10, 2010, Miami, FL, pp. 1-5.

39. M. C. Erturk, H. Aki, I. Güvenc and H. Arslan, "Fair and QoS-Oriented Spectrum Splitting in Macrocell-Femtocell Networks," IEEE Global Telecommunications Conference, GLOBECOM2010, December 6-10, 2010, Miami, FL, pp. 1-6.

40. M. C. Ertürk, I. Güvenc, and H. Arslan, "Femtocell Gateway Scheduling for Capacity and Fairness Improvement in Neighboring Femtocell Networks," 21st IEEE International Symposium on Personal, Indoor and Mobile Radio Communications, PIMRC2010, September 26-30, 2010, Istanbul, pp. 54-59.

41. C. H. Ko and H. Wei. "On-Demand Resource-Sharing Mechanism Design in Two-Tier OFDMA Femtocell Networks," *IEEE Transactions on Vehicular Technology*, **60**, 3, March 2011, pp. 1059-1071.

42. P. Lin, J. Zhang, Y. Chen and Q. Zhang. "Macro-Femto Heterogeneous Network Deployment and Management: From Business Models to Technical Solutions," *IEEE Wireless Communications Magazine*, **18**, 3, March 2011, pp. 64-70.

43. J. Kim, H. Kim, K. Cho and N. Park, "SON and Femtocell Technology for LTE-Advanced System," 6th International Conference on Wireless and Mobile Communications, ICWMC2010, September 2010, Valencia, Spain, pp. 286-290.

44. H. S. Jo, C. Mun, J. Moon, and J. G. Yook, "Self-Optimized Coverage Coordination and Coverage Analysis in Femtocell Networks," IEEE *Transactions on Wireless Communications*, **9**, 10, October 2010, pp. 2977-2982.

45. A. Ghosh, N. Mangalvedhe, R. Ratasuk and B. Mondal, "Heterogeneous Cellular Networks: From Theory to Practice," *IEEE Communications Magazine*, **50**, 6, June 2012, pp. 54-64.

46. S. Park, W. Seo, S. Choi and D. Hong, "A Beamforming Codebook Restriction for Cross-Tier Interference Coordination in Two-Tier Femtocell Networks," *IEEE Transactions on Vehicular Technology*, **60**, 4, April 2011, pp. 1651-1663.

47. C. Patel, M. Yavuz and S. Nanda, "Femtocells [Industry Perspectives]," *IEEE Wireless Communications Magazine*, **17**, 5, May 2010, pp. 6-7.

48. V. Chandrasekhar, M. Kountouris, J. G. Andrews, "Coverage in Multi-Antenna Two-Tier Networks," *IEEE Transactions on Wireless Communications*, **8**, 10, October 2009, pp. 5314-5327.

49. T. Alade, H. Zhu and J. Wang. "Uplink Co-Channel Interference Analysis and Cancellation in Femtocell Based Distributed Antenna System," 2010 IEEE International Conference on Communications, ICC, May 23-27, 2010, Cape Town, pp. 1-5.

50. J. M. Rigelsford, F. Collado and K. L. Ford, "Radiation Steering of a Low Profile Street Furniture Antenna Using An Active AMC," 2010 Antennas and Propagation Conference, LAPC, November 8-9, 2010, Loughborough, pp. 529-532

51. G. Gür, S. Bayhan and F. Alagöz, "Cognitive Femtocell Networks: An Overlay Architecture for Localized Dynamic Spectrum Access," *IEEE Wireless Communications Magazine*, **17**, 4, April 2010, pp. 62-70.

52. L. Giupponi, A. Galindo-Serrano, P. Blasco and M. Dohler, "Docitive Networks: An Emerging Paradigm for Dynamic Spectrum Management," *IEEE Wireless Communications Magazine*, **17**, 4, April 2010, pp. 47-54.

53. A. Galindo-Serrano, L. Giupponi and M. Dohler, "Cognition and Docition in OFDMA-Based Femtocell Networks," IEEE Global Telecommunications Conference, GLOBECOM2010, December 6-10, 2010, Miami, FL, pp. 1-6.

54. W. Hong and Z. Tsai, "On the Femtocell-Based MVNO Model: A Game Theoretic Approach for Optimal Power Setting," 71st IEEE Vehicular Technology Conference, VTC 2010-Spring, May 16-19, 2010, Taipei, Taiwan, pp. 1-5.

55. E. K. Paik, S.-H. Lee, C. Lee, J. Han, C. Park, T. Kwon and Y. Choi, "Service Differentiation Using Mobile Femtocell Virtualization," 7th IEEE Consumer Communications and Networking Conference, CCNC, January 9-12, 2010, Las Vegas, NV, pp. 1-4.

An Analog of Surface Tamn States in Periodic Structures on the Base of Microstrip Waveguides

D.P. Belozorov
A.A. Girich
S.I. Tarapov

Abstract

The Tamm state concept was formulated for periodic systems consisting of microstrip elements by analogy with the well-known Tamm state in photonic crystals. The unit cell, which determines the period of our microstrip system, consists of four elements: two segments with lengths L_1 and L_2, and two connections (1,2) and (2,1). The total period of the structure is equal to $L = L_1 + L_2$. The transfer matrix for the unit cell is written. The Bloch equation for the infinite system is formulated from the conditions of periodicity. The solutions of the Bloch equation determine the Bloch wave vector and the spectral structure of our infinite system. The numerical calculations of an important model system were performed. The model system consisted of two periodic subsystems (eight elements in either of the two), with different parameters of periodicity. The analog of the Tamm state was observed as a crowding of electromagnetic waves propagating through the system at the transition between two subsystems. The concentration of electromagnetic-wave energy takes place at the border point of one-dimensional subsystems. A corresponding transparency peak (a Tamm peak) appears in the coinciding forbidden frequency bands of two subsystems.

1. Special Properties of a Quadripole (Four-Pole) Medium

Currently, the study of bounded periodic structures (photonic crystals) and the condition for surface states to appear at the interface separating these structures had attracted the unceasing interest of researchers. The topic we are going to discuss now is connected with the well-known surface Tamm states appearing at the boundary of the bounded periodic structures: solid state lattices and photonic crystals [1, 2]. An important feature of such surface Tamm states is the absence of tangential components of the Bloch wave vector at the interface, which means that any physical transfer of energy along the boundary is absent.

A narrow transparency peak (the Tamm peak) appears in the spectrum bandgap of a bounded periodic structure. The position of the peak in the frequency bandgap depends on the parameters characterizing the whole system. This allows us to use this system in a variety of practical applications: for example, such as a controlled filter of electromagnetic radiation. The theoretical and experimental study of Tamm states in one-dimensional periodic crystals was discussed in a number of papers (see, e.g., [3, 4, 5, 6]).

The purpose of this paper is to study the analog of Tamm states for special bounded periodic structures consisting of microstrip elements, the elements of which are now widely used in various microwave applications. In particular, note the usage of microstrip photonic crystals for measurements of the permittivity of fluid substances [7].

We shall not dwell on the strengths and weaknesses of the existing theory of microstrip circuits [8]. However, it should be noted that because of complex mathematics, their detailed theory is far behind its practical applications, and is still far from being complete. However, there are a number of approximate formulas for quite accurately describing these waveguide systems, depending on their design features and the microwave frequency range [9-16].

If we are dealing with an infinite periodic structure, i.e., a symmetrical structure with respect to periodic translations by vector $\mathbf{L}$, all fields at points separated by a vector translation $\mathbf{L}$ are known to be connected by the relationships

D. P. Belozorov is with the Institute for Theoretical Physics, NSC "Kharkov Institute of Physics & Technology" NAS of Ukraine, Kharkov, Ukraine, Akademicheskaja St., Kharkov 61108, Ukraine; E-mail: belodi36@gmail.com. A. A. Girich and S. I. Tarapov are with the Institute of Radiophysics and Electronics NAS of Ukraine, 12 Ac. Proskura st., Kharkov, 61085, Ukraine; Tel: +38057-720-3463; Fax: +38057-315-2105; E-mail: girich82@mail.ru; tarapov@ire.kharkov.ua.

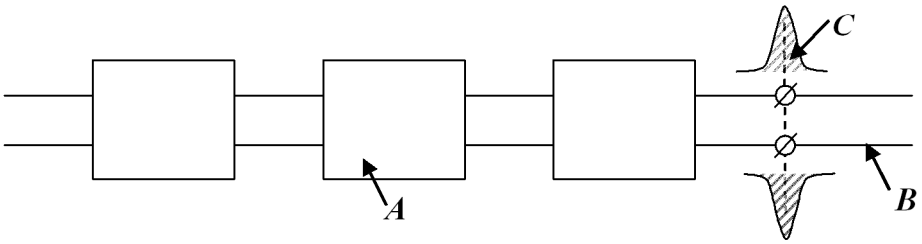

Figure 1. The schematic for observation of the Tamm states. A is the chain of four-poles (Medium 1), B is the line with strong attenuation or the similar subsystem with different parameters (Medium 2), and C is the analog of the Tamm states. C shows the "concentration" of the electromagnetic energy near the interface of four-pole systems A and B.

$$\mathbf{E}(x,y,z+L)\exp(ik_B L)=\mathbf{E}(x,y,z)\,, \qquad (1)$$

$$\mathbf{H}(x,y,z+L)\exp(ik_B L)=\mathbf{H}(x,y,z)\,.$$

For electromagnetic waves in one-dimensional periodic systems, the quantity k_B, called the Bloch vector, is scalar. The conditions of Equations (1) are known as the Floquet condition (Floquet theorem) for the case of one-dimensional periodicity, and the Bloch condition (Bloch theorem) when the system is periodic in two dimensions or three dimensions. The proof of the statement in Equation (1) reduces to the known fact from linear algebra that at least one solution, $\mathbf{U}$, exists for any square matrix, $\hat{\mathbf{A}}$, which satisfies the equation $\hat{\mathbf{A}}\mathbf{U}=\mu\mathbf{U}$ (see, e.g., [9]).

Below, we present our system as a chain of two-lines consisting of micro-stripes (see Figure 1). We use the well-known formalisms of a normalized wave-transmission matrix, $\hat{\mathbf{T}}$, a normalized wave-scattering matrix, $\hat{\mathbf{S}}$, and the normalized classical transmission matrix, $\hat{\mathbf{A}}$, for description of the chain. All of these matrices are related to each other, so elements of one matrix can be expressed in terms of another (for details about the properties of these matrices, see [10-12]). Note here the important property of the transmission matrix of the system, namely, that the transmission matrix of a cascade (chain) of four-poles is the product of the transmission matrices for individual four-poles:

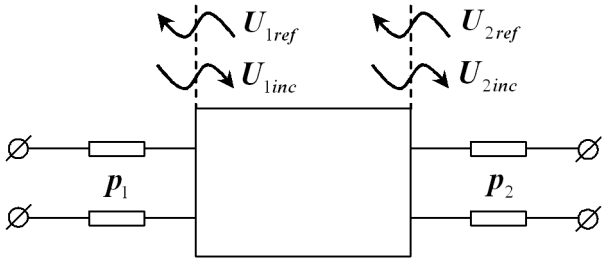

Figure 2. The circuit of a four-pole.

$$\hat{\mathbf{T}}=\prod_{i=1}^{k}\hat{\mathbf{T}}_i\,, \qquad (2)$$

where k is the number of four-poles in the chain.

Considering the wave processes in a medium that represents a periodic sequence of identical four-poles, we single out two variants of the medium. The first variant is the sequence of elementary cells unbounded in both directions (Medium 1). The second variant is the same sequence of cells bounded from one side. In the latter case, the sequence of four-poles is usually supposed to be bounded with a Medium 2, where the wave process becomes heavily attenuated. Tamm states are known to be surface states appearing at the interfaces of adjacent different photonic crystals. Here, we deal with one-dimensional systems of micro-stripes, so at the border point of two different subsystems, we shall speak only about the analog of the Tamm states. [1, 3, 4].

The process at the medium of the four-poles in approximation of the wave-transmission matrix is a voltage wave connected with a conditional wave process that takes place in a long line, equivalent to given system of four-poles. Here, properties of an individual four-pole are determined by its wave-transmission matrix, $\hat{\mathbf{T}}=(T_{ik})$ [10, 11], and (Figure 2)

$$U^n_{1inc}=T_{11}U^n_{2inc}+T_{12}U^n_{2ref}\,,$$

$$U^n_{1ref}=T_{21}U^n_{2inc}+T_{22}U^n_{2ref}\,, \qquad (3)$$

$$U_{1inc}=t_{11}U_{2inc}+t_{12}U_{2ref}\,,$$

$$U_{1ref}=t_{21}U_{2inc}+t_{22}U_{2ref}\,,$$

$$(T_{ik})=\sqrt{\rho_1\rho_2^{-1}}\,(t_{ik})\,.$$

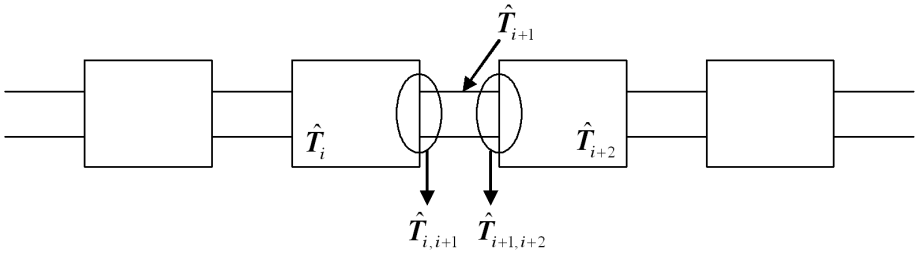

Figure 3a. An infinite periodic chain of four-poles.

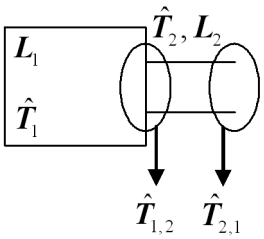

Figure 3b. The unit cell of the periodic structure of Figure 3a.

U^n_{1inc}, U^n_{1ref}, U^n_{2inc}, and U^n_{2ref} are the normalized incident and reflected voltage waves in the transmission lines at the input and output of the four-pole:

$$U^n_{1inc,ref}\sqrt{\rho_1} = U_{1inc,ref},$$

$$U^n_{2inc,ref}\sqrt{\rho_2} = U_{2inc,ref}.$$

Here, U_{1inc}, U_{2inc}, U_{1ref}, and U_{2ref} are the complex amplitudes of the incident and reflected waves, and ρ_1 and ρ_2 are the wave impedances of the input and output lines.

Note that in addition to a normalized wave in terms of the transmission matrix, as we shall see below an important physical meaning also has a normalized wave in terms of the scattering matrix $\hat{\mathbf{S}} = (S_{ik})$. The elements of the scattering matrix are expressed in terms of elements of the matrix $\hat{\mathbf{T}}$ in the following way:

$$U^n_{1ref} = S_{11}U^n_{1inc} + S_{12}U^n_{2ref},$$

$$U^n_{1inc} = S_{21}U^n_{1inc} + S_{22}U^n_{2ref}, \qquad (4)$$

$$\hat{\mathbf{S}} = \begin{pmatrix} S_{11} & S_{12} \\ S_{21} & S_{22} \end{pmatrix} = \begin{pmatrix} \frac{T_{21}}{T_{11}} & \frac{|T|}{T_{11}} \\ \frac{1}{T_{11}} & \frac{-T_{12}}{T_{11}} \end{pmatrix}.$$

Here, $|T| = \det\hat{\mathbf{T}}$.

One can mention here the physical meaning of the elements of both matrices $\hat{\mathbf{T}}$ and $\hat{\mathbf{S}}$, which are associated with a certain "characteristic" mode in the system of four-poles. In the wave theory, the role of such a "typical" mode is as a mode with zero parameter Γ_N, the reflection coefficient from a load of the output line:

$$\Gamma_N = \frac{U^n_{2ref}}{U^n_{2inc}}. \qquad (5)$$

In other words, $U^n_{2ref} = 0$. In this case,

$$T_{11} = \frac{U^n_{1inc}}{U^n_{2inc}},$$

$$T_{21} = \frac{U^n_{1ref}}{U^n_{2inc}}, \qquad (6)$$

$$S_{11} = \frac{U^n_{1ref}}{U^n_{1inc}},$$

$$S_{21} = \frac{U^n_{2inc}}{U^n_{1inc}}.$$

The elements of the matrices T_{11}, S_{21}, and S_{11} determine the properties of a four-pole loaded with a matched line at the definite forward direction of wave propagation (left to right). In particular, T_{11} determines the ratio of the normalized voltages in this mode, and is called the transmission coefficient. $S_{21} = T_{11}^{-1}$, and has an individual name, the "transmittance." $D = |T_{11}|^{-2}$ is used as the microwave power-transmission coefficient [7]. S_{11} is the reflection coefficient in the input line with matched output line. The microwave power reflection coefficient from the microstrip photonic structure is defined as $R = |S_{11}|^2$ [7].

2. Bloch Equation

We now consider an infinite periodic chain of identical four-poles (microstrip waveguides), and define the equation for the Bloch wave vector in such a structure. The transmission matrix for the elementary cell of the periodic structure, which consists of a complex four-pole (see Figure 3b), is the product of the wave-transmission matrices of four-poles constituting the elementary cell, and respectively including the following elements: the *i*th segment, a direct connection to the *i*th and $(i+1)$ segments, the $(i+1)$ segment, and the direct connection of the $(i+1)$ and $(i+2)$ segments of the microwave transmission line. The infinite periodic chain of four-poles and its unit cell are sketched in Figures 3a and 3b.

We see that the unit cell that determines the period of our structure consists of segments with lengths L_1 and L_2 and of two connections, (1,2) and (2,1). The total period of the structure is therefore equal to $L = L_1 + L_2$.

Using the wave-transmission matrices for the elements of the structure without considering attenuation [7],

$$\hat{T}_S = \begin{bmatrix} \exp(ik_S L_S) & 0 \\ 0 & \exp(-ik_S L_S) \end{bmatrix},$$

$$\hat{T}_{S,S+1} = \begin{pmatrix} \dfrac{r_{S,S+1}+1}{2\sqrt{r_{S,S+1}}} & \dfrac{r_{S,S+1}-1}{2\sqrt{r_{S,S+1}}} \\ \dfrac{r_{S,S+1}-1}{2\sqrt{r_{S,S+1}}} & \dfrac{r_{S,S+1}+1}{2\sqrt{r_{S,S+1}}} \end{pmatrix}, \qquad (7)$$

$$r_{S,S+1} = r_{S+1,S}^{-1} = \frac{\rho_{S+1}}{\rho_S},\ (s = 1,2).$$

We obtain the following expression for the transmission-wave matrix of the unit cell:

$$\hat{\mathbf{T}}_{EC} = \hat{\mathbf{T}}_1 \hat{\mathbf{T}}_{1,2} \hat{\mathbf{T}}_2 \hat{\mathbf{T}}_{2,1}, \qquad (8)$$

$$\hat{\mathbf{T}}_{EC} = \begin{pmatrix} T_{11}^{EC} & T_{12}^{EC} \\ T_{21}^{EC} & T_{22}^{EC} \end{pmatrix} \qquad (9)$$

$$\det \hat{\mathbf{T}}_{EC} = T_{11}^{EC} T_{22}^{EC} - T_{12}^{EC} T_{22}^{EC} = 1$$

(so the transmission matrix is unimodular). The elements of the matrix $\hat{\mathbf{T}}_{EC}$ are equal to

$$T_{11}^{EC} = 4^{-1}\left(2 + r_{1,2} + r_{1,2}^{-1}\right)\exp\left(ik_1 L_1 + ik_2 L_2\right) + 4^{-1}\left(2 - r_{1,2} - r_{1,2}^{-1}\right)\exp\left(ik_1 L_1 - ik_2 L_2\right),$$

$$T_{22}^{EC} = 4^{-1}\left(2 + r_{1,2} + r_{1,2}^{-1}\right)\exp\left(-ik_1 L_1 - ik_2 L_2\right) + 4^{-1}\left(2 - r_{1,2} - r_{1,2}^{-1}\right)\exp\left(-ik_1 L_1 + ik_2 L_2\right), \qquad (10)$$

$$T_{12}^{EC} = 4^{-1}\left(r_{1,2} - r_{1,2}^{-1}\right)\exp\left(ik_1 L_1 - ik_2 L_2\right) - 4^{-1}\left(r_{1,2} - r_{1,2}^{-1}\right)\exp\left(ik_1 L_1 + ik_2 L_2\right),$$

$$T_{21}^{EC} = 4^{-1}\left(r_{1,2} - r_{1,2}^{-1}\right)\exp\left(-ik_1 L_1 + ik_2 L_2\right) - 4^{-1}\left(r_{1,2} - r_{1,2}^{-1}\right)\exp\left(-ik_1 L_1 - ik_2 L_2\right).$$

We note that $(T_{11}^{EC})^* = T_{22}^{EC}$ and $(T_{12}^{EC})^* = T_{21}^{EC}$, as well as $|T_{11}|^2 = 1 + |T_{21}|^2$, so the wave matrix is a matrix of a reversible reactive four-pole [12].

The quantities ρ_S and k_S $(s = 1,2)$ entering Equations (7) and (10) are related to characteristics of structural elements (W_S is the width of the strip wire, h_S is the thickness of the microstrip-line substrate, and ε_S is the permittivity of the substrate). The wave resistance of the microstrip line according to [12, 14, 16] is therefore equal to

$$\rho_S = \frac{377 h_S}{\sqrt{\varepsilon_S} W_S \left[1 + 1.735\varepsilon^{-0.0724}\left(\dfrac{W_S}{h_S}\right)^{-0.836}\right]} \qquad (11)$$

where $k_S = 2\pi\Lambda_S^{-1}$.

The wavelength of the electromagnetic wave, Λ_S at the *s*th section of the microstrip line is defined by the known expression [7, 14, 16]

$$\Lambda_S = \begin{cases} \dfrac{\lambda}{\sqrt{\varepsilon_S}} \sqrt{\dfrac{\varepsilon_S}{1 + 0.63(\varepsilon_S - 1)\left(\dfrac{W_S}{h_S}\right)^{0.1255}}} & \text{for } \dfrac{W_S}{h_S} \geq 0.6 \\ \dfrac{\lambda}{\sqrt{\varepsilon_S}} \sqrt{\dfrac{\varepsilon_S}{1 + 0.6(\varepsilon_S - 1)\left(\dfrac{W_S}{h_S}\right)^{0.0297}}} & \text{for } \dfrac{W_S}{h_S} < 0.6 \end{cases} \qquad (12)$$

where λ is the wavelength in vacuum. The formulas in Equation (12) give dispersion relations for electromagnetic waves in the sth section of the microstrip line.

In what follows, we restrict our attention to the traveling-wave regime, which corresponds to the absence of the reflected wave in the system. The normalized classical transmission matrix relates currents and voltages on both sides of the four-pole [11], i.e.,

$$U_1^n = A_{11}U_1^n + A_{12}I_2^n, \qquad (13)$$

$$I_1^n = A_{21}U_2^n + A_{22}I_2^n,$$

$$\begin{pmatrix} U_1^n \\ I_1^n \end{pmatrix} = \hat{A}\begin{pmatrix} U_2^n \\ I_2^n \end{pmatrix},$$

where

$$U_l^n = U_{linc}^n + U_{lref}^n,\ I_l^n = U_{linc}^n - U_{lref}^n,\ (l = 1,2).$$

Under the traveling-wave conditions, the voltage and current are the same periodic functions of distance. Assuming the dependence $\exp(i\omega t - ikz)$, we have

$$U(z) = U(0)\exp(-ik_B z), \qquad (14)$$

$$I(z) = I(0)\exp(-ik_B z).$$

For the structure of an infinite chain of periodic four-poles, from the periodicity of the structure, it follows that the displacement at period L (where N is a number of unit cells) gives

$$U(N+1) = U(N)\exp(-ik_B L) \qquad (15)$$

$$I(N+1) = I(N)\exp(-ik_B L).$$

With the use of Equations (13) and (15), we have

$$\begin{pmatrix} U_N^n \\ I_N^n \end{pmatrix} = \hat{A}\begin{pmatrix} U_{N+1}^n \\ I_{N+1}^n \end{pmatrix} = \begin{bmatrix} U_{N+1}^n \exp(ik_B L) \\ I_{N+1}^n \exp(ik_B L) \end{bmatrix}. \qquad (16)$$

Elements of the unimodular matrix $\hat{\mathbf{A}}$, $\det\hat{\mathbf{A}} = 1$, are expressed through elements of the matrix $\hat{\mathbf{T}}_{EC}$ [11]:

$$\hat{\mathbf{A}} = \frac{1}{2}\begin{pmatrix} T_{11}^{EC} + T_{21}^{EC} + T_{12}^{EC} + T_{22}^{EC} & T_{11}^{EC} + T_{21}^{EC} - T_{12}^{EC} - T_{22}^{EC} \\ T_{11}^{EC} - T_{21}^{EC} + T_{12}^{EC} - T_{22}^{EC} & T_{11}^{EC} - T_{21}^{EC} - T_{12}^{EC} + T_{22}^{EC} \end{pmatrix}$$

$$Sp\hat{\mathbf{A}} = Sp\hat{\mathbf{T}}_{EC}.$$

With the use of Equations (16) and (17), we obtain

$$2\cos k_B L = Sp\hat{T}_{EC} = T_{11}^{EC} + T_{22}^{EC}. \qquad (18)$$

Finally, the Bloch equation (see, e.g., [13, 17]) has the form

$$\cos k_B L$$

$$= \cos k_1 L_1 \cos k_2 L_2 - \frac{1}{2}\left(r_{1,2} + r_{1,2}^{-1}\right)\sin k_1 L_1 \sin k_2 L_2. \qquad (19)$$

Equation (19) defines the Bloch wavevector, k_B. If the absolute value of the right-hand side of Equation (19) exceeds one at some frequency, then k_B is a complex number. It thus has an imaginary part, and the field dissipates when propagating inward through the medium, which is a periodic chain of four-poles. In these conditions, the propagation of electromagnetic energy through such medium is impossible. This is the so-called forbidden band (stop band) in the spectrum of electromagnetic waves. In the case of a real k_B, we are dealing with a pass band of the medium: the electromagnetic energy freely propagates through the medium (we consider a medium without attenuation). The appearance of pass and forbidden bands in the spectrum is a characteristic feature of any periodic super-lattice. Typical spectra for an "almost infinite structure" and a "finite structure" are given in Figure 4 (we neglected the absorption). The microwave power-transmission coefficient is $D = |T_{11}|^{-2}$. Gray regions correspond to the forbidden zones of the structures. It is easy to see that the frequencies of stop bands coincided for both super-lattices, and almost do not depend on the number of cells.

3. Tamm States

Surface Tamm states are known to appear (see, e.g., [1, 3, 4]) at the boundary separating the periodic super-lattice medium (Medium 1) from Medium 2, in which the propagation of electromagnetic waves is impossible. Metals and a wire medium [4] are the most illustrative examples of such a Medium 2, but any other media with

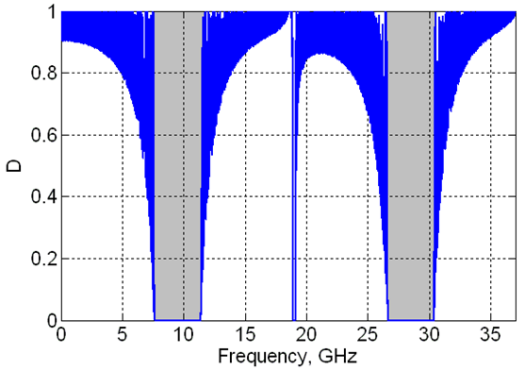

Figure 4a. The spectra for structures with various number of unit cells: The spectrum for an "almost infinite" periodic super-lattice (which means a very large number of unit cells N, ($N = 1000$)

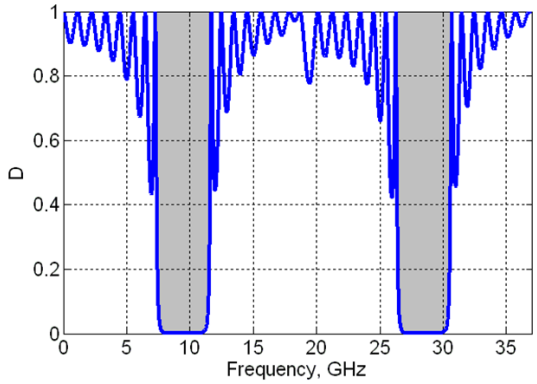

Figure 4b. The spectra for structures with various number of unit cells: The spectra for a finite structure with $N = 8$ (see Figure 5).

negative permittivity that results in strong attenuation of electromagnetic waves (Figure 1) can be used as a Medium 2. In any case, if the region of attenuation of electromagnetic waves coincides for given frequencies with the forbidden band of a periodic subsystem, the Tamm state appears, namely, the concentration of the field energy at the interface separating two media takes place. A characteristic feature of the state (as was stressed above for the two-dimensional boundary of a photonic crystal) is a homogeneous field distribution along the interface plane, between media 1 and 2. In the spectrum of the system, the Tamm state manifests itself as a sharp and narrow transmission peak, located at the frequency range where the forbidden states of both media coincide. The important case of the boundary Medium 2 can also be another periodic subsystem, the parameters of which differ from the parameters of Medium 1 (Figure 1). The only necessary condition is the coincidence of the bandgaps of both subsystems in a definite frequency range. A second subsystem (Medium 2) is a nonreflecting load line for the chain of four-poles that forms Medium 1. As in the case considered above, the Tamm states represent a sharp and narrow transmission peak in the frequency range where the forbidden bands of both media coincide. We consider this case in detail later. It should be mentioned here that due to the one-dimensionality of the considered problem, we can now speak only about an analog of the Tamm states, namely about the concentration of the electromagnetic field at the border points C between subsystems A and B.

We stress that matching of all parts of the line is an important condition in both cases, because the equality of the wave resistances (impedances) of both subsystems at the point of their contact prevents the appearance of a reflected wave in the system of four-poles.

The scheme for experimental observation of the Tamm states is presented in Figure 1. The already-mentioned condition of the equality of the impedances $Z_A = Z_B$ at the connection point is the condition of the electromagnetic waves not reflecting at this point (Z_A is the Bloch impedance of the chain of four-poles, and Z_B is the line impedance with strong attenuation or another subsystem chain, which are the loads of the chain A). The impedance condition provides the so-called mode matching between the source and the load, i.e., provides a traveling-wave regime for the line *A*. Note that if the matching condition is not satisfied between the load (B) and the line (A), in general it is possible to include some matching four-pole element, which ensures fulfillment of this condition. As a result, the traveling-wave regime is restored, i.e., the line will be matched to the load. Methods for calculation of matching four-poles are described, for example, in [18].

Using Equation (16) for the unit cell in the four-poles medium, we get

$$Z_A = \frac{U_{N+1}^n}{I_{N+1}^n}$$

$$= -\frac{A_{12}}{A_{11} - \exp(ik_B L)} \qquad (20)$$

$$= 2\frac{A_{12}}{(A_{11} - A_{22}) \pm \left[(A_{11} + A_{22})^2 - 4\right]^{1/2}}.$$

Substituting the expressions for the matrix elements of the matrix $\hat{A}$, we express the impedance, Z_A, in terms of known elements of the transmission matrix:

$$Z_A = 2\frac{T_{11}^{EC} + T_{21}^{EC} - T_{12}^{EC} - T_{22}^{EC}}{\left(T_{21}^{EC} + T_{12}^{EC}\right) \pm \left[\left(T_{11}^{EC} + T_{22}^{EC}\right)^2 - 4\right]^{1/2}}. \qquad (21)$$

Substituting the matrix elements of the transmission matrix, Equation (10), we obtain the following expressions for the quantities entering the numerator and denominator:

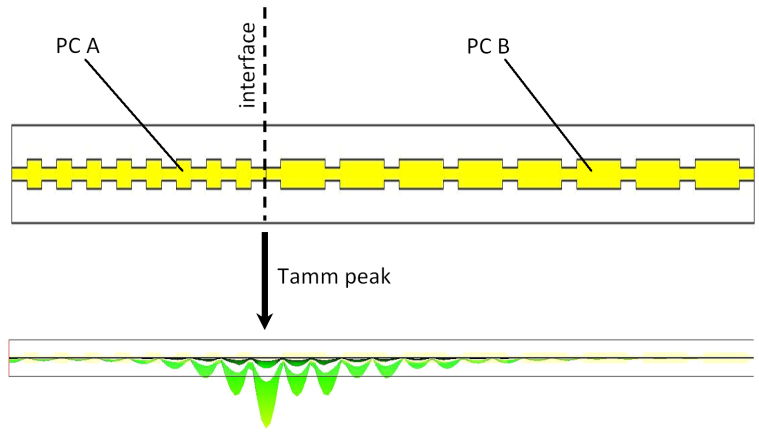

Figure 5. (top) The system used for the numerical calculations. Both super-lattices A and B consisted of eight elements. (bottom) The calculated spatial distribution of electromagnetic wave energy for the system of two subsystems.

$$T_{11}^{EC} + T_{21}^{EC} - T_{12}^{EC} - T_{22}^{EC}$$

$$= 2i\left(\sin k_1 L_1 \cos k_2 L_2 + r_{12} \sin k_2 L_2 \cos k_1 L_1\right),$$

$$T_{21} + T_{12} = \left(r_{12} + r_{12}^{-1}\right)\sin k_1 L_1 \sin k_2 L_2 , \qquad (22)$$

$$T_{11} + T_{22}$$

$$= 2\cos k_1 L_1 \cos k_2 L_2 - \left(r_{12} + r_{12}^{-1}\right)\sin k_1 L_1 \sin k_2 L_2$$

Note that corresponding expressions to Equation (22) were calculated for the infinite chain.

4. Numerical Calculations

In this section, we present some results of numerical calculations carried out for the system consisting of two subsystems with various parameters of four-poles [15]. The corresponding whole system is presented in Figure 5a.

The simulation of the model structure was performed, and the details are shown in Figure 5a. The structure was a microstrip line with the following parameters. Two copper upper strips were placed on the surface of a dielectric plate (Taconic TLC-30) with $\varepsilon = 3 + 0.003i$ and thickness $h = 0.5$ mm. The lower strip was a substrate strip. The upper strip was made of two periodic structures/subsystems A and B, connected in series. Each of these subsystems consisted of eight rectangular elements of equal width $D = 1.233$ mm, and their lengths were correspondingly $L_2^A = 5.0$ mm and $L_2^B = 14.2$ mm. These elements were connected with narrower rectangular elements correspondingly having equal widths $d = 3.0$ mm, and lengths $L_1^A = 5.0$ mm, mm. The characteristic impedance of such a microstrip structure equals 50 ohms at the "middle" frequency $f = 9$ GHz.

Note that in Figure 5b we can see a distribution of electromagnetic-wave energy in the system. We see the concentration of electromagnetic energy near the PC A/

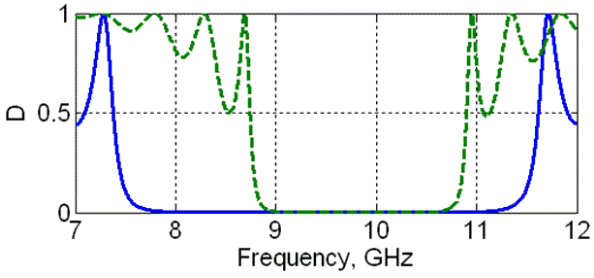

Figure 6a. The results of the numerical calculations for systems PC A and PC B: the forbidden bands for subsystems A (solid line) and B (dashed line).

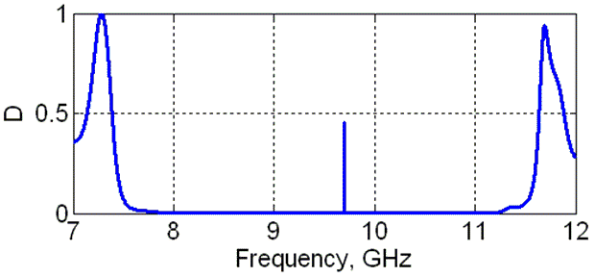

Figure 6b. The results of the numerical calculations for systems PC A and PC B: The Tamm peak at the frequency of 9.7 GHz.

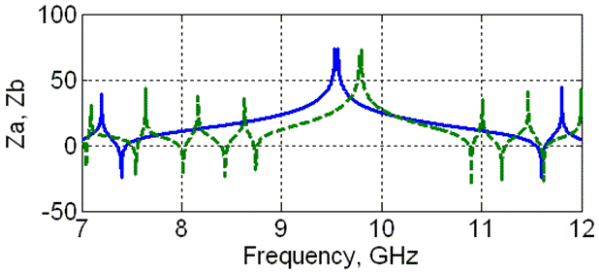

Figure 6c. The results of the numerical calculations for systems PC A and PC B: The impedances for the subsystems A (solid line) and B (dashed line).

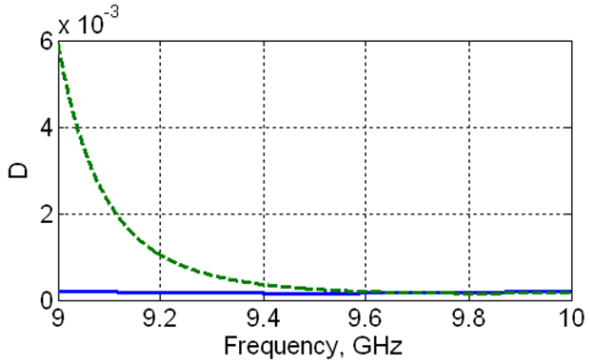

Figure 7a. The frequency dependence of the transmission coefficient in the vicinity of the Tamm peak (9 GHz to 10 GHz): The forbidden bands for each of subsystems A (solid line) and B (dashed line).

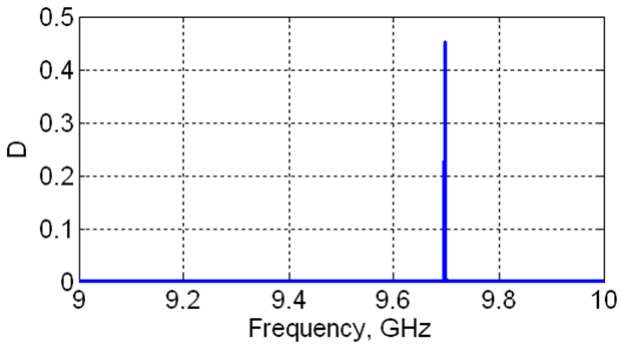

Figure 7b. The frequency dependence of the transmission coefficient in the vicinity of the Tamm peak (9 GHz to 10 GHz): The forbidden band for the joined subsystems and the position of the Tamm peak.

PC B interface. Such a concentration of energy is the analog of the Tamm state for our system.

Figure 6a presents two stop bands of two separate subsystems (PC A and PC B). The coincidence of two forbidden bands of separate subsystems takes place in the region of approximately 9 GHz to 11 GHz (the values of the transmission coefficient, D, are plotted along the y axis). The characteristic sharp increase of the microwave power-transmission coefficient, D, near a frequency of 9.7 GHz (Figure 6b) corresponds to the analog of the Tamm peak.

For the purpose of detailed analysis, we carried out numerical calculations in the vicinity of the Tamm peak, namely in the range of 9 GHz to 11 GHz. The results are presented in Figure 7.

As was stated above, the frequency position of the Tamm peak depends on the characteristics of the system. This feature of the Tamm peak is very important for various practical applications, because it enables us to control the position of the narrow transparency peak by changing the parameters of the system.

In Figure 8, we present the results of numerical calculations of the dependence of the position of the Tamm peak on the magnitude L_2^B (the length of elements of the subsystem (B)). Here is also shown the dependence on L_2^B of the characteristic frequency ($f_{(ZA=ZB)}$), which is the frequency of impedance equality for both structures. Both dependencies, $f_{TS} = \varphi\left(L_2^B\right)$ (open squares) and $f_{(ZA=ZB)} = \varphi\left(L_2^B\right)$ (the solid line) coincided, and demonstrated almost linear behavior. We saw that an increase of L_2^B shifts the Tamm-state's frequency position toward the lower frequencies.

In addition, an important question is the investigation of this dependence as a function of the number of unit cells (N) in the system. According to Figure 8a, for $N = 4,6,8,10,12,14$, all curves coincided with high accuracy. Only a small divergence took place in the vicinity of the stop band edges (Figure 8b): the divergence was higher for smaller N. This tendency is quite natural, because with the decrease of N, the system becomes more transparent, and the quality factor of the Tamm peak also decreases. The energy dissipation thus begins to play a role, and leads to the shift of the Tamm peak's frequency.

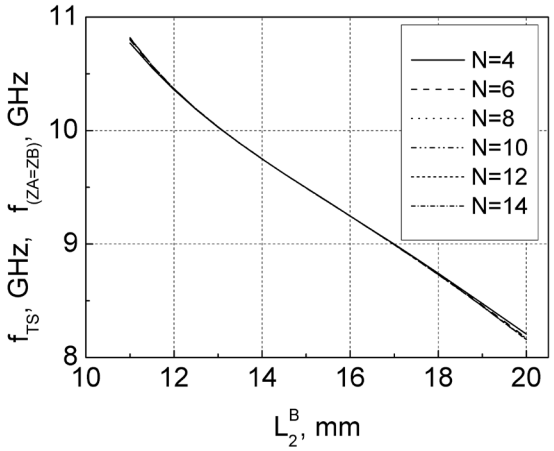

Figure 8a. The Tamm-state frequency position as a function of the value of L_2^B for various values of N: for the whole stop band, 8 GHz to 10 GHz.

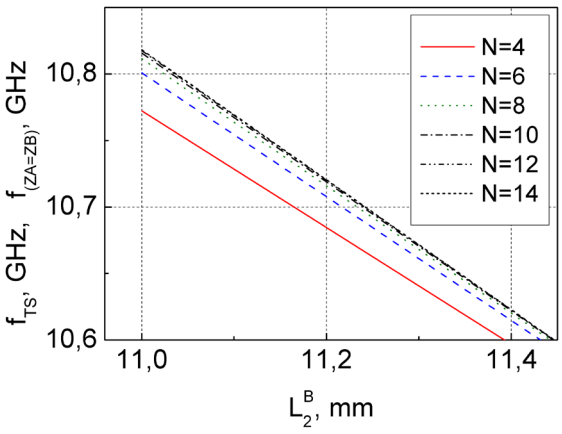

Figure 8b. The Tamm-state frequency position as a function of the value of L_2^B for various values of N: A detailed picture of the region from 10.60 GHz to 10.65 GHz on the band's edge.

5. Conclusions

1. The propagation of electromagnetic waves in systems of infinite and bounded periodical chains of four-poles was analyzed. The equation for the Bloch wave vector, determining the band structure of the infinite chain, was formulated and numerically solved.

2. A concept of the Tamm state was formulated for a periodic chain consisting of two periodic subsystems with different constitutive parameters. We revealed that this state gives rise to a concentration of electromagnetic energy in the vicinity of the interface of the two subsystems. The Tamm frequency peak corresponding to the Tamm state is located in that frequency range where the forbidden bands of the two subsystems coincide.

3. The Tamm peak's position depends on the parameters of the system, and can be changed if the parameters are changed. This feature is of great value for various practical applications of systems with Tamm states.

4. Detailed numerical calculations were carried out for the system consisting of two periodic subsystems with differing lengths of their four-pole elements. These numerical calculations verified all of the properties of the Tamm states as stated above.

6. References

1. A. P. Vinogradov, A. V. Dorofeenko, S. G. Erokhin, M. Inoue, A. A. Lisyansky, A. M. Merzlikin, A. B. Granovsky "Surface State Peculiarities in One-Dimensional Photonic Crystal Interfaces," *Phys. Rev. B*, **74**, 2006, pp. 045128.

2. I. M. Lifshitz and S. I. Pekar, "Tamm Bounded States of Electrons on the Crystal Surface and Surface Oscillations of Lattice Atoms," *Phys.-Usp.*, **56**, 4, 1955, pp. 531-568

3. A. P. Vinogradov, A. V. Dorofeenko, F. M. Merzlikin and A. A. Lisyansky, "Surface States in the Photonic Crystals," *Phys.-Usp.*, **53**, 2010, pp. 243-256.

4. S. I. Tarapov and D. P. Belozorov, "Microwaves in Dispersive Magnetic Composite Media," *Low Temperature Physics*, **38**, 7, 2012, pp. 766-792.

5. C. A. Valagiannopoulos, "Electromagnetic Propagation into Parallel-Plate Waveguide in the Presence of a Skew Metallic Surface," *Electromagnetics*, **31**, 2011, pp. 593-605.

6. C. A. Valagiannopoulos and N. K. Uzanoglu, "Green's Function of a Parallel Plate Waveguide with Multiple Abrupt Changes of Interwall Distances," *Radio Science*, **44**, 5, 2009.

7. D. A. Usanov, A. V. Skripal, A. V. Abramov, A. S. Bogolyubov, M. Y. Kulikov, D. V. Ponomarev, "Microstrip Photonic Crystals Used for Measuring Parameters of Liquids," *Technical Physics*, **55**, 8, 2010, pp. 1216-1221.

8. V. A. Neganov, *Electrodynamic Theory of Flat-Gap EHF Structures*, Saratov University, 1991 (in Russian).

9. R. A. Silin, *Periodic Waveguides*, Moscow, Phasis, 2002 (in Russian).

10. F. L. Feldshtein, L. R. Yavich, and V. P. Smirnov, *Handbook on Elements Waveguide Technology*, Moscow, Soviet Radio, 1966 (in Russian).

11. A. L. Feldshtein and L. R. Yavich, *Synthesis of 4-Pole and 8-Pole for Microwave*, Moscow, Svyaz, 1971 (in Russian).

12. L. G. Maloratsky and L. R. Yavich, *Design and Calculation Microwave Components for Strip Lines*, Moscow, Soviet Radio, 1972 (in Russian).

13. D. V. Pozar, *Microwave Engineering*, New York, John Wiley & Sons, Inc., 1998.

14. Koryu Ishii (ed.), *Handbook of Microwave Technology, Volume 1, Components and Devices*, New York, Academic Press, 1995, Chapters 2, 4.

15. R. C. Booton, *Computational Methods for Electromagnetics and Microwaves*, New York, Wiley-Interscience, 1992.

16. K. C. Gupta, R. Garg, J. Bahl, and P. Bhartia, *Microstripe Lines and Slotlines*, Norwood, MA, Artech House, 1996.

17. F. G. Bass and A. A. Bulgakov, *Kinetic and Electrodynamic Phenomena in Classical and Quantum Semiconductor Superlattices*, Nova Science Pub Inc., 1997.

18. G. D. Malushkov, *Antennas and Microwave Devices, Part 1, Transmission Lines and Microwaves Devices*, Moscow, 1973 (in Russian).

Book Reviews for Radioscientists

Understanding Space Weather and the Physics Beghind It

by Delores D. Knipp, New York, McGraw-Hill, 2911m 727+xiv pp; ISBN-13: 978-0-07-340890-3;
ISBN-10: 0-07-340890-5; US$93.

The term "space weather" rose to common usage between 1990 and 1995. There is also anecdotal evidence for the term being used earlier than this. Subsequently, space weather has been embraced in textbooks and conferences. There are two scientific journals dedicated to the subject, and many more that support the discipline. That is the environment in which this textbook has been written.

Right at the outset, I will admit I am a biased reviewer. I really like this book, and have enjoyed reviewing it. I knew that within five minutes of seeing a copy, and bought several for our library on the strength of that first look. It has taken a great deal longer to work through the book, and my first impressions have not changed.

Chapter structure: An opening page summarizes in bullets what the readers should already know, what they will now learn, and outlines the section headings. Each section (subsection and sub-subsection) starts with a summary of what the reader will be able to describe after reading the section. Sections are interspersed with "Pause for inquiry" problems, well-connected to the section content, and often developing a feel for the scale and substance of the main physical concepts. Important concepts are also illustrated by worked examples. Each chapter concludes with a summary section drawing the ideas together. This is followed by a list of key words introduced in the chapter, together with any new notation, and the answers to all the questions posed in the chapter. The chapter then concludes with a list of references referred to in the chapter, and a list for further reading. Throughout the chapters are also interspersed "Focus Boxes," describing specific – sometimes, niche – aspects of space weather linked to the chapter content, as well as a large number of useful tables. Throughout, there is a fine array of supporting figures. The high degree of structure in each chapter is impressive, and breaks concepts down into digestible elements. There is also an extensive contents page opening the book, and a comprehensive index together with four short useful appendices to close it.

To give a further feel for the general content: spread across 14 chapters (727+xiv pages), there are about 435 figures (all in color); 100 worked examples; 205 problems and answers; 69 focus boxes; and 59 tables. All of these add significantly to the content of the chapter in which they are placed. In addition, the first sentence of many sections and subsections has been crafted to capture the essence of the large-scale concepts being introduced. Some of these are gems, and a tribute to the care taken preparing the text. This is also a very well-illustrated book: almost every page contains carefully selected, color figures to illustrate the concepts being discussed. These demonstrate that the author has a very good eye for choosing figures, which are drawn from diverse sources.

The content of the book is divided among 14 chapters, split into three units and four appendices.

The first unit of nine chapters (roughly two-thirds of the book) initially introduces space weather through description and historical background (Chapter 1) and physical concepts (Chapter 2). Chapters 3 to 6 start at the sun and solar wind. They provide a background for the plasma environment that defines space weather, and the rich source of electric currents and magnetic fields that embody the interactions that make space weather both pleasurably illuminating (the aurora), and dangerously destructive (just about everything else). Chapter 7 deals with the Earth enveloped in the solar-wind plasma, leading to the formation of the quiescent magnetosphere. Chapter 9 introduces the atmosphere and, I'd claim, historically the first major battlefield for understanding and controlling space weather rather, than just describing its effects: the ionosphere (the home of high-frequency communications). The unit concludes with an introduction to what lifts space weather from the benign to the hazardous: the active sun.

The second unit (a little over a third of the book) has three chapters, and deals with active space weather. Disturbances on the sun are tracked through the solar medium (Chapter 10) to the magnetosphere (Chapter 11) and into the atmosphere (Chapter 12). This is the heart of hazardous space weather, and draws on the ideas and concepts of the earlier chapters. The third unit (of similar length) deals with the impacts of these disturbances. Chapter 13 covers the damaging effects of high-energy particles on space-based assets, both hardware and humans. The final chapter (14) covers its effects on signals and systems. The book closes with four short appendices and an index.

What's missing? Like any discipline, space weather is now vast, and cannot be encompassed by even a 700+ page book. All the same, almost every reviewer has their pet list of topics they like to see represented, so I dipped into the index at the end of the book to seek missing topics. I was surprised to find only one reference to the K_p index. However, this turned out to be a weakness in a very comprehensive index, as the K_p index appears in

other locations in the book, as it should. In a way, that is a metaphor for the scope of space weather: everything cannot be covered in equal detail without obscuring the message, which in this case is the physics of space weather.

Typos/spelling errors, grammatical mistakes, and other simple errors of detail are all an indication of production standards: I gave up looking for them. There must be a few, but if there are, the subject matter swept me past them. However, after a while, as a reviewer, you feel you are not paying attention if you don't find some small errors. I did find one incorrect reference, and I assume somebody must have added the error on the last page of the contents to encourage people like me. That's not really a surprise. This is a very encouraging book that guides people into the first-rate physical domain of space weather. As the author states, "In space, electricity, magnetism and gravity wage an unending battle for control of matter." That embraces a large amount of physics. At times, this will prove challenging for students, but at least they have a great book to help them tackle this immense field.

Summary: will this book produce space-weather experts? No, but it doesn't intend to. It aims to produce better-prepared space-weather specialists. It will engage people so that they reach this goal with confidence, and go on to enjoy the richness of the discipline.

Reviewed by

Phil Wilkinson
IPS Radio and Space Services, PO Box 1386, Haymarket, NSW 1240, Australia
E-mail: phil_wilkinson@internode.on.net

[Editor's note: The Young Scientists who received an award at the 2011 Istanbul URSI GASS were asked to review their favorite textbook, even if it was a classic book. This is in contrast to our usual reviews, where we try to have new books reviewed. The review below is from a Young Scientist.]

Sequence Design for Communications Applications

by Michael Darnell and Pingzhi Fan, London, Research Studies Press (RSP), John Wiley & Sons, 1996;
ISBN086380201X, 9780863802010

This book is an excellent reference for all students or/and researchers working in the digital-communications field and related areas. It gives an amazing review of all types of sequences. The book's material provides the reader with full information about the design of various sequences and their implementation. This is either interesting for readers with a mathematical background, or practical interests. Moreover, the book provides practical information about the utilization of each sequence, and considers it in current or emerging applications.

The book consists of four main parts. Part I is an introduction to sequence classification, correlation properties, structural properties, and mathematical prerequisites. Part II addresses binary sequences. Part III is dedicated to non-binary sequences, and Part IV discuss special types of sequences.

Part I starts with mandatory information about sequences. An interesting yet compact brief is given about the correlation properties of sequences and their relationships to sequence applications. This part also introduces some mathematical prerequisites, such as integer division, the Euclidean algorithm, Euler's toting function, residue classes, block design, irreducible polynomials, primitive polynomials, and the trace function. These details are discussed through Chapters 1, 2, and 3.

Part II starts with Chapter 4. It begins with the generation of some of the most commonly used spreading sequences, the pseudo-random sequences. Various types of M-sequences are considered, such as binary, non-binary, and Gaussian. Their generation and applications in different cellular systems are discussed. Chapter 5 considers binary sequences with good periodic correlations, such as special pairs of M-sequences, Gold sequences, and Kasami sets of sequences. Chapter 6 focuses on some binary sequences with large linear span. The construction and properties of Gold-Like sequences, Kasami-like sequences, and Bent-function sequences are highlighted, as well as their quaternary implementation, when available. The last part of the chapter presents some optimal sequences derived from interleaved M-sequences.

Part III of the book is oriented to non-binary sequences. Sequences with perfect periodic correlations are discussed in Chapter 7. This shows the properties, spectrum properties, correlation properties, and construction of the sequences. It also highlights types such as perfect sequences, two-valued perfect sequences, ternary perfect sequences, polyphase perfect sequences, and perfect sequences that can be modulated. Chapter 8 discusses non-binary sequences with two levels of periodic correlation. The chapter shows their group character, and then displays their types and makes comparisons among them. The chapter considers

Luke polyphase sequences, power-residue sequences, and cubic-phase sequences. Chapters 9 and 10 are concerned with quadriphase and polyphase sequences with good periodic correlation.

Finally comes Part VII, which discusses special types of sequences. It starts by displaying a selection of particular codes through Chapter 11. Examples include Barker sequences, Golay sequences, Huffman sequences, Ghu sequences, and Frank sequences. The chapter also considers their utilization in several applications. In particular, Chapter 12 considers array sequences. It focuses on pseudorandom arrays and perfect arrays. Their spectra, properties, and synthesis methods are shown. Chapter 13 addresses the complementary sequences: both code pairs and sets are highlighted. The chapter classifies three classes of complementary codes: periodic, orthogonal, and uncorrelated. Their use in current and future applications is discussed.

Chapter 14 discuss frequency-hopping (FH) sequences. It starts with the constructions of both types of one-coincidence frequency-hopping sequences. The properties of Greenberger frequency-hopping sequences and large-linear-span frequency-hopping sequences are then displayed, followed by a brief discussion of Costas arrays. The chapter is terminated by presenting frequency-hopping sequences with good auto- and cross-ambiguity functions. The last chapter is 15, which is addressed toward optical orthogonal sequences. It shows their basic concept, upper and lower bounds, and several construction methods.

This book is recommended both as a reference for researchers and professionals, and as a textbook.

Reviewed by:

Noha El-Ganainy
Arab Academy of Science and Technology.
E-mail: noha_elganainy@yahoo.co.uk

Have you written a book? Do you know a book written by a colleague that might be of interest for the URSI community? We would be glad to publish a review of such books in our URSI *Radio Science Bulletin*. Please contact our Associate Editor on book reviews, Kristian Schlegel (ks-ursi@email.de).

Conferences

CONFERENCE REPORTS

Report on International Reference Ionosphere (IRI) 2013 Workshop

Olsztyn, Poland, 24 - 28 June 2013

The 2013 Workshop of the International Reference Ionosphere (IRI) project was held at the University of Mazury and Warmia in Olsztyn, Poland, from June 24 to 28, 2013. The IRI is a joint undertaking by the Committee on Space Research (COSPAR) and the International Union of Radio Science (URSI), with the goal of developing and improving an international standard for the parameters in the Earth's ionosphere. This endeavor was originally triggered by the need for an ionospheric model for satellite/experiment design and satellite data analysis (COSPAR), and for radio propagation studies (URSI). However, it has meanwhile found a much broader range of users with space-weather concerns. As requested by these international unions, the IRI was built as an empirical model, representing the syntheses of all (or most) of the available ground and space measurements of ionospheric characteristics. IRI workshops bring together scientists from different countries, representing different measurement and modeling techniques, with the goal of improving the IRI model in a collaborative effort.

This was again nicely illustrated by the spectrum of participants attending the 2013 workshop, and the main collaborative studies presented during the week-long meeting. The meeting was attended by close to 70 scientists, representing 20 countries (Poland, USA, South Africa, Nigeria, Zambia, Uganda, Russia, China, Taiwan, Spain, Czech Republic, Italy, Turkey, Japan, Thailand, Sweden, Belgium, Argentina, Ukraine, Malaysia). 56 oral and 20 poster presentations were made. The meeting was divided into nine sessions, dealing with "Improvement of IRI with GNSS Data," "Real-Time IRI and the Representation of Storm Effects," "GNSS Monitoring of Ionosphere (TEC, Fluctuation, and Scintillation)," "Modeling of the High-Latitude Ionosphere," "New Inputs for IRI," "Mapping of Ionospheric Peak Parameters," "The Ionosphere and IRI During the Recent Solar Cycle," "IRI Applications," and "Posters." Prof. Andrzej Krankowski and his local organizing committee worked around the clock. They did a splendid job of hosting and organizing the workshop. The IRI team gratefully acknowledges financial support received for the meeting from COSPAR, URSI, the University of Warmia and Mazury, Leica Geosystems Poland, the National Space Organization (NSPO) in Taiwan, and INS Ltd. Poland.

Scientific Results and Future Plans

In line with the main topic of the workshop, many of the presentations involved GNSS (global navigation satellite system) measurements. TEC (total electron content) comparisons with the IRI (Oyeyemi et al., Nigeria; Bhoo Pathy et al., Malaysia; Wang et al., China; Habarulema et al., South Africa) showed generally good to fair agreement, with shortcomings in describing solar-cycle changes and variations at dawn and dusk. Tomographic and other techniques are being used to obtain the electron-density profile and foF2 from GNSS measurements (Sessanga and McKinnell, South Africa; Sibanda et al., Zambia). Combining different GNSS data sets, Zakharenkova et al. (WestIZMIRAN, Russia) were able to deduce information about the variability of the ionosphere and plasmasphere parts of the TEC. Krankowski (UMW, Poland) reviewed the activities of the IGS IONO group, and highlighted their new plans for higher time resolution (from two hours now to 15 minutes), and additional products, such as the irregularity index ROTI. Other GNSS services and products reviewed during this meeting included the IONOLAB-TEC (Arikan et al., Turkey), gAGE/UPC (Garcia-Rigo et al., Spain), DRAWING-TEC (Tsugawa et al., Japan), NICT products (Ishii et al., Japan), and COSMIC products and research (Liu et al., Taiwan). The ingest of TEC data into IRI was discussed by Migoya-Orue et al. (ICTP, Italy).

In the topside, IRI modeling is progressing, with promising new results for the Vary-Chap approach for the electron density presented by Reinisch et al. (LDI-UML, EDU). Of benefit will also be the study of Verhulst and Stankov (Belgium), which showed that for optimal results, different mathematical functions should be used for different conditions. Truhlik et al. (IAP, Czech Republic) improved the IRI topside ion-composition model by including a more-accurate description of solar-activity variations. Watanabe et al. (U. Hokkaido, Japan) used satellite in-situ data to study the correlation between electron temperature and density in the F region and topside, with the goal of including this relationship in the IRI. The IRI currently includes three options for the topside density (NeQuick, IRI-2001corr, and

IRI-2001). As a fourth option, the topside model of Gulyaeva (IZMIRAN, Russia) will be added in the next IRI release. This model uses the half-F-peak-density (0.5×NmF2) height h0.5 as an anchor point for an extension of the IRI to the plasmasphere, and was developed with ISIS and Alouette topside-sounder data.

There are exciting new developments regarding the representation of the F-peak height, hmF2, in the IRI. So far, the IRI has relied on the anti-correlation between hmF2 and the propagation factor M(3000)F2 and the CCIR models for this factor. This is because M(3000)F2 is easily obtainable from ionograms, while a much more involved analysis is required for getting hmF2. This modeling approach did well in reproducing the average global- and temporal-variation patterns, but it did not succeed in describing short-period variations such as the evening peak at equatorial latitudes. It was also found that this formalism produced hmF2 values that were too high during the past solar minimum, indicating a breakdown of the simple anti-correlation between the two parameters. Three groups are involved in developing models directly for hmF2. Altadill et al. (Ebro, Spain) used a spherical-harmonic representation of hmF2 data from a set of globally distributed ionosonde stations. The model of Gulyaeva et al. (IZMIRAN, Russia) was based on Alouette and ISIS topside sounder data, and used the correlation between hmF2 and NmF2. Karpachev et al. (SibIZMIRAN, Russia) based their model on carefully selected COSMIC radio-occultation data. It is planned to include these models as different options in the IRI.

Two efforts are underway to provide IRI users with more information than just the monthly averages, as they are given now: (1) A quantitative description of the monthly average of ionospheric variability, and (2) the real-time IRI, based on assimilating real-time data into the IRI. A description of the standard deviation from the monthly mean has long been a goal. Progress made during several IRI Task Force Activity meetings at the International Centre for Theoretical Physics (ICTP, Radicella) is now being picked up by the Argentinean Network for Atmospheric Research (RAPEAS) project. First results were presented at this meeting. Bilitza et al. (GMU, USA), studying topside-sounder data, found that ionospheric relative variability reaches a maximum in the topside (500 km to 700 km). Mosert et al. (CONICET, Argentina) presented a first table of representative values for the foF2 variability based on global ionosonde measurements. Good progress is being made in producing a real-time IRI. The IRI Real-Time Assimilative Mapping (IRTAM) of foF2 by Galkin et al. (UML, USA) updated the CCIR spherical-harmonic maps with global data from the Global Ionospheric Radio Observatory (GIRO) network of digisondes. They also discussed the use of IRTAM for studying the effects of sudden stratospheric warmings on the ionosphere. Altadill et al. (Ebro, Spain) presented a prediction of hmF2 storm-time changes based on IMF Bz measurements by the ACE satellite.

Publications, Meetings, and New Members

The refereed and accepted papers from the 2010 COSPAR session on the "Representation of the Auroral and Polar Ionosphere in IRI" were published in a dedicated issue of *Advances in Space Research* (**51**, 4, February 15, 2013), with D. Bilitza and B. Reinisch as guest editors. Editing is in the final stages for a special *Advances in Space Research* issue with papers from the 2011 IRI workshop that was held in Hermanus, South Africa, which was focused on "Improvements of IRI over the African Region." The 14 papers finally accepted for this issue gave a good overview over ionospheric activities on the African continent.

The year 2014 will see several meetings of interest to the IRI team and community. Considerable progress is expected with regard to the development of the real-time IRI, through two meetings organized by the IRI team in 2014. There will be a one-day session during the Digisonde/GIRO Forum in Lowell, USA, May 19-21, 2014 (which will follow the Ionospheric Effects Symposium held in Alexandria near Washington, DC). There will also be a session entitled "Improved Representation of the Ionosphere in Real Time and Retrospective Mode" during the COSPAR Scientific Assembly in Moscow, Russia, August 2-10, 2014. The URSI General Assembly will be held in Beijing, China, August 16-23, 2014, and will include a session on "Ionosphere and Plasmasphere Electron Density Profiles," with L.-A. McKinnell as the main organizer. For the 2015 IRI Workshop, the IRI Working Group accepted an invitation by Prof. Pornchai Supnithi to host the meeting in Bangkok, Thailand. The meeting's focus will be on scintillations and spread-F.

Irina Zkharenkova (Russia) was elected as a new member of the IRI team. Irina is a researcher from the West Department of IZMIRAN in Kaliningrad, Russia. She is currently working at the Geodynamics Research Laboratory of the University of Warmia and Mazury in Olsztyn, Poland. Irina has made important contributions to determining the plasmaspheric electron content (PEC) from GNSS measurements, and to studying the variability of the PEC. As a member of the Local Organizing Committee for the 2013 IRI Workshop, she helped to make this a very successful and productive meeting.

Dieter Bilitza
George Mason University, Fairfax, VA, USA
E-mail: dbilitza@gmu.edu

CONFERENCE ANNOUNCEMENT

International School on Atmosphere-Ionosphere Radar
ISAR-NCU-2013

National Central University, Jhongli, Taiwan, 11 - 20 November 2013

The National Central University has decided to continue the series of International Radar Schools and to organise the eighth ISAR-NCU-2013 from 11 to 20 November 2013 in the National Central University (NCU) in Jhongli, Taiwan, which is, together with the National Research Council (NSC) of Taiwan, the main sponsor of this school.

The general topics of ISAR-NCU-2013 will again be a basic overview and introduction on radar systems and methods for atmosphere and ionosphere research. These span from Doppler weather radars, wind profilers, mesosphere-stratosphere-troposphere radars to meteor and ionosphere coherent and incoherent scatter radars. Some limited special highlights of weather observations with these radar methods will be explained, such as extreme weather developments, typhoon passages, frontal systems, tropopause detection, mountain lee waves, development of convective clouds, precipitation and lightning radar localizing by interferometry, two dimensional turbulence as well as applied meteorology and lower and middle atmosphere and ionosphere refractivity irregularities The technical and signal processing of radar data will be handled more intensely during this year's school, and will also treat some basics of atmosphere/ionosphere radar imaging.

An important goal of ISAR-NCU 2013 is to attract students to this atmosphere and ionosphere research by means of radar. It is not required for the applicants to have established relations or expert knowledge of radar techniques, but to show basic interest and some experience in meteorology and/or atmosphere and ionosphere physics.

Lecturers will again be from the NCU and the international community of weather radar and atmosphere-ionosphere research using ground-based radar methods. The school lectures and training will aim towards graduate and PhD students, young postdoctoral research scientists from South-East Asian countries and India, who have not yet specifically worked but have developed interest in radar atmosphere and/or ionosphere science.

Financial support for young students to participate at ISAR-NCU-2013 can be provided by NSC/NCU on proven demand.

Contact

http://isarncu.tw

URSI CONFERENCE CALENDAR

An up-to-date version of this conference calendar, with links to various conference web sites can be found at http://www.ursi.org/en/events.asp

July 2013

IconSpace 2013 - 2013 International Conference on Space and Communication
Malacca, Malaysia, 1-3 July 2013
Contact: iconspace@ukm.my, http://www.ukm.my/iconspace2011

Beacon Satellite Symposium
Bath, UK, 8-12 July 2013
Contact: Prof. Cathryn Mitchell, University of Bath, Electronic and Electrical Engineering, University of Bath, Clavertown Down, BATH, BA2 7AY, UK, E-mail: c.n.mitchell@bath.ac.uk, http://www.bc.edu/research/isr/ibss.html

ISSS-11 - The 11th International School/Symposium for Space Simulations
Jhongli City, China SRS, 21-28 July 2013
Contact: isss11@jupiter.ss.ncu.edu.tw, http://isss11.ss.ncu.edu.tw/

August 2013

HF 13 - 10th nordic HF conference
Fårö, Baltic Sea, 12-14 August 2013
Contact: HF 10, Saab AB, Support and Services,SE-581 82 Linköping, Sweden , Phone: +46 13231321, Fax: int +46 13231121, E-mail: margareta.samuelsson@saabgroup.com, http://www.nordichf.org

Joint Workshop of URSI Commission K and ICNIRP
Paris, France, 29-30 August 2013
Contact: emmanuelle.conil@orange.com, http://whist.institut-telecom.fr/URSI2013/ursi_icnirp.html

September 2013

EMC Europe 2013 Brugge
Brugge, Belgium, 2-6 September 2013
Contact: Davy Pissoort, Head FMEC, Zeedijk 101, B8400 Oostende, Belgium, Fax: +32 59 56 90 01, E-mail: davy.pissoort@khbo.be, http://www.emceurope2013.eu

AP-RASC 2013 - 2013 Asia-Pacific Radio Science Conference
Taipei, China SRS, 3-7 September 2013
Contact: Prof. K. Kobayashi, Chair, AP-RASC International Advisory Board, Fax: +886-2-23632090, E-mail: ctshih@tl.ntu.edu.tw, http://aprasc13.ntu.edu.tw/

Africon 2013 - Sustainable Engineering for a Better Future
Mauritius, 9-12 September 2013
Contact: generalchair@africon2013.org, http://africon2013.org

ICEAA-APWC-EMS conferences - The first Electromagnetic Metrology Symposium
Torino, Italy, 9-13 September 2013
Contacts: Prof. W.A. Davis, EMS Chair wadavis@vt.edu and Prof. Y. Koyama, EMS Vice-Chair koyama@nict.go.jp, http://www.iceaa.net

Metamaterials 2013 - The Seventh International Congress on Advanced Electromagnetic Materials in Microwaves and Optics
Bordeaux, France, 16-21 September 2013
Contact: Prof. Sergei A. Tretyakov, Dept. Of Radio Science and Engineering, Aalto, School of Electrical Engineering, PO Box 13000, FI-00076 Aalto, Finland, E-mail: sergei.tretyako@aalto.fi, fax: +358 9 470 22152, http://congress2013.metamorphose-vi.org/

October 2013

OCOSS 2013 - Ocean and Coastal Observation Sensors and Observing Systems, Numerical Models and Information Systems
Nice, France, 28-31 October 2013
Contact: Ms. M. Dechambre, LATMOS, Quartier des Garennes, 11, Bd des Garennes, F-78280 Guyancourt, France, E-mail: monique.dechambre@latmos.ipsl.fr, http://2013.ocoss.org/

November 2013

First COSPAR Symposium - Planetary Systems of our Sun and other Stars, and the Future of Space Astronomy
Bangkok, Thailand, 11-15 November 2013
Contact:Geo-Informatics and Space Technology Development Agency, Ratthaprasasanabhakti Bdg 6th and 7th Floor, Chaeng Wattana Road, Lak Si, Bangkok 10210, THAILAND, E-mail:cospar2013@gistda.or.th, http://www.cospar2013.gistda.or.th

December 2013

4th International Colloquium on Scientific and Fundamental Aspects of the Galileo Programme
Prague, Czech Republic, 4-6 December 2013
Contact: ESA Conference Bureau, PO Box 299, NL-2200 AG Noordwijk, Netherlands, Fax: +31 (0) 71 565 6558, E-mail: esa.conference.bureau@esa.int, http://www.congrexprojects.com/2013-events/13c15/introduction

ICMAP 2013 - International Conference on Microwaves and Photonics
Dhanbad, India, 13-15 December 2013
Contact: http://icmap2013.org, http://icmap2013.org/

January 2014

RCRS 2014 – Regional Conference in Radio Science
Pune, India, 2-5 January 2014
Contact: Prof. Akshay Malhotra, Deputy Director, SIT, Pune, Symbiosis Institute of Technology (SIT), Symbiosis International University, Tel : +91 20 39116300, 6404 / 6407, e-mail: rcrs2014@sitpune.edu.in, http://www.sitpune.edu.in/abstract_submission_form.php

URSI National Radio Science Meeting
Boulder, Colorado, USA, 8-11 January 2014
Contact: Prof. Steven C. Reising, Director of Microwave Systems Laboratory, Colorado State University, 1373 Campus Delivery, Fort Collins, CO 80523-1373, USA, Fax: +1-970-491-2249, Email: steven.reising@colostate.edu, http://www.nrsmboulder.org/

VERSIM-6 - Sixth VERSIM Workshop
Dunedin, New Zealand, 20-23 January 2014
Contact: Prof. Craig J. Rodger, Department of Physics, University of Otago, PO Box 56, Dunedin 9016, NEW ZEALAND, Fax: +64 3 479 0964, E-mail: crodger@physics.otago.ac.nz, http://www.physics.otago.ac.nz/versim/VERSIM_workshop_Dunedin_2014.html

April 2014

RADIO 2014 - Radio and Antenna Days of the Indian Ocean 2014
Flic-en-Flac, Mauritius, 7-10 April 2014
Contact: Conference Secretariat RADIO 2012, University of Mauritius, Réduit, Mauritius, Fax: +230 4656928, E-mail: radio@uom.ac.mu, http://sites.uom.ac.mu/radio2012/

May 2014

EMC'2014 - 2014 International Symposium on Electromagnetic Compatibility
Tokyo, Japan, 13-26 May 2014
Contact: E-mail: emc14-contact@mail.ieice.org, http://www.ieice.org/~emc14/

June 2014

EUSAR 2014 – 10th European Conference on Synthetic Aperture Radar
Berlin, Germany, 2-6 June 2014
Contact: Mr. Jens Fischer (DLR), EUSAR 2014 Executive, Oberpfaffenhofen, 82234 Wessling, Germany, Fax: +49 8153-28-1449, E-mail: eusar2014@dlr.de, http://conference.vde.com/eusar/2014

August 2014

COSPAR 2014 ("COSMOS")
40th Scientific Assembly of the Committee on Space Research (COSPAR) and Associated Events
Moscow, Russia, 2-10 August 2014
Contact: COSPAR Secretariat, c/o CNES, 2 place Maurice Quentin, 75039 Paris Cedex 01, France, Tel: +33 1 44 76 75 10, Fax: +33 1 44 76 74 37, cospar@cosparhq.cnes.fr, http://www.cospar-assembly.org/

ICEAA 2014 - International Conference on Electromagnetics in Advanced Applications
Palm Beach, Aruba, 3-9 August 2014
Contact: Prof. P.L.E. Uslenghi, Dept. of ECE (MC 154), University of Illinois at Chicago, 851 So. Morgan St., Chicago, IL 60607-7053, USA, E-mail: uslenghi@uic.edu, http://www.iceaa.net/

XXXIth URSI General Assembly and Scientific Symposium
Beijing, China, 16-23 August 2014
Contact : URSI Secretariat, c/o Intec, Sint-Pietersnieuwstraat 41, B-9000 Ghent, Belgium, Email : info@ursi.org, http://www.chinaursigass.com

September 2014

EMC Europe 2014
Gothenburg, Sweden, 1-4 September 2014
Contacts: Symposium Chair: jan.carlsson@sp.se, Technical Program Chair: peterst@foi.se, http://www.emceurope2014.org/

URSI cannot be held responsible for any errors contained in this list of meetings

News from the URSI Community

NEWS FROM THE MEMBER COMMITTEES

FRANCE
Médaille du CNFRS

La Médaille du Comité national français de radioélectricité scientifique (CNFRS), membre de l'Union radio scientifique internationale (URSI), a été décernée le 26 mars 2013 à Jean-Pierre Bérenger.

Le CNFRS/URSI-France souhaite ainsi souligner l'importance des contributions de Jean-Pierre Bérenger à l'électromagnétisme. Sa contribution scientifique majeure porte sur l'invention de «conditions aux limites absorbantes» (PML : Perfectly Matched Layers) beaucoup plus performantes que les conditions utilisées jusqu'alors. Il s'agit de conditions aux limites imposées dans la résolution numérique des équations de Maxwell par la méthode FDTD (Finite Difference Time Domain), qui maille un volume d'espace nécessairement fini bien que le rayonnement s'étende à l'infini. La technique PML est maintenant universellement utilisée et la contribution de Jean-Pierre Bérenger est reconnue dans le monde entier pour avoir fortement fait progresser la performance de la FDTD. Jean-Pierre Bérenger a également développé des codes numériques efficaces dans le domaine de la compatibilité électromagnétique et des très basses fréquences.

La Médaille du CNFRS/URSI-France est « destinée à honorer une personnalité scientifique qui a contribué à des avancées remarquables en radioélectricité et qui a participé à l'animation scientifique de la communauté française et internationale ».

Biographie de Jean-Pierre Bérenger

Titulaire de la Maîtrise de physique de l'Université de Grenoble (1973) et Ingénieur de l'École supérieure d'optique (1975), Jean-Pierre Bérenger a rejoint le département Études théoriques d'Arcueil de la Délégation générale de l'armement (DGA) en 1975 pour se consacrer a de la recherche appliquée sur la propagation dans les milieux perturbés par les rayonnements nucléaires et les effets de l'impulsion électromagnétique. Il s'est particulièrement attaché à la résolution numérique des équations de Maxwell et aux problèmes ouverts nécessitant l'utilisation d'une condition aux limites absorbante. Il a ainsi introduit en 1979 une condition originale, la couche adaptée, et est l'auteur du premier logiciel aux différences finies (FDTD) développé en France.

Au Centre d'analyse de défense, à partir de 1984, et en parallèle avec d'autres activités dans la simulation informatique de défense, Jean-Pierre Bérenger a effectué des travaux de recherche sur les conditions absorbantes et les structures subcellulaires dans la méthode FDTD. Il introduit en 1990 la couche parfaitement adaptée (PML). Publiée en 1994 et rapidement adoptée par la communauté de l'électromagnétisme, cette condition a suscité de nombreux travaux et a été transposée à toutes les équations aux dérivées partielles de la physique. Ses travaux sur ce thème se sont poursuivis pendant une dizaine d'années pour optimiser la condition PML dans l'espace discrétisé des techniques numériques. Au cours des années 90, il a aussi développé l'application de la méthode FDTD à la propagation VLF-LF dans le guide d'onde Terre-Ionosphère, travaux ayant abouti à un logiciel fournissant le bilan de liaison VLF-LF dans des conditions très générales.

Depuis 2003, à côté d'un rôle d'expert DGA sur les effets électromagnétiques des rayonnements nucléaires et de responsable d'études prospectives, Jean-Pierre Bérenger a poursuivi ses recherches sur :

- les problèmes de sous-maillage dans les techniques numériques avec l'introduction d'une méthode originale (Huygens subgridding) qui élimine la plupart des inconvénients des méthodes antérieures ;
- la propagation VLF-LF avec le développement d'un nouveau schéma plus performant ;
- et, depuis peu, l'introduction d'un nouveau concept de conditions aux limites absorbantes (Huygens absorbing boundary condition) moins général que la condition PML mais aussi efficace et plus simple à utiliser.

Fellow IEEE, Jean-Pierre Bérenger a été Associate Editor du journal IEEE Transactions on Antennas and Propagation de 2006 à 2010. Dans les années 90, il a collaboré sur divers sujets avec l'équipe électromagnétisme de l'Université de Limoges, et depuis 2005 avec l'Université de Manchester (UMIST) sur le développement de la méthode FDTD pour le bioélectromagnétisme.

FINLAND
Finnish URSI Radio Science Days 2013

The first Finnish Radio Science Days took place April 24-25, 1953. This convention, "Radio Days" (in Finnish, "Radiopäivät") was a successful effort of the newly formed Finnish member committee of URSI. The two-day seminar highlighted the active work that Finnish radio scientists had accomplished in various domains of URSI during these years of great activity in the 1950s (Figure 1).

Exactly 60 years later, April 24-25, 2013, the Finnish Member Committee of URSI (Figure 2) organized the XXXIII Finnish Convention on Radio Science. This meeting brought together a more-global collection of radio scientists than in early times: Finnish research groups are nowadays truly international, and the convention itself attracted several researchers from abroad. The meeting served also as a SMARAD seminar. SMARAD is an Academy of Finland –selected Centre of Excellence in Smart Radios and Wireless Research. This center, the operations of which started in 2000, is a research network of three departments in the Aalto University School of Electrical Engineering: namely, the Department of Radio Science and Engineering, the Department of Signal Processing and Acoustics, and the Department of Micro and Nanosciences.

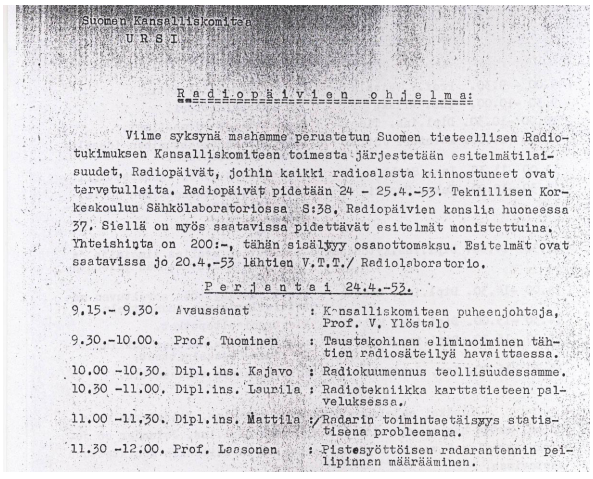

Suomen Kansalliskomitea
U R S I

R a d i o p ä i v i e n o h j e l m a:

Viime syksynä meshamme perustetun Suomen tieteellisen Radiotukimuksen Kansalliskomitean toimesta järjestetään esitelmätilaisuudet, Radiopäivät, joihin kaikki radioelosta kiinnostuneet ovat tervetulleita. Radiopäivät pidetään 24 - 25.4.-53. Teknillisen Korkeakoulun Sähkölaboratoriossa S:38. Radiopäivien konsiia huoneessa 37. Siellä on myös saatavissa pidettävät esitelmät monistettuina. Yhteishinta on 200:-, tähän sisältyy osanottomaksu. Esitelmät ovat saatavissa jo 20.4.-53 lähtien V.T.T./ Radiolaboratorio.

P e r j a n t a i 24.4.-53.

9.15.- 9.30.	Avaussanat	: Kansalliskomitean puheenjohtaja, Prof. V. Ylöstalo
9.30.-10.00.	Prof. Tuominen	: Taustakohinan eliminoiminen tähtien radiosäteilyä havaittaessa.
10.00 -10.30.	Dipl.ins. Kajavo	: Radiokuumennus teollisuudessamme.
10.30 -11.00.	Dipl.ins. Launila	: Radiotekniikka karttatieteen palveluksessa.
11.00 -11.30.	Dipl.ins. Mattila	: Radarin toimintaetäisyys statistisena probleemana.
11.30 -12.00.	Prof. Leesonen	: Pistesyöttöisen radarantennin peilipinnan määrääminen.

Figure 1. The first lectures of the Radio Days in 1953: after the opening, the talks focused on "Eliminating the Background Noise in the Observation of the Radio Emission from Stars," "Radio Heating in our Industry," "Radio in Service of the Science of Mapping," "The Operation Distance of Radar as a Statistical Problem," and "Determining the Reflector Surface of a Point-Fed Radar Antenna."

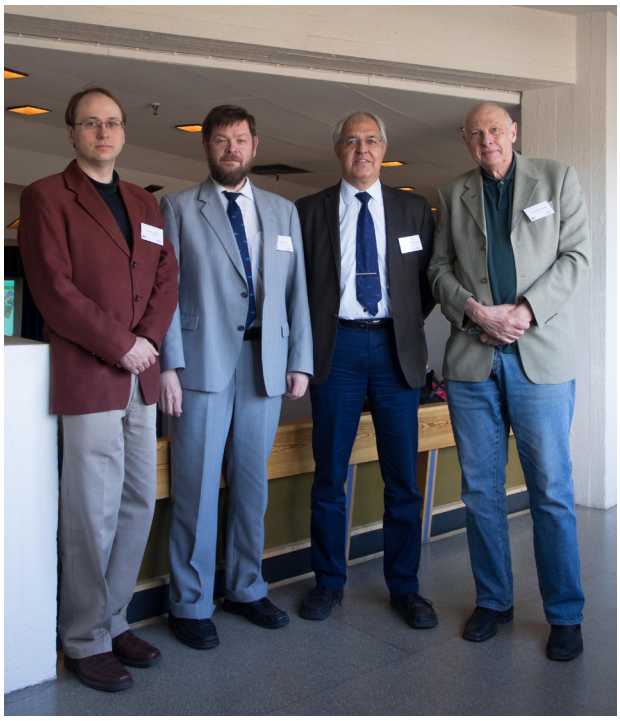

Figure 2. The Swedish Member Committee was respectfully present at the convention: (l-r) Henrik Wallén (Secretary, URSI Finland); Ari Sihvola (Chair, URSI Finland); Gerhard Kristensson (Chair, URSI Sweden); Carl-Henrik Walde (Secretary, URSI Sweden). Note the URSI ties (photo: Juhani Kataja)!

During the two days in late April, 46 contributed presentations were given within all of the URSI Commissions. In addition, eight plenary presentations provided the state-of-the-art in various domains of radio science:

- Prof. Esko Valtaoja (University of Turku): "Radio Astronomy, Planck, and the Evolution of the Universe?"
- Dr. Mikko Uusitalo (Nokia Research Center): "What is there Beyond 4G?"
- Prof. Danielle Vanhoenacker-Janvier (University of Louvain-la-Neuve): "Impact of Tropospheric Turbulence on Non-Geostationary Communication Systems"

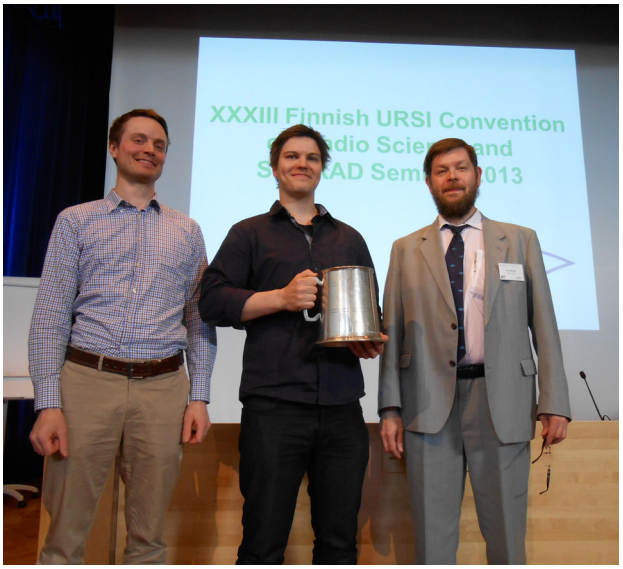

Figure 3. The Young Scientist Award for the best paper and presentation by a radio scientist younger than 35 years was given to Dr. Tero Kiuru from VTT, Technical Research Centre of Finland (here, between Ville Viikari, Chair of the YSA Committee, and Ari Sihvola) for his contribution, "Thermal Characterization as a Part of Reliability Testing of THz Schottky Diodes" (photo: Tommi Rimpiläinen).

Figure 4. Prof. Martti Tiuri was one of the organizers of the first Finnish "Radio Days" exactly 60 years ago. He later served as the Chair of the Finnish URSI Committee during 1966-1991. At the banquet of the 2013 convention, he shared his recollections of the early times of Finnish radio science (photo: Janne Lahtinen).

- Dr. Ville Kangas (European Space Agency): "Current and Future Microwave Remote Sensing Instruments at ESA"
- Prof. Yrjö Neuvo (Aalto University): "Internet and Wireless Go Everywhere"
- Prof. Heli Jantunen (University of Oulu): "Printed Antennas"
- Prof. Björn Ottersten (Kungliga tekniska högskolan, Stockholm, and University of Luxembourg): "Satellite Communications – Signal Processing Challenges"
- Dr. Antti Manninen (Centre for Metrology and Accreditation in Finland): "Towards the New SI System of Units"

The Young Scientist Award for the best paper and presentation by a radio scientist younger than 35 years was presented at the conference (Figure 3).

At the evening banquet, the true history of Finnish radio science was present. We were fortunate to have Prof. Martti Tiuri among us (Figure 4). Prof. Tiuri served as one of the organizers of the very first Radio Days in 1953, exactly 60 years ago. During the banquet, he described the way radio science was performed those early days. The presentations during the 1953 convention by Martti Tiuri dealt with magnetic attenuators, and with the manner of how a reactive element could be matched to a circuit. To solve this problem, today's electrical engineering student would use Smith's chart. However, in those days it was not very well known: when Tiuri in the next year went to Stanford University for graduate studies, he had to work as a missionary for the Smith chart!

A few copies of the *Proceedings of the XXXIII Finnish Radio Science Convention* are available from the organizers.

Links: Finnish Member Committee of URSI: http://www.ursi.fi/

XXXIII Finnish URSI Convention on Radio Science and SMARAD Seminar 2013: http://www.ursi.fi/2013/

SMARAD: http://smarad.aalto.fi/en/

Ari Sihvola and Henrik Wallén
Aalto University, Department of Radio Science and Engineering, Espoo, Finland
E-mail: ari.sihvola@aalto.fi

SWEDEN
Radio Science in Latvia

The Swedish national member committee of radio science in URSI, SNRV (Svenska Nationalkommittén för radiovetenskap), combined its annual meeting with a spring excursion to Latvia by cruising over the Baltic Sea on *M/S Romantika*. For a few years, we have had the tradition of making social visits to some of the neighboring national committees. Earlier, we visited Finland and Denmark. Discussions during these visits pointed out that some of our neighbors – the three Baltic countries, Estonia, Latvia, and Lithuania – are not members of URSI.

These countries met hardships during World War II, due to their geographical location between Nazi Germany and the Soviet Union. They lost their independence for half a century. When the Baltic countries re-emerged in the early 1990s, the previous Soviet URSI membership went over to Russia, while Estonia, Latvia, and Lithuania were left outside. In two decades, these countries have made enormous progress to reach a modern level of communication and technology. It would thus be a benefit both for URSI and the Baltic countries if they joined URSI as part of its ambition to stimulate and coordinate, on an international basis, studies, research, applications, scientific exchange, and communication in the field of radio science.

Latvia has a very special role in radio science. When the Russian army withdrew from Latvia in 1994, the country inherited the remains of a Soviet space communication facility. This station, located in Irbene, was top secret.

Figure 2. The Swedish SNRV delegation and some members of the staff admire the 32-m telescope.

Although it was the home of about 2000 Soviet officers and their family members, Latvians did not know of its existence. Today, we can only imagine the tasks of this cold-war facility in the western-most part of the former Soviet Union.

Our group disembarked at the port a few kilometers upstream from the mouth of the river Daugava at the bottom of the Gulf of Riga, on Sunday morning, April 21. Our eight delegates started the three-hour drive through the beautiful spring landscape, towards the city of Ventspils on the west

Figure 1. Our host, Director Valdis Avotins, at VIRAC.

Figure 3. The impressive VIRAC antenna.

Figure 4. The 32-m antenna drives are still partially controlled with the old (vacuum-tube-based) steering system (photo: Gudmund Wannberg).

Figure 5. This shows parts of the new receiver system. The timing and frequency control are provided by a hydrogen maser (center) (photo: Joakim Johansson).

coast. Our hosts had arranged a rendezvous at a lay-by along the road. At the right place and time, we met the Director of VIRAC (the Ventspils International Radio Astronomy Centre), Dr. Valdis Avotins (Figure 1). This was good, since the rest of the route to the former top-secret facility went along small, narrow roads.

The Ventspils International Radio Astronomy Center

When approaching the destination, we were overwhelmed by the massive 32-m parabolic dish, towering above the top of the pine forest (Figures 2 and 3). The Ventspils International Radio Astronomy Center (http://virac.venta.lv/en/) hosts one of world's eight largest radio telescopes. The facility was used for signal intelligence during the Cold War years by the Soviets, to intercept radio signals and telephone conversations in the NATO countries. Soon after Latvia's independence was restored in 1994, the Russian military personnel left the place. When they withdrew, a lot of the equipment, such as the electric motors and the cables, were destroyed. Fortunately, the huge antenna dishes were left intact. We were told that the Russian Academy of Science played a role in this. Even the Swedish Academy of Science was involved. This is the origin of the word "International" in VIRAC's name.

Once at our destination, the earlier secrecy changed to a warmly welcoming atmosphere, with coffee, pies, and cakes. We were given a very friendly greeting by a group of enthusiastic employees, who proudly presented their work and international collaboration, and gave us a tour around their facilities. In addition to Director Avotins, there was their leading researcher, Janis Trokss; Miks Klapers, a researcher and engineer; as well as engineer Agris Berzins. We had a presentation of the history of the place, about the upgrades since the turnover, and a review of their education and science programs. While much of the hardware still revealed the history of the place, the electronics associated with the software was definitively up-to-date (Figures 4 and 5).

With assistance from the European Union and support by many scientists with their roots in Latvia, the former military receiver was transformed to serve scientific purposes. The interests extend from basic research to signal processing and radio hardware, and the staff has received very good training while refurbishing the antenna systems. VIRAC runs projects to observe the sun in the microwave range, and interferometric and radio astronomy studies with the ambition of become a member of the European VLBI (Very Long Baseline Interferometry Network) EVN. VIRAC recently participated in an initial EVN test, and sent data at 5 Gb/s to The Netherlands. Observed fringes confirmed that the facility worked properly. The VIRAC staff also work on projects to improve the detection, analysis, and processing of satellite images and satellite navigation signals. They do research on the efficiency of electric-drive control, adaptation of antenna control, and data-registration software.

The 32-m wide antenna, weighting 600 tons, is the largest radio telescope in Northern Europe. A smaller, 16-m radio telescope has also been renovated in Irbene. This instrument will soon be used to track the first Latvian satellite, currently being built by Latvian students in cooperation with the University of Bremen. VIRAC is associated with the Ventspils University College as an Engineering Research Institute. It has four departments: electronic engineering, high-performance computing, astronomy and astrophysics, and space technology. In addition, the college has a strong profile in languages, which is considered important in Latvia. During our whole visit, we noted that all the professionals spoke very good English.

We were invited to climb up to the external platforms on the upper floors of the telescopes, and enjoy the beautiful views extending across the surrounding Kurzeme forests

Figure 6. The mechanical structures are massive; the way to the top alternates between tunnels and ladders (photo: Joakim Johansson).

Figure 7. The Chair of the Swedish delegation, almost at the top of the antenna.

(Figures 6 to 8). We also saw the underground kilometer-long tunnels connecting the radio telescope with the technical headquarters (Figure 9). The views of the abandoned military town were very sad (http://englishrussia.com/2012/01/06/irbene-a-secret-object-of-the-soviet-past/).

Latvian Electrical and Electronics Industry Association (LEtERA)

On Monday morning, we visited the Latvian Electrical and Electronics Industry Association (LEtERA). Again, we were met with great hospitality from the Executive Director of the organization, Inese Cvetkova, and the President, Normunds Bergs. They gave us a detailed description of the development of the Latvian industry after the Soviet period. About 200,000 people had been employed in the electronic industry at that time, many of them in defense electronics. This branch collapsed overnight in 1991.

In the new stage of independence, a hard-working period of renewed entrepreneurship to build up modern industry for the country commenced. Isolated pockets of expertise existed, such as the pocket associated with VIRAC, and new pockets emerged. LEtERA is present to encourage companies to develop their own products. The Investment and Development Agency of Latvia (LIAA) also promotes business development by facilitating foreign investments in parallel with the increasing competitiveness of Latvian entrepreneurs expanding in domestic and foreign markets. The geographical position that made Latvia so vulnerable 70 years ago has turned into an advantage. The country is a member of the European Union, and has a cultural connection towards the emerging markets of its eastern neighbors: Russia, etc.

Figure 8. The shadow of the antenna, photographed from its top, and the wide beautiful pine forests, which for decades hid the huge facility from the Latvians.

Figure 9. The old kilometer-long tunnels connecting the antennas to the HQ (photo: Gudmund Wannberg).

Figure 10. Normunds Bergs and Inese Cvetkova at LEtERA, with Guntars Balonis from RTU sitting between them.

We left LEtERA sharing the positive expectations of the future of the Latvian electrical engineering industry. However, we were still aware of the problem that many young people, especially those with a good education, want to try their luck abroad. Before our next stop our host, professor Guntars Balodis, invited us for lunch (Figure 10).

Figure 12. There were many very beautiful old buildings in Riga (photo: Mats Bäckström).

Figure 11. The Swedish delegation and the hosts from RTU at a nice dinner: (l-r) Peteris Misans, Gudmund Wannberg, Arnis Gulbis, Carl-Henrik Walde, Jan Kjellgren, Asta Pellinen-Wannberg, Mats Bäckström, Gerhard Kristensson, Guntars Balodis, Annika Grönberg Johansson, and Joakim Johansson.

Riga Technical University

In the afternoon, we visited the Faculty of Electronics and Telecommunications (ETF) of the Riga Technical University (RTU). We were welcomed by Prof. Guntars Balodis, who told us about the university, which was founded 1862. The Institute of Electronics and Computer Science has about 80 researchers and a total staff of 200. They have 18 PhD students.

Both PhD students and senior staff gave us talks about their research activities. The topics covered fiber-optics transmission systems, wireless communications for vehicles and transport systems, signal processing for medical applications, high-frequency measurements in an anechoic chamber, and the more-theoretical signal syntheses by rotational matrixes.

We were also informed about some of the problems at the university. The age distribution is skewed towards the oldest employees. Most students want to study communications, only a few want to study electronics. We were told that there was one female staff member and six to seven female PhD students, even though we did not meet any.

Postscript

During discussions at the different institutions on our tour, it became clear that there are many activities related to URSI, and an interest in joining the organization. The Statutes of URSI say that the Members of the Union are

the Committees whose applications for membership have been adopted at an Ordinary General Assembly, and that a Member Committee is established in a territory by its Academy of Sciences or Research Council, or by a similar institution or association of institutions. The problem in Latvia seems to be that there are no radio scientists within the Latvian Academy of Sciences. The option of starting with an Associate Membership was discussed, and SNRV will continue to negotiate this issue.

We finished the official part of our visit by hosting a dinner together with some of our new friends from RTU in a traditional Latvian restaurant (Figure 11). The Chair of the Swedish delegation, Prof. Gerhard Kristensson, assured the Swedish support for the Latvians to find a way to join the radio science family of URSI.

We were very impressed by the beauty of Riga in the parks and all the renovated buildings (Figure 12). We had heard about Latvia from our parents, but the country existed only in history, not in the geography books during our school time. We are happy to see them back in business, and especially in radio science.

Asta Pellinen-Wannberg
Umeå University and Swedish Institute of Space Physics, Box 812, SE-98128, Kiruna, Sweden
E-mail: asta.pellinen-wannberg@irf.se

ORGANIZERS

Technical sponsors

NICE (FRENCH RIVIERA), FRANCE
OCTOBER 28-31, 2013

Call for Papers

About OCOSS'2013

OCOSS'2013 aims at taking stock of recent projections and future developments of research and technologies related to sea and ocean observation.
It is also an opportunity to pursue -at an European level- the targets put forward in the *Aberdeen declaration* or -at the French level- in the ***«Grenelle de la mer»***.

It offers a broad spectrum covering physical oceanography (waves, tide, currents, thermocline, salinity, turbidity...) and marine geoscience, meteorology and climatology, monitoring of the environment and the coastal ecosystem as well as the optimization of fishing resources, assistance with exploration and exploitation of the oceans (offshore oil rigs, marine energy: tides, wind, oil spills...). The cartography of sea-beds (bathymetry, imagery, geology...), space oceanography and underwater robot-like systems are of primary importance. Other relevant topics include command and detection systems for control of civil and naval forces' sea traffic.

The general topics of this conference will be organized around the following research topics (unexhaustive list):

- Sensors for Environmental Ecosystem Assessment: Multiscales & Multi-physics Models,
- Sensors for Green-Energy: Off-shore Wind-Farm, hydrolic energy, ...
- Bio-sensors for real time monitoring of bio-hazard and man-made chemical pollution,
- Innovative multifunctional sensors for in-situ monitoring of marine environment and related maritime activities,
- Operating Environment Assessment for EM, EO/IR & Acoustic Sensors,
- Remote Sensing Technics, Processing and Data management,
- METOC (Meteorology Oceanography) Systems,
- Underwater, Onshore/Offshore & Airborne Observation Platforms,
- Maritime Safety & Security Surveillance Systems (Sea and Harbors),
- Awareness system and risk management,
- Rules of Access to the Frequency Spectrum,
- Innovative antifouling materials for maritime applications,
- Innovative transport and deployment systems for the offshore wind energy sector METOC...

OCOSS'2013 will also focus on subjects developed by various local laboratories and research centres:

- Measurement Instruments for field experimentation (space, airborne, etc.),
- Maritime risk modeling,
- Multi-scale and multi-physical models for the evaluation of environmental ecosystems,
- Risk and Disaster management,
- Physical conditions of the sea-air interface...

WELCOME

The BENELUX Antenna & Propagation Community welcomes EuCAP 2014 to The Hague, situated on the North Sea Coast, close to Amsterdam Schiphol Airport.

EuCAP 2014 is the 8th European Conference on Antennas & Propagation organised by the European Association on Antennas and Propagation (EurAAP) since 2006. The previous successful editions took place in Nice, Edinburgh, Berlin, Barcelona, Rome, Prague and Gothenburg. The average attendance is around 1000 delegates.

EuCAP is supported by the top level Associations in Antennas and Propagation, thus fostering true collaboration at European and global levels. AMTA will support the organisation of the Exhibition, provide special AMTA sessions, and cooperate in the application tracks.

SCOPE OF THE CONFERENCE

To provide a forum on the major challenges faced by the Antenna, Propagation and Measurement communities with the aim of fostering exchange of ideas between experts in their respective fields. Contributions from European and non-European industries, organisations, universities and institutions are solicited. This conference will provide an overview of the current state-of-the-art in the field, highlighting the latest developments and innovations required for future applications.

FORMAT OF THE CONFERENCE

The conference combines the following formats:

- Plenary sessions with invited keynote speakers
- Oral sessions (both convened and regular)
- Posters (presented in the same central area as the exhibition)
- Short Courses & Workshops
- Exhibition

ABSTRACT SUBMISSION

AAuthors are kindly invited to submit their abstract by 13 October 2013. The on-line submission form is available via the conference website.

APPLICATION TRACKS

EuCAP 2014 will feature a session track focussing on applications. This will increase interaction between academia and industry. During abstract submission, authors will be invited to allocate their contributions to one or more applications, enabling the formation of application tracks in the final program. Contributions not targeting a particular application will be allocated to regular sessions all along the week.

SHORT COURSES & WORKSHOPS

In the spirit of the previous EuCAP editions, EuCAP 2014 will also provide a series of short courses and workshops. Those interested are invited to submit a firm proposal for a Course before August 20th, 2013.

EXHIBITION & SPONSORSHIP

EuCAP 2014 will provide ample opportunities for exhibitors and sponsors. Contact the conference service provider for further information and floor plans.

Organised by

EurAAP

Supporting Associations

URSI · IEEE · IET The Institution of Engineering and Technology · AMTA · APS

Important Deadlines

- **Submission of Abstracts**
  13 October 2013
- **Notification of Acceptance**
  15 December 2013
- **Submission of Final Papers**
  17 January 2014

Contact

Congrex Holland/
ESA Conference Bureau

Phone: +31715656507
eucap2014@congrex.com

Platinum Sponsors

esa · TU Delft Delft University of Technology · TICRA · TU/e Technische Universiteit Eindhoven University of Technology · CST

Gold Sponsors

FEKO · TNO innovation for life

www.eucap2014.org

CALL FOR PAPERS

ICEAA - IEEE APWC

August 3-9, 2014 **Palm Beach, Aruba**

ICEAA 2014
International Conference on Electromagnetics in Advanced Applications

www.iceaa-offshore.org

IEEE APWC 2014
IEEE-APS Topical Conference on Antennas and Propagation in Wireless Communications

The sixteenth edition of the International Conference on Electromagnetics in Advanced Applications (ICEAA 2014) is supported by the Politecnico di Torino, by the University of Illinois at Chicago, by the Istituto Superiore Mario Boella and by the Torino Wireless Foundation, with the principal cosponsorship of the IEEE Antennas and Propagation Society and the technical cosponsorship of the International Union of Radio Science (URSI). It is coupled to the fourth edition of the IEEE-APS Topical Conference on Antennas and Propagation in Wireless Communications (IEEE APWC 2014). The two conferences consist of invited and contributed papers, and share a common organization, registration fee, submission site, workshops and short courses, and social events. The proceedings of both conferences will be published on IEEE Xplore.

Suggested Topics for ICEAA

Adaptive antennas
Complex media
Electromagnetic applications to biomedicine
Electromagnetic applications to nanotechnology
Electromagnetic education
Electromagnetic measurements
Electromagnetic modeling of devices and circuits
Electromagnetic packaging
Electromagnetic properties of materials
Electromagnetic theory
EMC/EMI/EMP
Finite methods
Frequency selective surfaces
Integral equation and hybrid methods
Intentional EMI
Inverse scattering and remote sensing
Metamaterials
Optoelectronics and photonics
Phased and adaptive arrays
Plasma and plasma-wave interactions
Printed and conformal antennas
Radar cross section and asymptotic techniques
Radar imaging
Radio astronomy (including SKA)
Random and nonlinear electromagnetics
Reflector antennas
Technologies for mm and sub-mm waves

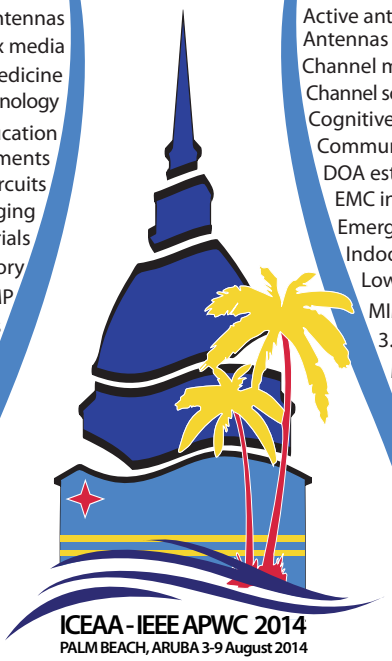

Suggested Topics for APWC

Active antennas
Antennas and arrays for security systems
Channel modeling
Channel sounding techniques for MIMO systems
Cognitive radio
Communication satellite antennas
DOA estimation
EMC in communication systems
Emergency communication technologies
Indoor and urban propagation
Low-profile wideband antennas
MIMO systems
3.5G and 4G mobile networks
Multi-band and UWB antennas
OFDM and multi-carrier systems
Propagation over rough terrain
Propagation through forested areas
Radio astronomy (including SKA)
RFID technologies
Signal processing antennas and arrays
Small mobile device antennas
Smart antennas and arrays
Space-time coding
Vehicular antennas
Wireless mesh networks
Wireless security
Wireless sensor networks

Information for Authors

Authors must submit a full-page abstract electronically by March 7, 2014. Authors of accepted contributions must submit the full paper, executed copyright form and registration electronically by June 6, 2014. Instructions are found on the website. Each registered author may present no more than two papers. All papers must be presented by one of the authors.

Deadlines	Abstract submission	March 7, 2014
	Notification of acceptance	April 11, 2014
	Full paper and presenter registration	June 6, 2014
Inquiries	Prof. Roberto D. Graglia Chair of Organizing Committee Politecnico di Torino *roberto.graglia@polito.it*	Prof. Piergiorgio L. E. Uslenghi Chair of Scientific Committee University of Illinois at Chicago *uslenghi@uic.edu*

Information for authors

Content

The *Radio Science Bulletin* is published four times per year by the Radio Science Press on behalf of URSI, the International Union of Radio Science. The content of the *Bulletin* falls into three categories: peer-reviewed scientific papers, correspondence items (short technical notes, letters to the editor, reports on meetings, and reviews), and general and administrative information issued by the URSI Secretariat. Scientific papers may be invited (such as papers in the *Reviews of Radio Science* series, from the Commissions of URSI) or contributed. Papers may include original contributions, but should preferably also be of a sufficiently tutorial or review nature to be of interest to a wide range of radio scientists. The *Radio Science Bulletin* is indexed and abstracted by INSPEC.

Scientific papers are subjected to peer review. The content should be original and should not duplicate information or material that has been previously published (if use is made of previously published material, this must be identified to the Editor at the time of submission). Submission of a manuscript constitutes an implicit statement by the author(s) that it has not been submitted, accepted for publication, published, or copyrighted elsewhere, unless stated differently by the author(s) at time of submission. Accepted material will not be returned unless requested by the author(s) at time of submission.

Submissions

Material submitted for publication in the scientific section of the *Bulletin* should be addressed to the Editor, whereas administrative material is handled directly with the Secretariat. Submission in electronic format according to the instructions below is preferred. There are typically no page charges for contributions following the guidelines. No free reprints are provided.

Style and Format

There are no set limits on the length of papers, but they typically range from three to 15 published pages including figures. The official languages of URSI are French and English: contributions in either language are acceptable. No specific style for the manuscript is required as the final layout of the material is done by the URSI Secretariat. Manuscripts should generally be prepared in one column for printing on one side of the paper, with as little use of automatic formatting features of word processors as possible. A complete style guide for the *Reviews of Radio Science* can be downloaded from http://www.ips.gov.au/IPSHosted/NCRS/reviews/. The style instructions in this can be followed for all other *Bulletin* contributions, as well. The name, affiliation, address, telephone and fax numbers, and e-mail address for all authors must be included with

All papers accepted for publication are subject to editing to provide uniformity of style and clarity of language. The publication schedule does not usually permit providing galleys to the author.

Figure captions should be on a separate page in proper style; see the above guide or any issue for examples. All lettering on figures must be of sufficient size to be at least 9 pt in size after reduction to column width. Each illustration should be identified on the back or at the bottom of the sheet with the figure number and name of author(s). If possible, the figures should also be provided in electronic format. TIF is preferred, although other formats are possible as well: please contact the Editor. Electronic versions of figures *must* be of sufficient resolution to permit good quality in print. As a rough guideline, when sized to column width, line art should have a minimum resolution of 300 dpi; color photographs should have a minimum resolution of 150 dpi with a color depth of 24 bits. 72 dpi images intended for the Web are generally *not* acceptable. Contact the Editor for further information.

Electronic Submission

A version of Microsoft *Word* is the preferred format for submissions. Submissions in versions of T_EX can be accepted in some circumstances: please contact the Editor before submitting. *A paper copy of all electronic submissions must be mailed to the Editor, including originals of all figures.* Please do *not* include figures in the same file as the text of a contribution. Electronic files can be send to the Editor in three ways: (1) By sending a floppy diskette or CD-R; (2) By attachment to an e-mail message to the Editor (the maximum size for attachments *after* MIME encoding is about 7 MB); (3) By e-mailing the Editor instructions for downloading the material from an ftp site.

Review Process

The review process usually requires about three months. Authors may be asked to modify the manuscript if it is not accepted in its original form. The elapsed time between receipt of a manuscript and publication is usually less than twelve months.

Copyright

Submission of a contribution to the *Radio Science Bulletin* will be interpreted as assignment and release of copyright and any and all other rights to the Radio Science Press, acting as agent and trustee for URSI. Submission for publication implicitly indicates the author(s) agreement with such assignment, and certification that publication will not violate any other copyrights or other rights associated with the submitted material.

APPLICATION FOR AN URSI RADIOSCIENTIST

I have not attended the last URSI General Assembly, and I wish to remain/become an URSI Radioscientist in the 2012-2014 triennium. Subscription to *The Radio Science Bulletin* is included in the fee.

(please type or print in BLOCK LETTERS)

Name : Prof./Dr./Mr./Mrs./Ms. _____
Family Name First Name Middle Initials

Present job title: _____

Years of professional experience: _____

Professional affiliation: _____

I request that all information be sent to my ☐ home ☐ business address, i.e.:

Company name: _____

Department: _____

Street address: _____

City and postal/zip code: _____

Province/State: _____ Country: _____

Phone: _____ ext._____ Fax: _____

E-mail: _____

Areas of interest (Please tick)

☐ A Electromagnetic Metrology
☐ B Fields and Waves
☐ C Radio-Communication Systems & Signal Processing
☐ D Electronics and Photonics
☐ E Electromagnetic Environment & Interference
☐ F Wave Propagation & Remote Sensing
☐ G Ionospheric Radio and Propagation
☐ H Waves in Plasmas
☐ J Radio Astronomy
☐ K Electromagnetics in Biology & Medicine

I would like to order :

☐ An electronic version of the RSB downloadable from the URSI web site
(The URSI Board of Officers will consider waiving the fee if a case is made to them in writing.) 40 Euro

Method of payment : VISA / MASTERCARD (we do not accept cheques)

Credit card No ☐☐☐☐ ☐☐☐☐ ☐☐☐☐ ☐☐☐☐ Exp. date _____

CVC Code: _____ Date : _____ Signed _____

Please return this signed form to :

The URSI Secretariat
c/o Ghent University / INTEC
Sint-Pietersnieuwstraat 41
B-9000 GHENT, BELGIUM
fax (32) 9-264.42.88